Understanding of Tumor Heterogeneity in Glioblastoma Multiforme Cell Lines with Differential Apoptotic Threshold

by

Ahmet CİNGÖZ

A Dissertation Submitted to the

Graduate School of Health Sciences

in Partial Fulfillment of the Requirements for

the Degree of

Doctor of Philosophy

in

Cellular and Molecular Medicine



KOÇ
UNIVERSITY

24.06.2019

Understanding of Tumor Heterogeneity in Glioblastoma Multiforme Cell Lines with Differential Apoptotic Threshold

Koç University

Graduate School of Health Sciences

This is to certify that I have examined this copy of a doctoral dissertation by

Ahmet CİNGÖZ

and have found that it is complete and satisfactory in all respects,

and that any and all revisions required by the final

examining committee have been made.

Committee Members:

Assoc. Prof. Tuğba BAĞCI-ÖNDER (Advisor)

Prof. Nesrin ÖZÖREN

Prof. İhsan SOLAROĞLU

Assoc. Prof. Tamer ÖNDER

Assist. Prof. Emre DENİZ

Date: 24.06.19

I would like to dedicate this thesis to my beloved family,
who always support me…

ABSTRACT

Understanding of Tumor Heterogeneity in Glioblastoma Multiforme Cell Lines With Differential Apoptotic Threshold

Ahmet CİNGÖZ

Doctor of Philosophy in Cellular and Molecular Medicine

June 24, 2019

Glioblastoma multiforme (GBM) is the most common and aggressive primary brain tumor, with very low survival rate after diagnosis. Current treatment approaches include radio and chemotherapy following resection of tumor by surgery. Tumor necrosis factor–related apoptosis-inducing ligand (TRAIL) induces apoptosis specifically in tumor cells, making it a prime therapeutic candidate. However, many tumor cells, including GBM, are either innately TRAIL-resistant, or they acquire resistance with adaptive mechanisms that remain poorly understood. In this thesis, we generated acquired TRAIL resistance models using multiple GBM cell lines to assess the molecular alterations in the TRAIL-resistant state. We selected TRAIL-resistant cells through chronic and long-term TRAIL exposure and showed that these cells showed persistent resistance *in vitro* and *in vivo*. Among known TRAIL-sensitizers, proteasome inhibitor Bortezomib, but not HDAC inhibitor MS-275, was effective in overcoming resistance in all cell models. This was partly achieved through upregulating death receptors and pro-apoptotic proteins, and downregulating major anti-apoptotic members, Bcl-2 and Bcl-xL. We showed that CRISPR/Cas9 mediated silencing of DR5 could block Bortezomib-mediated re-sensitization, demonstrating its critical requirement. While overexpression of Bcl-2 or Bcl-xL was sufficient to confer resistance to TRAIL-sensitive cells, it failed to override Bortezomib-mediated re-sensitization. With RNA sequencing in multiple paired TRAIL-sensitive and TRAIL-resistant cells, we identified major alterations in the inflammatory signaling, particularly in the NF-kB pathway. Inhibiting NF-kB with QNZ substantially sensitized the most resistant cells to TRAIL, albeit its sensitization ability was lower than that of Bortezomib. Together, our findings provide new models of acquired TRAIL resistance, which will provide essential tools to gain further insight into the heterogeneous therapy responses within GBM tumors. Additionally, these findings emphasize the critical importance of combining proteasome inhibitors and pro-apoptotic ligands to overcome acquired resistance.

ÖZETÇE

Glioblastoma Multiforme Hücre Hatlarında Diferansiyel Apoptotik Yanıt ile Hücre Heterojenitesinin Anlaşılması

Ahmet CİNGÖZ

Hücresel ve Moleküler Tıp, Doktora

24 Haziran 2019

Glioblastoma multiforme (GBM), tanı sonrası yaşam süresi çok kısa olan en yaygın ve agresif primer beyin tümörüdür. Güncel tedavi yaklaşımları, tümörün cerrahi olarak rezeksiyonunu takiben radyo ve kemoterapiyi içerir. Tümör Nekroz Faktörü ile İlişkili Apoptoz-İndükleyici Ligand (TRAIL), özellikle tümör hücrelerinde apoptozu indüklediği için kanserde önemli bir terapötik adaydır. Bununla birlikte, GBM de dahil olmak üzere birçok tümör hücresi, ya TRAIL'a baştan dirençlidir ya da henüz yeterince anlaşılamamış sonradan gelişen mekanizmalarla direnç kazanır. Bu tez çalışmasında, TRAIL direncindeki moleküler değişiklikleri değerlendirmek için farklı GBM hücre dizileri kullanarak TRAIL-dirençli hücre modelleri geliştirilmiştir. TRAIL'a dirençli hücreler kronik ve uzun süreli TRAIL'a maruz kalma yoluyla seçilmiş, bu hücrelerin direncinin kalıcı olduğu *in vitro* ve *in vivo* çalışmalarla gösterilmiştir. Tüm hücre modellerinde TRAIL direncini kırabildiği bilinen TRAIL-duyarlılaştırıcılarından HDAC inhibitörü MS-275 değil, proteazom inhibitörü Bortezomib etkili olmuştur. Bu durum, ölüm reseptörleri, pro-apoptotik proteinler ve majör anti-apoptotik proteinler olan Bcl-2 ve Bcl-xL'nin ekspresyonunun düzenlenmesiyle sağlanmıştır. Ayrıca, CRISPR/Cas9 aracılı DR5 susturulmasının Bortezomib aracılı hassaslaştırmayı engelleyebileceği gösterilmiştir. Bcl-2 veya Bcl-xL'nin yüksek ifadesinin, TRAIL'a duyarlı hücrelere direnç kazandırmak için yeterli olduğu, fakat Bortezomib aracılı yeniden hassaslaştırmayı engelleyemediği bulunmuştur. TRAIL'e duyarlı ve dirençli hücrelerde yaptığımız RNA dizilimi ile özellikle NF-kB yolu gibi inflamasyon sinyallerinde büyük değişiklikler tespit edilmiştir. NF-kB'nin QNZ ile engellenmesi, Bortezomib'den daha düşük olsa da TRAIL'a dirençli hücreleri büyük ölçüde hassaslaştırmıştır. Sonuç olarak, çalışmamız GBM tümörleri içindeki heterojen terapi yanıtları hakkında daha fazla bilgi edinmek için gerekli araçları sağlayacak olan yeni kazanılmış TRAIL-direnci modellerini sunmaktadır. Ek olarak, bu bulgular kazanılmış direncin üstesinden gelmek için proteazom inhibitörlerinin ve pro-apoptotik ligandların birleştirilmesinin kritik önemini vurgulamaktadır.

ACKNOWLEDGMENTS

First of all, I would like to thank to my advisor, Dr. Tuğba BAĞCI-ÖNDER for her guidance, support, and encouragement throughout my PhD life. She trusted me and opened the doors of her laboratory to me, and I have completed this thesis. Her excellent support and guidance on both my PhD life and future are priceless.

Secondly, I would like to thank my PhD thesis committee members Dr. Nesrin ÖZÖREN, and Dr. İhsan SOLAROĞLU for their support and guidance throughout my PhD. I owe special thanks to Dr. Tamer ÖNDER and Dr. Emre DENİZ for being in my thesis defense committee and sparing their precious time for me.

I would like to thank Koç University, Graduate School of Health Sciences (GSHS), School of Medicine (KUSOM), Koç University Research Center for Translational Medicine (KUTTAM) and The Scientific and Technological Research Council of Turkey (TÜBİTAK) for the funding and the research environment they provided.

Also, I would like to thank to Dr. Khalid SHAH and Deepak BHERE from Harvard University, for their collaboration and help with stem-cells and animal experiments, and their precious advices.

My sincere thanks also go to current members of the TBO Lab., Fidan Şeker, Ezgi Özyerli-Göknar, Dr. Filiz Şenbabaoğlu, Nareg Pınarbaşı, Alişan Kayabölen, Özlem Yedier-Bayram, Dr. İlknur Sur-Erdem, Seher Emreoğlu, E. Yağmur Kala, Göktuğ Karabıyık, A. Cenk Aksu and Birsu Kölemen; and also alumni of TBO Lab., Ezgi Kaya, Tolga Lokumcu, İ. Çağrı Kurt, Selena Kazancıoğlu, and Nastaran Langarizadeh for helping me at every step of my PhD life and studies. I re-defined brotherhood without blood relation with them.

Also, I owe special thanks to my lovely friends and colleagues Dr. Fatma Özgün, Eray Enüstün. Dr. Pelin Erkoç, and Dr. Benay Uzer for their support in any aspect of my life and research.

Additionally, I would like to thank to my best friends Gökhan Türkoğlu and Semin Özkan for their friendship and their unconditional support.

Last but definitely not the least, I wish to thank my family, my mother, father, sister, brother, and cousins. I could not be what I am today without their trust, love, endless and unconditional support throughout my whole life.

TABLE OF CONTENTS

LIST OF TABLES x

LIST OF FIGURES xi

RESEARCH PROPOSAL xiv

SPECIFIC AIMS xiv

Specific Aim 1: Isolation of TRAIL resistant sub-populations from GBM cell lines. xiv

Specific Aim 2: To investigate the molecular determinants of TRAIL resistance. xiv

Specific Aim 3: To examine the re-sensitization of TRAIL-resistant sub-population. xiv

1. REVIEW OF LITERATURE 1

1.1 Overview of primary brain tumors 1

1.2 Glioblastoma multiforme (GBM) 1

1.2.1 Molecular structure of GBM 3

1.3 Treatment of GBM 6

1.3.1 Targeted therapies in GBM 7

1.4 APOPTOSIS 9

1.5 TRAIL and TRAIL receptors 10

1.5.1 TRAIL Signals 10

1.5.2 TRAIL resistance 13

1.5.3 TRAIL Therapy 15

1.6 Tumor heterogeneity in GBM 17

1.7 Therapy resistance 20

1.7.1 Acquired resistant models for TRAIL 21

2. MATERIALS AND METHODS 22

2.1 Cell Culture 22

2.2 Production of TRAIL protein 22

2.3 Cell viability 22

2.4 Caspase 3/7 Activity and Caspase Inhibition Assay 23

2.5 Real-time Cell Growth Analysis 23

2.6 Live Cell Imaging 23

2.7 YO-PRO-1/PI Staining 24

2.8 Cell Cycle Assay 24

2.9 Cloning 25

2.9.1 shRNA Cloning 25

sh-Bcl-XL: 25

sh-Bcl-2: 25

sh-IGFBP-2: 25

2.9.2 Overexpression vectors: 25

pLEX307-HES1 vector cloning: 25

2.9.3 gRNA cloning 26

2.10 Viral Packaging and Transduction 27

2.11 Quantitative Real Time-PCR 28

2.12 Western Blot 30
2.13 RNA-Sequencing and Analysis 32
2.13.1 Statistical and functional analysis of RNA seq data and differentially expressed gene Identification 32
2.13.2 Functional analysis of RNA seq data 32
2.14 Co-culture Experiments 33
2.15 In vivo Studies 33
3. RESULTS 34
3.1 Generation of TRAIL-resistant cell populations from GBM cell lines 34
3.1.1 TRAIL response of TRAIL-resistant sub-populations 35
3.1.2 Re-generation of TRAIL-resistant sub-populations 36
3.1.3 Caspase activity of TRAIL-resistant sub-populations 37
3.1.4 Apoptotic protein levels in TRAIL-resistant sub-populations after TRAIL treatment 38
3.1.5 TRAIL resistance in long term 39
3.2 TRAIL-resistant cell generation from U87MG cells 42
3.2.1 TRAIL response of TRAIL-resistant U87MG-R10 and R50 Cells 42
3.2.2 Caspase Activity of TRAIL-resistant U87MG-R10 and R50 Cells 43
3.2.3 Long term effects of TRAIL in U87MG-R10 and R50 Cells 43
3.3 Resistance of sub-populations was specific to TRAIL 44
3.4 Re-sensitization of TRAIL-resistant cells 47
3.4.1 MS-275 cannot re-sensitize sub-populations to TRAIL 47
3.4.2 Bortezomib re-sensitizes TRAIL-resistant sub-populations to TRAIL 48
3.5 Regulation of apoptotic cell death pathway by Bortezomib 50
3.6 Maintenance of DR5 expression for TRAIL resistance 53
3.7 Regulation of TRAIL response in GBM cells by Bcl-2 And Bcl-xL expression 57
3.7.1 The effects of Bcl-2 and Bcl-xL overexpression on Bortezomib-mediated re-Sensitization 60
3.7.2 The Effects of Bcl-2 And Bcl-xL Downregulation on TRAIL-resistance 60
3.8 Re-sensitization of TRAIL-resistant cells by BH3 mimetics 63
3.9 RNA-sequencing of TRAIL-sensitive and -resistant cells 64
3.9.1 qRT-PCR confirmation of common gene expressions 67
3.9.2 The effects of Bortezomib on RNA-sequencing related common gene expressions 69
3.9.3 Functional analysis of RNA sequencing data 70
3.9.4 Gene Set Enrichment Analysis (GSEA) 71
3.9.5 Functional analysis of NF- κB pathway 75
3.9.6 Functional analysis of PI3K pathway 76
4. DISCUSSION 77
5. Appendix I 84
5.1 Knock-Out of Up-Regulated Genes by CRISPR/Cas9 84
5.2 Overexpression of HES1 Gene 86
5.3 Inhibition of PPARG Pathway 87
6. Appendix II 89
6.1 RNA sequencing of U87MG TRAIL-resistant Sub-Populations 89
6.2 Functional Analysis of RNA-Seq Data of R50 and 250 Cells 89
6.3 Differentially Expressed Gene Alterations 91

7. Appendix III 93
7.1 Insulin-like Growth Factor Binding Proteins (IGFBPs) 93
7.1.1 IGF-Binding Protein-2 (IGFBP-2) 93
7.1.2 IGFBP-2 in Glioblastoma 94
7.1.3 IGFBP-2 was Common Upregulated Top Gene 95
7.1.4 Correlation of IGFBP-2 Expression with Patient Survival 96
7.2 Knock-down of IGFBP-2 in U87MG-R250 cells 96
7.3 The Effects of Down-regulation of IGFBP-2 on TRAIL-resistance 97
7.4 Overexpression of IGFBP2 97
7.5 The Effects of Up-regulation of IGFBP-2 on TRAIL-resistance 98
7.6 The Effects of Secreted IGFBP-2 on TRAIL-resistance 98
BIBLIOGRAPHY 101

LIST OF TABLES

Table 1.1. Genetic alterations in different grades of GBM. 19
Table 2.1. List and DNA sequences of gRNAs used in CRISPR/Cas9 experiments. 26
Table 2.2. List of vectors used in experiments. 27
Table 2.3. List of primers used in quantitative real-time PCR experiments. 30
Table 2.4. List of primary and secondary antibodies used in western-blot experiments. 31
Table 3.1. Clean reads quality metrics of sequenced samples. 64
Table 3.2. Common up- and down-regulated gene list. 67
Table 5.1. List of gRNA sequences used in CRISPR/Cas9 experiments. 84
Table 6.1. Table showing of common top 25 up-regulated genes in U87MG-R50 and R250 cell lines. 92
Table 6.2. Table showing of common top 25 down-regulated genes in U87MG-R50 and R250 cell lines. 92

LIST OF FIGURES

Figure 1.1. MRI scan of a GBM patient. 2
Figure 1.2. Oncogenic pathways in GBM. 6
Figure 1.3. Signaling pathways of TRAIL-induced apoptosis. 12
Figure 1.4. Mechanisms of resistance to TRAIL. 15
Figure 1.5. Hierarchical model for GBM tumor evolution. 18
Figure 3.1. Experimental approach to isolation of TRAIL-resistant sub-populations. 34
Figure 3.2. Viability of TRAIL-resistant subpopulations. 35
Figure 3.3. Light microscopy snapshots of A172-S and -R cells. 36
Figure 3.4. Viability results of all resistant subpopulations. 36
Figure 3.5. Caspase 3/7 activity of TRAIL-resistant subpopulations. 37
Figure 3.6. Western blot results of TRAIL-resistant subpopulations. 38
Figure 3.7. Yo-Pro staining of A172-S and -R cells. 38
Figure 3.8. Long-term real time cell survival analysis of TRAIL-resistant cells. 39
Figure 3.9. Representative snapshots of co-culture experiments. 40
Figure 3.10. Schematic showing of in vivo experiment. 41
Figure 3.11. Representative snapshots of tumor imaging and quantification. 41
Figure 3.12. Experimental approach to isolation of TRAIL-resistant sub-populations from U87MG cells. 42
Figure 3.13. Viability of U87MG-R10 and R50 cells. 42
Figure 3.14. Caspase 3/7 activity of U87MG-R10 and R50 cells. 43
Figure 3.15. Real-time cell survival analysis of U87MG-R10 and R50 cells. 43
Figure 3.16. Viability of TRAIL-resistant cells treated with Temozolomide. 44
Figure 3.17. Viability of TRAIL-resistant cells treated with Fas-ligand. 45
Figure 3.18. Viability of TRAIL-resistant cells treated with Staurosporine. 46
Figure 3.19. Viability of TRAIL-resistant cells treated with MS-275. 47
Figure 3.20. Viability results of TRAIL-resistant cells treated with Bortezomib. 48
Figure 3.22. Quantification of live cell imaging data. 49
Figure 3.21. Representative snapshots from live cell imaging of A172-S and -R cells. 49
Figure 3.23. Caspase 3/7 activity of TRAIL-resistant cells treated with Bortezomib. 50
Figure 3.24. Viability analysis A172-S and –R cells pretreated with caspase inhibitors followed by TRAIL and Bortezomib. 51
Figure 3.25. Western blot results of A172-S and -R cells treated with Bortezomib. 52
Figure 3.26. Endogenous DR4 and DR5 expression levels of TRAIL-S and R cells. 53
Figure 3.27. Pro- and anti-apoptotic gene expression levels of TRAIL pathway in Bortezomib treated TRAIL-resistant cells. 54
Figure 3.28. Western blot showing of major TRAIL pathway related proteins in Bortezomib treated A172-R cells. 55
Figure 3.29. Western blot showing the CRISPR knockouts of DR5 protein levels in A172-S and –R cells. 55
Figure 3.30. Viability analysis of DR5 knockout A172-S and -R cells. 56
Figure 3.31. Overexpression of Bcl-2 and Bcl-xL genes in A172-S and -R cells. 57
Figure 3.32. Overexpression of Bcl-2 and Bcl-xL genes in LN18-S and -R cells. 57
Figure 3.33. Overexpression of Bcl-2 and Bcl-xL genes in T98G-S and -R cells. 58
Figure 3.34. Overexpression of Bcl-2 and Bcl-xL genes in U87MG-S and -R cells. 58
Figure 3.35. Viability of Bcl-2 and Bcl-xL overexpressed cells. 59
Figure 3.36. Viability analysis of Bcl-2 and Bcl-xL overexpressed A172-S and A172-R cells upon Bortezomib treatment. 60

Figure 3.37. Knock-down of Bcl-2 and Bcl-xL in TRAIL-S and -R cells. 61
Figure 3.38. Viability analysis of Bcl-2 and Bcl-xL knocked-down cells. 62
Figure 3.39. Viability results of A172-S and -R cells treated with BH3 mimetics. 63
Figure 3.40. Hierarchical clustering between samples. 65
Figure 3.41. Bar graph showing of differentially expressed genes (DEGs). 65
Figure 3.42. Volcano plots showing of differentially expressed genes (DEGs). 66
Figure 3.43. Common upregulated and downregulated DEGs in all cell lines. 66
Figure 3.44. qRT-PCR confirmation of common genes. 68
Figure 3.45. Expression of common genes in A172-R cells treated with Bortezomib. 69
Figure 3.46. Ingenutiy pathway analysis of DEGs. 70
Figure 3.47. Gene Set Enrichment Analysis (GSEA). 72
Figure 3.48. Enrichment plots for hallmark of NF-kB pathway. 73
Figure 3.49. Expression of NF-kB related genes in all TRAIL-R cells. 74
Figure 3.50. Viability of A172-S and -R cells treated with QNZ. 75
Figure 3.51. Viability of A172-S and -R cells treated with QNZ and TRAIL combination. 75
Figure 3.52. Viability of A172-S and –R cells treated with PI3K inhibitor. 76
Figure 4.1. Model for generation of TRAIL resistance and re-sensitization of resistant cells with different agents. 83
Figure 5.1. Representative showing of genomic map of PPARGC1A gene. 84
Figure 5.2. Viability of PPARGC1A, CXCL14, MEST, and DAAM genes by CRISPR/Cas9 in A172 cells treated with TRAIL. 85
Figure 5.3. Confirmation of HES1 overexpression in A172-S and R cells. 86
Figure 5.4. Viability of HES1 overexpressed A172 cells treated with TRAIL. 86
Figure 5.5. Viability of A172-S and -R cells treated with GW9662. 87
Figure 5.6. Viability of A172-S and -R cells treated with GW9662 and TRAIL combination. 88
Figure 6.1. Disease and Functions of IPA analysis in U87MG TRAIL-R cells. 89
Figure 6.2. Canonical pathways and upstream regulators of R50 and R250 cells. 90
Figure 6.3. Common up- and down-regulated genes in U87MG-R50 and R250 cells. 91
Figure 7.1. IGFBP2 gene expression levels in U87MG-TRAIL-R cells. 95
Figure 7.2. Survival analysis of IGFBP-2 expression in both LGG and LGG&GBM patients. 96
Figure 7.3. Knockdown of IGFBP2 in U87MG-S (R0) and -R (R250) cells. 96
Figure 7.4. Viability of IGFBP2 knocked-down U87MG-S and R cells treated with TRAIL. 97
Figure 7.5. Overexpression of IGFBP2 in U87MG cells. 97
Figure 7.6. Viability of IGFBP-2 overexpressed U87MG cells treated with TRAIL. 98
Figure 7.7. Schematic view of IGFBP-2 recombinant protein or conditioned medium experiment timeline. 98
Figure 7.8. Representative snapshots of U87MG cells treated with TRAIL and IGFBP-2. 99
Figure 7.9. Viability of U87MG cells treated with TRAIL and IGFBP-2. 99
Figure 7.10. Viability of U87MG cells treated with TRAIL upon IGFBP-2 conditioned medium applying. 100

NOMENCLATURE

2-HG	2-hydroxyglutarate
2-OG	2-oxoglutarate
APAF-1	Apoptotic protease activating factor 1
Bak	Bcl-2 homologous antagonist/killer
Bax	Bcl-2-associated X protein
BBB	Blood–brain barrier
Bcl-2	B-cell CLL/lymphoma 2
Bcl-xL	B-cell lymphoma-extra large
BH	Bcl-2 Homology Domain
Bid	BH3 interacting-domain death agonist
Cyt C	Cytochrome C
DISC	Death-inducing signaling complex
DR4/5	Death Receptor-4/5
EGFR	Epidermal growth factor receptor
EOC	Epithelial ovarian cancer
FADD	Fas-Associated protein with Death Domain
FDA	Food and Drug Administration
FLIP	Flice-like inhibitory protein
Fluc	Firefly luciferase
FMC	Fluc-mCherry
GBM	Glioblastoma Multiforme
HRK	Harakiri
IAP	Inhibitor of Apoptosis protein
IDH1/2	Isocitrate Dehydrogenase 1/2
IGFBP2	Insulin like growth factor binding protein-2
LGG	Lower-grade Glioma
MGMT	O-6-methylguanine-DNA methytransferase
MOMP	mitochondrial outer membrane permeabilization
NF-κB	Nuclear Factor kappa B
NOD/SCID	Nonobese diabetic/severe combined immunodeficiency
PDGF	Platelet-derived growth factor
PI3K	Phosphoinositide 3-kinase
PTEN	Phosphatase and tensin homolog
RNA-seq	RNA sequencing
TMZ	Temozolomide
TNF	Tumor necrosis factor
TRAIL	TNF-related apoptosis inducing ligand
VEGF	Vascular endothelial growth factor
WHO	World Health Organization
XIAP	X-linked inhibitor of apoptosis

RESEARCH PROPOSAL

In this thesis, we hypothesized that differential apoptotic thresholds of Glioblastoma multiforme (GBM) cell lines are caused by genetic and epigenetic heterogeneity. For this purpose, we focused on understanding tumor heterogeneity in GBM with following aims:

SPECIFIC AIMS

Specific Aim 1: Isolation of TRAIL resistant sub-populations from GBM cell lines.

GBM cells exhibit heterogeneity in their responses to TRAIL. In order to study heterogeneity in the context of apoptosis response, the first aim was isolation of TRAIL resistant sub-populations through several approaches in parallel.

Specific Aim 2: To investigate the molecular determinants of TRAIL resistance.

After establishing TRAIL-resistant cells, we aimed to characterize the molecular mechanisms underlying the heterogeneity by transcriptome profiling. We employed RNA sequencing to dissect out the differences between TRAIL-sensitive and their matched TRAIL-resistant cell populations.

Specific Aim 3: To examine the re-sensitization of TRAIL-resistant sub-populations.

To assess whether the acquired resistance is reversible with secondary therapeutic agents, we addressed the efficacy and potential of several secondary drugs to overcome resistance.

1 REVIEW OF LITERATURE

1.1 Overview of primary brain tumors

Primary brain tumors arise in the central nervous system (CNS) and they have numerous types such as gliomas, meningiomas and schwannomas [1]. Gliomas are the major form with 77% of all malignant primary tumors [2]. Gliomas are in 4 different group, namely, astrocytomas, oligodendrogliomas, ependymomas and oligo-astrocytomas [3]. According to World Health Organization (WHO), astrocytomas are the most common brain tumor type, further classified into 4 grades with respect to their malignancy: benign astrocytoma (Grade I), low-grade astrocytoma (Grade II), anaplastic astrocytoma (Grade III), and glioblastoma (GBM) (Grade IV) [4]. Grade I, pilocytic astrocytomas have benign tumor biology and are generally seen in children and young patients. Grade I astrocytomas can be mainly treated by surgery. Low grade or diffuse astrocytomas are Grade II tumors, which slowly grow and invade into the brain. The patient survival rate is approximately 4-5 years. Generally, treatment options are resection of tumor by surgery, then radio and chemotherapy. Grade III, anaplastic oligodendro-gliomas and astrocytomas, and Grade IV, GBM are high grade malignant gliomas [5]. Approximately 7/100.000 individuals are diagnosed with the brain tumor every year [6], and the incidence of gliomas is 5/100.000 individuals every year [7]. Even though GBM incidence is only 1% in all adult cancers, it is the fourth deadly cancer [8].

1.2 Glioblastoma multiforme (GBM)

GBM is the most frequent and aggressive type of primary brain cancer [9] with 3/100.000 diagnoses every year [10]. GBM is among the most malignant cancer types with median survival of approximately 15 months [11], less than 5% of GBM patients survive 5 years [12].

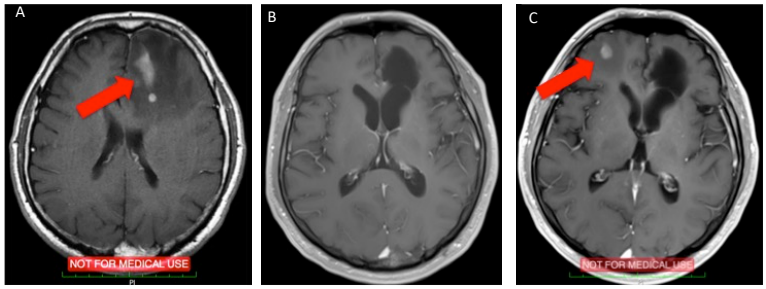


Figure 1.1. MRI results of a GBM patient. **(A)** Preoperative MR image of left frontal lobe located GBM. **(B)** Demonstrates post-operative loss of contrast-enhancing lesion post gross total resection **(C)** Recurrence of tumor after 14 months of initial operation.
(MRI scan, kindly provided by Prof. Dr. Ihsan Solaroğlu)

GBM can develop in two ways: de novo, as defined primary GBM, directly appears as Grade IV, or gradually increasing from lower grades by accumulation of mutations. This type of tumors is defined as secondary GBM. Both primary and secondary GBMs are the last grade of astrocytic tumors, show highly malignant and invasive phenotype. The mitotic index of GBMs is highly elevated compared to the low-grade gliomas (LGG), and as a hallmark of GBM, it has necrotic regions in the core of the tumor mass. Another characteristic phenotype of GBM is increased proliferation rate and angiogenic activity. Other hallmarks of GBM are diffuse invasion phenotype into the brain parenchyma, resistance to apoptosis and chemotherapy drugs, and genomic instability [6,13].

The complex structure of tumor is one of the reasons to therapy resistance. Glioblastoma is "multiforme", which describes heterogeneous tumor populations affecting morphology, proliferation, gene expression, and drugs response of cells. Also, these multiforme structure causes necrotic and hemorrhagic regions. These regions include pleomorphic cells and nucleus, microvascular proliferation, and pseudopalisading necrosis. Additionally, multiforme structure of GBM is accompanied by a variety of point mutations, deletions and amplifications causing hyper-activation of signal transduction pathways [13,14].

1.2.1 Molecular structure of GBM

Different signaling pathways are altered during the malignant transformation of GBM. The most important of these altered pathways are receptor tyrosine kinases (RTKs). RTKs are on cell surface that activate after growth-factors (GFs) binding. In the absence of GFs, receptors are embedded as a monomeric form (single subunit) in the plasma membrane. When ligand is present, two adjacent subunits are dimerized resultings in conformational shift that activates the kinase function of RTKs. Active RTKs transduce the signal by phosphorylation to downstream signaling cascades. Epidermal growth factor receptors (EGFR) signaling is one of the important RTKs in GBM. EGFR signaling activates survival functions, including differentiation, proliferation and migration in all types of CNS cells [15,16]. EGFR can be highly activated in GBMs through mutations of receptors, overexpression of receptor or ligand, or amplification of the EGFR locus. As a result of these abnormalities, EGFR pathway is constitutively activated. The most common EGFR mutation in GBM is the EGFRvIII, which depends on the loss of exon 2-7, causing of the deletion of 267 amino acids in the extracellular domain. Mutated receptors are phosphorylated ligand independently and constitutively active. This mutation is observed in only primary GBMs, not secondary GBMs or healthy tissues [17,18].

Ras is another common altered pathway in GBM. Although Ras mutation is rare in GBM, elevated activity of Ras pathway is observed in almost all GBM tumors [19]. Ras, like the heterotrimeric G-proteins (Guanosine-binding protein), is regulated as the binary switches. When GDP is bound to Ras, pathway is in inactive form, then it is activated by GTP binding and signal emits to downstream [16]. GTP-bound, active Ras promotes the cell cycle, migration and survival. Ras is the downstream of RTKs, therefore, presence of mutated Ras results in increasing the downstream signaling. Additionally, one of the targets of Ras is PI3K/Akt pathway. PI3K/Akt (Phosphatidylinositol-4,5-Bisphosphate 3-Kinase/Phosphatase /serine threonine kinase Akt) pathway is also activated by growth-factor receptors (GFRs). PI3K generates the PIP3 (phosphatidylinositol (3,4,5)-trisphosphate), as a secondary messenger, upon GFR activation [20]. Akt is activated by PIP3 as a downstream molecule, causing cell proliferation, survival and inhibition of apoptosis [16]. On the other hand, PTEN (Phosphatase and Tensin Homolog) negatively regulates the PI3K signaling pathway in normal conditions. However, PTEN is frequently mutated and cannot work as a tumor suppressor in GBM. PTEN activity loss is frequently

observed because of the chromosomal mutations, loss of heterozygosity (LOH), silencing of expression through DNA methylation, or overexpression of some microRNAs that suppress PTEN expression [16,21].

A tumor suppressor protein, retinoblastoma (RB), regulates the cell cycle on G1/S check-point by sequestering E2F. Hypo-phosphorylated RB binds to the E2F transcription factor and prevents the transcription of cell cycle and mitosis related genes in non-proliferating cells. When GFs induce Cyclin D1, CDK/cyclin (cyclin-dependent kinase/cyclin) complex is activated, then RB is phosphorylated, and E2F is released from RB. Free E2F promotes the transcription of DNA synthesis and cell proliferation related genes [6]. Mutation of genes in the RB pathway increases the mitotic activity in transformed cells. RB inactivation is frequently observed due to mutations of $p16^{INK4a}$, CDK4, and methylation of RB promoter in GBM. Alteration of these pathways leads to imbalances of cell cycle [22].

The TP53 pathway regulates the DNA damage response, cell cycle, and cell death. If DNA damage cannot be repaired, TP53 will promote apoptosis. Additionally, TP53 is negatively controlled by MDM2 proto-oncogene, and MDM2 is degraded by CDKN2A-$p14^{ARF}$ for maintaining the TP53. MDM4 is an activator of TP53 through binding to the transcriptional activation domain [23]. In gliomas, missense mutations of TP53, MDM2 and MDM4 amplifications, and CDKN2A-$p14^{ARF}$ deletions inactivate the tumor suppressor function of TP53 [24].

Recent discoveries identified either, not together, isocitrate dehydrogenase (IDH) 1 or IDH2 mutations in secondary GBMs [25]. IDH enzymes are responsible for producing of 2-OG (2-oxoglutarate), however mutation of IDH leads to accumulation of 2-HG (2-hydroxyglutarate) instead of 2-OG. 2-HG, called as “oncometabolite”, is a competitive inhibitor of some epigenetic enzymes such as TET hydroxylases and histone lysine demethylases. Mutant IDHs causes hypermethylation by inhibiting TET enzymes in glioma. Interestingly, patients with IDH-mutant gliomas have better prognosis against TMZ treatment [26–28].

In summary, primary GBMs have frequent loss of heterozygosity of 10q (70%), amplification of EGFR (35%), deletion of $p16^{INK4a}$ (31%), and PTEN mutations (25%). On the other hand secondary GBMs have mostly TP53 mutations [6,29,30] and IDH mutations. Mutations in these genes ultimately lead to uncontrolled mitosis, cell proliferation, and resistance to apoptosis.

Additionally, tumor necrosis factor (TNF) super-family and NF-kB pathway (RELB, TNFRSF1A, and TRADD), Notch (JAG1, LFNG, and NOTCH3), Sonic-hedgehog (GLI2, GAS1, and SMO), IDH1/2, STAT3, CEBP, HCLS1, MAFB, TAZ, and YAP were reported as a regulatory signaling pathway in different GBM sub-types (Verhaak RGW 2010, Turcan S 2012, Carro 2010, Bhat KPL 2011, Bozdag S 2014).

Besides these oncogenic pathways, some transcriptional regulators are linked with GBM progression, such as POU3F2, SOX2, SALL2, and OLIG2. These neural-developmental transcriptional factors regulate the (de)differentiation of cancer-propagating cells (Suva, 2014). OLIG2 (Oligodendrocyte lineage genes-2) is a key regulator transcriptional factor of oligodendrocyte precursor cells (OPC) differentiation and proliferation (Lu QR, 2002). Interestingly, OLIG2 was found as ubiquitously expressed in glioma cells and plays an important role in glioma initiation and tumor progression Kupp et al., 2016; Ligon et al., 2004-2007; F. Lu et al., 2016; S. K. Singh et al., 2016). Deletion of *Olig2* resulted slow-growing tumor cells and decreased the PDGFRa expression in murine GBM model (Lu, F 2016). Additionally, knockdown of OLIG2 downregulated the PDGFRa signaling in human GBM cell lines (Kupp 2016). Similarly, OLIG2 function is dependent on the mutant p53, suggesting it negatively regulates p53 and p21 tumor suppressor genes.

One of the mechanisms controlling the expression of transcriptional regulators is RTK signaling. For example, SOX2 and OLIG2 are elevated by EGFRvIII oncogenic signaling [18]. These findings suggest that glial lineage specific transcriptional factors play key role in oncogenic re-programming in glioma **(Figure 1.2)**.

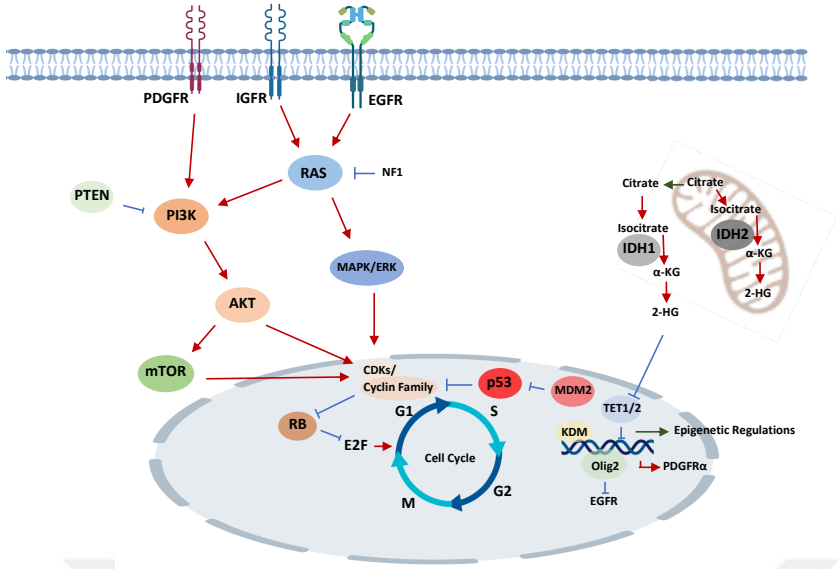


Figure 1.2. Oncogenic pathways in GBM. (Adapted by Lu, 2018, and Weinberg, 2014.)

1.3 Treatment of GBM

Treatment of gliomas is extremely difficult and one of the biggest challenges in oncology [5]. There are several factors for these difficulties. First, GBM is a heterogenous tumor that easily acquires resistance to conventional therapies. Second problem is the blood-brain barrier (BBB). The BBB permeability allows very limited delivery of chemotherapy drugs into the brain, therefore most of the novel anti-cancer drugs cannot be used in glioma therapy. Also, limited repair capacity of brain decreases the therapy options [31].

Standard of care for GBM involves maximal tumor resection, radiotherapy and chemotherapy [32]. Standard chemotherapy drug in clinical use is Temozolomide (TMZ), a DNA alkylating agent approved by FDA in 2005 [33]. TMZ causes cell death by generating of O6-methylguainine in DNA, resulting missmatches with thymine during the DNA replication. These miss-pairs cause double-strand breaks leading to apoptosis [7]. Also, TMZ can pass the BBB, is much more able to penetrate into the core regions of tumors and has fewer side effects. Therefore, it is preferred in GBM therapy [7]. However, resistance to TMZ is frequently seen in GBM patients.

Despite the recent advances in these therapies, tumor recurrence with a therapy-resistant state is very common [34]. Aggressive phenotype of tumor as well as the complex structure of brain leads to poor prognosis in GBM patients. For this purpose, new therapeutic options are necessary for GBM therapy.

1.3.1 Targeted therapies in GBM

New discoveries focus on the targeted therapies to overcome the therapy resistance in cancer in recent years. The common altered molecular mechanisms have become the first line choices of targeted therapeutics.

1.3.1.1 Targeting growth factor receptors and ligands

Growth factor receptors are relatively easy to target, because of their extracellular components, making the access with small molecules and monoclonal antibodies (mAb) possible. mAbs can target either the transmembrane RTK or growth factor ligands. When they bind, they can inhibit the signaling pathway and induce cell death. Pharmaceutically developed small molecules can penetrate the cell membrane and inhibit the enzymatic activity of tyrosine kinase domain of RTKs [35].

EGFR is frequently mutated or amplified receptor in GBM, therefore it is a potential target for therapy. Recent clinical trials on EGFR status of GBM involve both mAbs and small molecules. Cetuximab is a monoclonal antibody that target the receptor dimerization of EGFR. Small molecules, Gefitinib (AstraZeneca, USA) and Erlotinib (Genentech, USA), are tyrosine kinase inhibitors and prevent the phosphorylation of EGFR and inhibit downstream signaling. These molecules have been tested alone or in combination with TMZ for GBM therapy [36,37].

1.3.1.2 Targeting of angiogenesis

Malignant gliomas have high angiogenesis capability. Bevacizumab is the only approved mAb by FDA for recurrent GBM therapy [38]. Bevacizumab targets vascular endothelial growth factor (VEGF) ligand to inhibit its binding to receptor (VEGFR). AZD2171 (AstraZeneca, USA) and Vatalanib (Novartis, Switzerland) are other VEGFR inhibitors currently in clinical trials for GBM [39]. Sorafenib and Pazopanib are small

molecule inhibitors of PDGFR and VEGFR tried in GBM, however there is has been no significant benefits for therapy [35]. Imatinib (Novartis, Switzerland) is a tyrosine kinase inhibitor and also tried for glioma, however, it was not successful in clinic [40]. Clinical trials of Bevacizumab and Irinotecan combination showed improvement of progression-free survival and overall median survival in high grade gliomas [41,42], however severe side effects and development of resistance were reported for long term use of Bevacizumab [43,44]. These findings suggest that simultaneously targeting multiple pathways with combinational therapies might be beneficial, however long-term effects need to be comprehensively analyzed.

1.3.1.3 Targeting intracellular pathways

Most of the malignant gliomas have several altered intracellular effectors such as RAS, PI3K, and PTEN [40]. For this reason, targeting these intracellular pathways became potential therapy approaches in GBM. Several PI3K, mTOR, and MAPK pathway inhibitors were evaluated in clinical trial studies alone or in combination with TMZ, or other anti-cancer drugs in GBM. [4546]. DNA repair and cell cycle pathway are other important targets for GBM therapy. P53 activation or MDM2 inhibition have recently been a center of attention. However, poor BBB penetration problem has been a disadvantage for these drugs as well [47]. Although most of these studies resulted as negative, they carry promising perspectives for the future of targeted therapies [48].

1.3.1.4 Proteasome inhibitors

Ubiquitin-proteasome system plays a vital role for cellular homeostasis by regulating protein balance in cell. Bortezomib is a proteasome inhibitor that is approved for clinical use [49,50]. Many studies showed the efficacy of combinatory treatment with Bortezomib and other chemotherapy drugs or apoptosis inducers in GBM cell lines [51–53].

1.4 APOPTOSIS

Apoptosis is an indispensable physiological process of embryonic development and adult tissue homeostasis. The "apoptosis" (a-po-toe-sis) term was first used by Kerr et. al. to describe a new type of cell death, and was characterized by distinct morphological changes of dying cells [54]. The programmed cell death term is used for apoptosis for several reasons: the cell death is programmed for embryonic development, and the cellular death process is controlled by different mechanisms [55]. Apoptosis causes morphological changes in dying cells, like cell shrinkage, plasma membrane blebbing, and chromatin condensation, which result in the separation of apoptotic bodies [56]. Disruption of the balance between the cell survival and death mechanisms causes deregulation of apoptosis, therefore uncontrolled cell proliferation leads to cancer development. These controlled mechanisms are well-characterized in mammalian cells and grouped as two main apoptotic pathways. The first one is the extrinsic pathway which starts with the death receptor activation, a subgroup of the tumor necrosis factor (TNF) receptor superfamily. The second mechanism is the intrinsic pathway, also known the mitochondrial pathway, which is controlled by the Bcl-2 family proteins [57]. Both of these pathways cause the caspase cascade activation with first "initiator", then "effector" caspases. Caspases which are endoproteases, hydrolyze cysteine dependent, aspartate specific peptide bonds. Caspases are classified by their roles in apoptosis, and in inflammation (caspase-1, -4, -5, -12) in humans. Apoptotic caspases (caspase-3, -6, -7, -8, -9, -10) are grouped by their mechanisms, as either initiator (caspase-8, -9, -10) or executioner (caspase-3, -6, and -7) caspases. Initially, caspases are in procaspases form, then are activated by cleavage. Additionally, different caspases have different protein-protein interaction domains. Caspase-1, -2, -4, -5, -9 have a caspase recruitment domain (CARD), and caspase-8 and caspase-10 contains a death effector domain (DED) [58,59].

1.5 TRAIL and TRAIL receptors

Tumor necrosis factor-related apoptosis-inducing ligand (TRAIL) was discovered as a new member of TNF superfamily proteins [60,61]. TRAIL is a type II transmembrane protein and its sequence is homologous with the extracellular domain of TNF and CD95 ligand (Fas-L) (23% and 28%, respectively). TRAIL forms a homotrimer and binds to TRAIL receptors expressed on cell surfaces, and trimeric-form enhances the biologic activity as compared to monomeric form [61].

TRAIL interacts with five receptors, including death receptors (DR4/TRAIL-R1/TNFRSF10A and DR5/TRAIL-R2/TNFRSF10B) and decoy receptors (DcR1/TRAIL-R3/TNFRSF10C and DcR2/TRAIL-R4/ TNFRSF10D) [62–64]. In addition to these receptors, osteoprotegerin (OPG, a RANK ligand inhibitor), a soluble receptor, is another TRAIL-binding receptor with low affinity [65]. After TRAIL binding to death receptors, DR4 and DR5, oligomerize and apoptotic signaling starts. However, decoy receptors, DcR1 and DcR2, cannot transduce apoptotic signals; because DcR1 has not cytoplasmic domain, it binds to membrane via only glycosylphosphatidylinositol (GPI) anchor, and DcR2 has non-functional death domain. Competition that occurs at the receptor binding level is involved in apoptotic resistance. [66].

1.5.1 TRAIL Signals

1.5.1.1 Apoptotic signaling

The first step of induction of apoptosis via extrinsic pathway is the binding of TRAIL to death receptors on the cell surface. After the binding of TRAIL to death receptors, conformational changes are induced at death domains of receptors; and following oligomerization and clustering, functional activation occurs. The first affected member is Fas-associated protein with death domain (FADD) interacting with death domains that plays an adaptor role. FADD is also required for activation of pro-caspase-8/-10 via death effector domains. These protein complexes are called Death-inducing signaling complex (DISC) and they activate initiator caspases. As a result of this activation, caspase cascade auto-activation and cellular apoptosis process are induced. Cellular FLICE-like inhibitory protein (c-FLIP) is another death effector protein binding to FADD. Also, c-FLIP is one of the major inhibitor proteins of extrinsic pathway of cell

death, because c-FLIP has three different isoforms: c-FLIP$_S$, c-FLIP$_L$ and c-FLIP$_R$. c-FLIP$_S$ and c-FLIP$_R$ show a strong homology to caspase-8 and c-FLIP$_L$ is catalytically inactive. The targets of active caspase-8/-10 are other caspases including pro-caspase-3 and many structural and regulatory proteins. The activation of caspases results in DNA fragmentation and nuclear shrinkage and membrane blebbing, which are hallmarks of apoptosis. In addition, the active caspase-8/-10 is able to activate Bid (BH3-interacting domain death agonist), which is a pro-apoptotic Bcl-2 (B-cell CLL/lymphoma 2) member. Bid activation occurs through cleavage of Bid into form called truncated Bid (tBid). Bid cleavage plays a primary role in type II cells for enhancing intrinsic pathway by binding BAX (Bcl-2-associated X protein) and BAK (Bcl-2 homologous antagonist killer). After BAX and BAK oligomerization and translocation to the mitochondrial outer membrane, the mitochondrial membrane potential decreases and the outer membrane permeabilization (MOMP) occur. Cytocrome c and Smac/DIABLO (Second mitochondrial-derived activator of caspases/direct inhibitor of apoptosis-binding protein with low PI) are released to cytoplasm because of MOMP. Cytochrome c binds to APAF-1 (Apoptotic peptidase activating factor 1) with ATP. This complex is called "apoptosome" and it is necessary for activation of pro-caspase-9. Active caspase-9 activates caspase-3, -6 and -7. There are some inhibitors of executioner caspase activation or/and their activity, such as Inhibitor of Apoptosis Proteins (IAPs). XIAP (X-linked IAP), c-IAP1 and c-IAP2 (cellular-IAP-1, -2) and survivin are important IAP family members, and these members can directly inhibit caspase-3/-7 activation or block apoptosome activation [66,67] **(Figure 1.3)**.

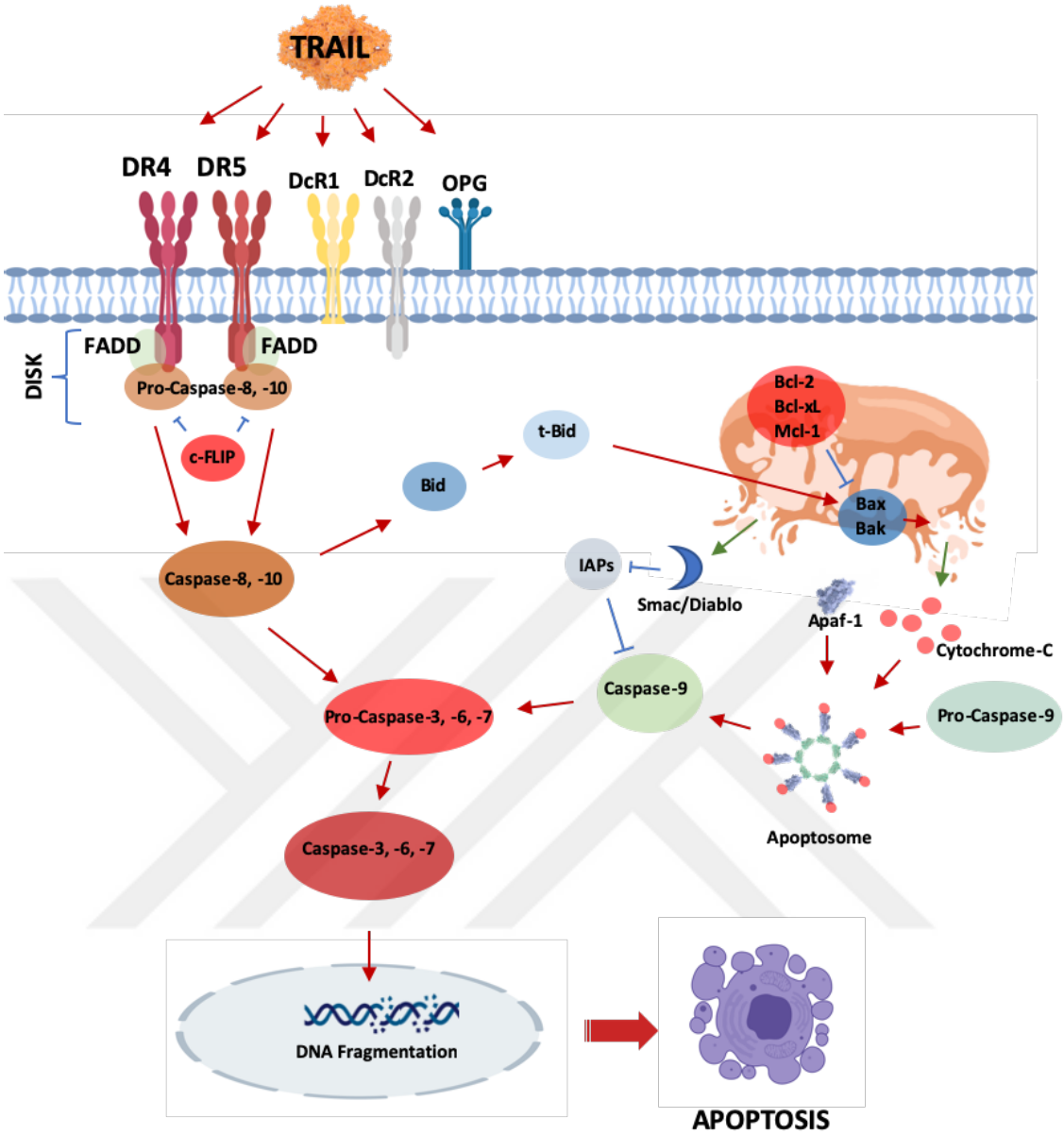


Figure 1.3 Signaling pathways of TRAIL-induced apoptosis. (Adapted by Karstedt, 2017.)

1.5.2 TRAIL resistance

Most malignant tumors exhibit resistance to TRAIL-induced apoptosis. TRAIL resistance can occur due to deregulation in different components of apoptosis. For example, expression levels of death receptors, upregulation of c-FLIP and apoptotic inhibitory proteins, or deterioration of pro-/anti-apoptotic Bcl-2 protein balance can cause to TRAIL resistance.

1.5.2.1 TRAIL resistance caused by death receptors and DISC

Surface expression levels of death receptors affect binding of TRAIL to the cell. Some researchers suggest that, TRAIL resistance can occur by lack of DR4 and DR5 expression. For example, Horak et al. showed that epigenetically silenced DR4 expression correlated with TRAIL resistance in ovarian cancer [68]. Similarly, TRAIL resistance was determined to be caused by loss-of-function mutations in DR4 and DR5 in breast cancer, head and neck squamous cell carcinoma, and non-Hodgkin's lymphoma. Also, ratio of death receptors and decoy receptors expressions competitively affects TRAIL-induced apoptosis [66,69]. Post-translational modifications such as O-glycosylation [70], S-palmitoylation [71] of DR4 and DR5 change the receptor structure, therefore TRAIL cannot ligate to receptors and apoptotic signal cannot be initiated.

As a caspase-8 homolog, c-FLIP can bind to FADD by competition with pro-caspase-8, and TRAIL-induced apoptosis is inhibited [72]. There is an interaction between c-FLIP and cell survival related pathways such as NF-κB and ERK and it promotes cell survival by these pathways' activation [73]. In contrast, c-myc directly represses the c-FLIP transcription and sensitizes $Bax^{-/-}$ cells to TRAIL induced apoptosis [74].

1.5.2.2 Resistance caused by deregulation of mitochondrial components

The intrinsic apoptotic pathway is the dominant pathway in type II cells for TRAIL-induced apoptosis. Although mitochondria is active in both cell types, it is not required for the apoptosis of type I cells [75,76]. Bid plays a bridge role between these two pathways and Bax is required for activation of pro-apoptotic Bcl-2 proteins in TRAIL-induced apoptosis via intrinsic pathway [72]. The ratio between pro- and anti-apoptotic proteins is critical for cell death or surviving. Song and colleagues showed that Bcl-xL overexpression increased TRAIL resistance and cells were resensitized to TRAIL when Bcl-xL was knockdown in prostate carcinoma cell lines [77]. Similarly, other anti-apoptotic proteins, including Bcl-2, Mcl-1 were reported for TRAIL resistance.

Another important group is IAP family for inhibition of TRAIL-induced apoptosis. High XIAP expression made resistant cells to TRAIL; conversely, inhibition of IAP members restored TRAIL sensitivity has been reported [66].

1.5.2.3 Resistance caused by epigenetic regulations

Epigenetic regulation of genes plays important role in cancer. Histone modifications, loss and gain-of-methylations of DNA involve to epigenetic mechanisms. Deregulation of gene expression is achieved by DNA methylations, particularly with the hypermethylation of important regions of genes, such as CpG islands and promoters [78–80]. Another way of epigenetic regulation is upregulation of histone-deacetylases (HDACs) [81]. The relationship between TRAIL resistance and epigenetic silencing has been showed. For example, epigenetic silencing of DR4 leads to TRAIL resistance in ovarian cancer [68]. Additionally, caspase-8 inhibition by DNA methylation caused TRAIL resistance in medulloblastoma [82]. Recently, using some HDAC inhibitors combined with TRAIL restored to TRAIL sensitivity in different type of cancers [83–87] **(Figure 1.4)**.

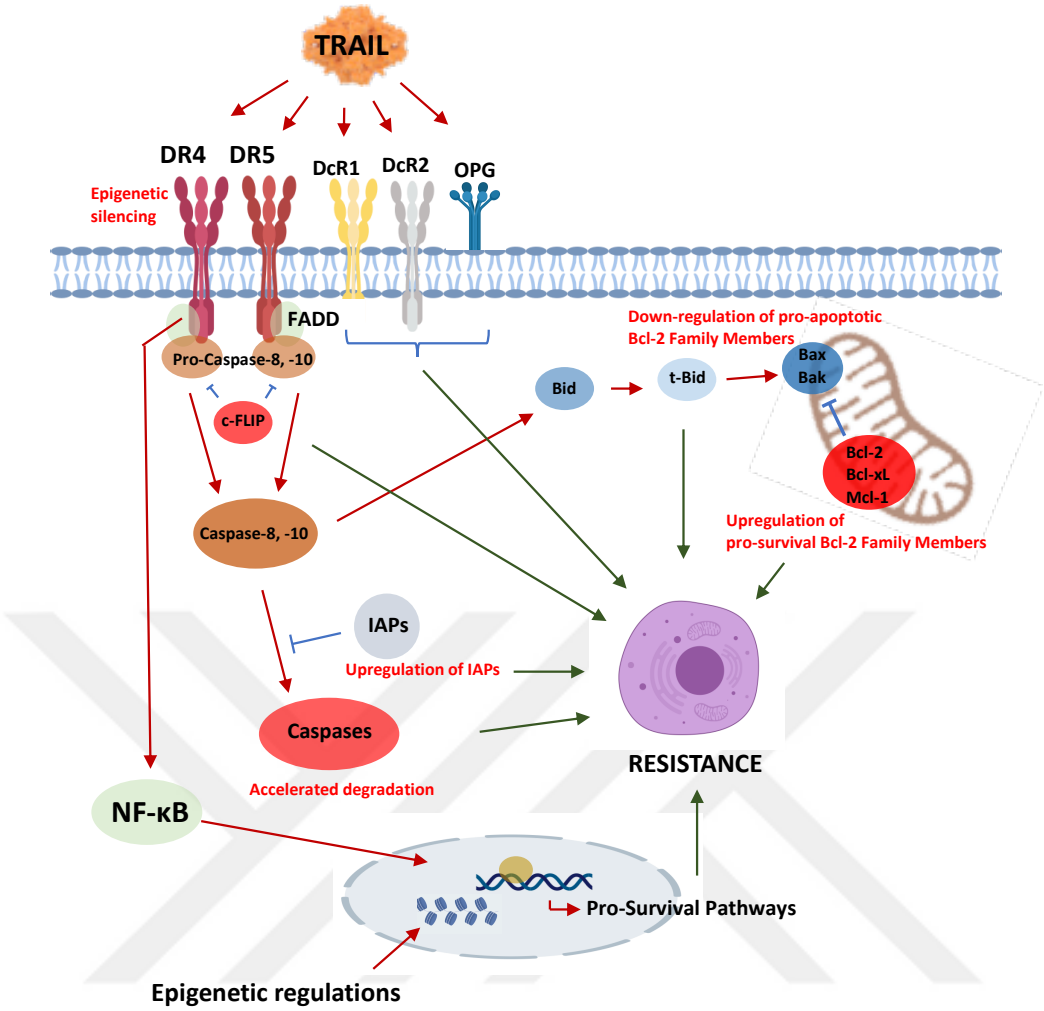


Figure 1.4. Mechanisms of resistance to TRAIL. (Adapted by Mellier, 2010.)

1.5.3 TRAIL Therapy

TRAIL has been a prime candidate for cancer therapies. Because of the short half-life of TRAIL, many recombinant versions have been created to increase the therapeutic potential of TRAIL. Naked (untagged) soluble human TRAIL has an approximately 30 min half-life in serum, and systemically administered TRAIL is rapidly removed from the body in short time [88]. New delivery options or modifications on TRAIL molecule can improve the half-life in circulation and the tumor-killing property. One of the new approaches for modification on TRAIL is noncovalent tags, such as FLAG tag [89], leucine/isoleucine zipper tag [90,91], or tenascin-C oligomerization domain [92]. All of these modifications reduce the degradation of TRAIL in circulation and enhance the biological activity. Additionally, covalently linked molecules such as serum albumin increase the

half-life of recombinant TRAIL *in vivo* [93]. Similarly, nanoparticles are another strategy for maintaining the TRAIL activity for long term [94–96].

Another problem for TRAIL therapy is the delivery of TRAIL to complex organs such as brain, or tumor site. Viral delivery or stem cell-based delivery options are some approaches to overcome this problem. Adeno-associated viruses (AAV), adenoviruses (AV), lentiviruses (LV), and oncolytic herpes simplex viruses (oHSV) have been used for viral delivery of TRAIL. Targeted delivery of TRAIL using engineered stem cells that express and release TRAIL within tumor site has been an effective approach [97]. Indeed, there have been several studies that showed the efficacy and success of stem-cell delivered TRAIL in preclinical GBM models [98,99].

1.5.3.1 TRAIL in clinical trials

Targeting of TRAIL receptors with different agents are promising candidates for TRAIL therapy in clinic. Both death receptor agonists (DR4 monoclonal antibody (mAb) agonist Mapatumumab [100] and DR5 mAb agonists Tigatuzumab, Apomab and Lezatumumab [101–103] and soluble recombinant TRAIL (Dulanermin) [104] are single agents in Phase I clinical trials for solid tumors. Mapatumumab monotherapy, the most promising agent, entered the Phase II trial for non-Hodgkin lymphoma with response of one third of enrolled patients [105].

Combination therapies with different agents passed the Phase I-b trials and entered the Phase II, and sponsored by different companies such as Genentech, Amgen and GlaxoSmithKline. As an example of combination trials, conatumumab (AMG655) is a DR5 mAb and used in combination with FOLFOX6 (folinic acid, 5-fluorouraci, and oxaplatin), and bevacizumab (Avastin, an angiogenesis inhibitor) in colorectal carcinoma (NCT00625651), lymphoma, and non-small cell lung cancer patients (NCT01327612). Also, conatumumab and FOLFIRI (folinic acid, 5-fluorouraci, and irinotecan) combination has been started for trials in colorectal carcinoma patients (NCT00813605) [98]. Clinical trials of combination with FOLFOX6 in colorectal cancer patients were completed, however any significant outcomes has not been reported in progression-free survival. Other studies are currently in clinical trials for different cancer types [106].

Additionally, new clinical trials with mesenchymal stem cell expressing TRAIL (NCT03298763) and recombinant-TRAIL (NCT03443674) has been started in recent years. These studies are promising and will help to overcome of delivery and resistance of TRAIL.

1.6 Tumor heterogeneity in GBM

Tumor heterogeneity is the biggest challenge of the clinical success. Stochastic events affect the clonal growing populations, therefore cells within the same tumor bulk exhibit different properties. Intra-tumoral heterogeneity confers an advantage to survival against microenvironmental fluctuations and generate resistance to chemo-and radio-therapy [107].

There are two key models that helps to understand tumor heterogeneity: Cancer stem cell (CSC) model (the hierarchy model), and clonal evolution model (the stochastic model). In CSC model, tumor population is rooted from a single cancer stem cell, which has self-renewal and differentiation capacity. CSCs generate differentiated tumor cells by asymmetrical division, and accumulated mutations cause heterogeneity. In clonal evolution model, heterogeneity is dependent on randomly acquired mutations during cell division. “Driver” mutations as a result of DNA damage confer malignant advantages to cells and accumulation of these mutations cause a serious cancerous phenotype [22,107,108].

Brain tumors are among the highly heterogeneous cancers; and defining of driver oncogenes and cell of origins are difficult. Recently, the CSC model has been used for explaining the cancer initiation theory in GBM. Glioma cancer stem cells were defined by CD133 (prominin-1) cell surface expression marker and not expressing of this marker was thought to be attributed to the lack of tumor generation capacity [109]. Moreover, CD44 and Id1 were associated with glioma stem-like phenotype [110]. On the other hand, a study showed that CD133 negative cells formed tumors in mice, suggesting that the new markers are needed for identifying the heterogenous nature of GBM **(Figure 1.5)**.

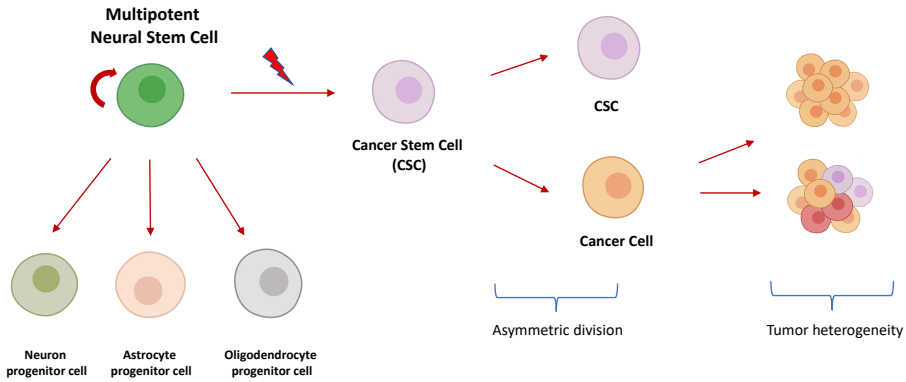


Figure 1.5. Hierarchical model for GBM tumor evolution. (Adapted by Lu, 2019.)

Classification of tumors can help the understanding of heterogeneity. New techniques used in molecular biology, such as RNA sequencing or single-cell sequencing, revolutionized our understanding of tumor heterogeneity by providing a new level in genomic and transcriptomic analysis. GBMs are classified into four molecular subtypes, depending on the gene expression profiles: proneural, classical, neural, and mesenchymal. The proneural GBMs have oligodendrocyte precursor cell gene signature and PDGFRa amplification, TP53 and/or IDH mutations. The classical subtype has astrocyte (CD44+) gene signature, and EGFR activation and CDKN2A loss. The mesenchymal GBM subtypes have astrocyte and microglia signatures, TNF-a and NF-kB activation and NF1 deletion [111]. There are some speculations about the neural GBM subtype that to be contaminated with normal brain tissue sample profiles [112]. Additionally, TNF-a treated proneural glioma stem cells shifted to mesenchymal state with CD44 expression, and activation of NF-kB, suggesting tumor microenvironment plays a role in transition between states [22,113]. Barcoded primary GBM cell experiments in xenograft models showed that tumors developed with hierarchy model from slow-cycling GBM stem-like cells to rapid growing progenitors [114].

Additionally, single cell studies revealed detailed molecular landscape, characterizing the heterogeneity between tumor samples, somatic mutation pattern, DNA methylation profiles, and copy number alterations in GBM. However, roots of tumorigenicity and lineage tracing are still unknown and needed to be identified in GBM [22].

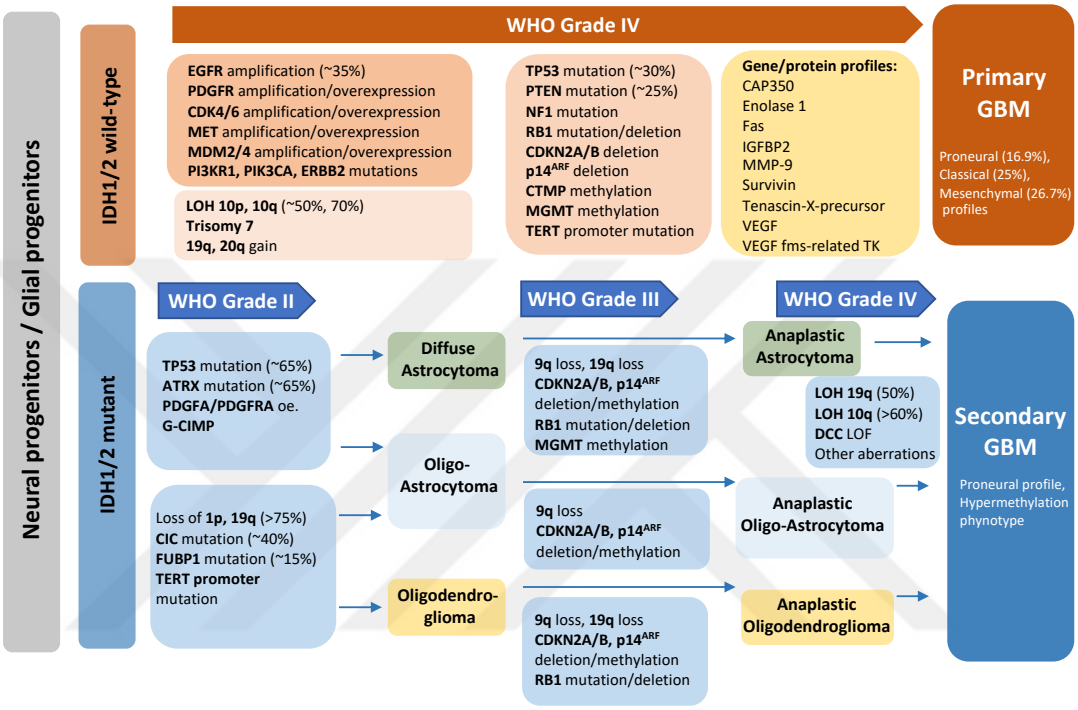


Table 1.1. Genetic alterations in different grades of GBM. (Adapted by de Vleeschouwer, 2017; and Lu, 2019.)

1.7 Therapy resistance

One of the main approaches to cancer therapy is chemotherapy. Many different types of chemotherapeutic agents are used in cancer, such as DNA alkylating agents, RTK inhibitors, anti-metabolites, microtubule target agents, platinum-based compounds, and etc. However, intrinsic structure of cancer cells or acquired resistance to chemotherapy is the major problem for the effective treatment [115].

Drug resistance is an unwanted but common phenomenon observed in cancer. Although initial state of many types of cancer are susceptible to anti-cancer drugs, they can develop resistance to only specific drugs or multiple drugs during the treatment. Several factors play key roles in developing drug resistance in cancer, these are DNA mutations, epigenetic and metabolic changes, cell death inhibition, drug efflux, epithelial to mesenchymal transition, and drug inactivation [116]. Drug resistance can be innate, which is present within the tumor from the beginning, or acquired resistance, which is developed during the treatment.

One of the reasons for the therapeutic resistance of GBM is intratumoral heterogeneity [11,117,118]. Indeed, large scale genetic and epigenetic variety can be observed within the resistant "drug-tolerant" cell populations [119,120]. Therefore, the acquired therapy resistance might be a consequence of both the clonal expansion of already existing resistant tumor cells and the acquisition of resistant state during the treatment period. However, the mechanisms behind acquired TRAIL resistance in GBM cells have not yet been resolved.

1.7.1 Acquired resistant models for TRAIL

When clonally growing drug sensitive populations are exposed to apoptosis inducers such as TRAIL, a subset of cells can be affected and undergo apoptotic cell death. The heterogeneity of such cells has previously been studied and interestingly, these dying cells exhibited heterogeneity in the time required for apoptotic execution. The variability range was from 40 mins to more than 12 hours [121]. This "fractional killing" arose from the different levels of pro- and anti-apoptotic proteins [122,123].

Flusberg et. al. examined the cause of fractional killing to TRAIL-induced apoptosis. Upon exposure to TRAIL for 6 hours, surviving tumor cells exhibited short term resistance phenotype for 1 day, but then reset to the naïve state within several days in culture. Also, their survivors were resistant to second TRAIL application at 24 hours later, however resistance of survivor cells disappeared in following days. Additionally, they showed the NF-kB mediated inflammatory phenotype was activated, and suggesting that this transient resistance was caused by inflammatory response of cells [124].

In another study, researchers generated acquired TRAIL resistance in prostate and pancreatic carcinoma cells within 1 day. First, they treated cells with TRAIL for 4 hours, then detached cells were removed and attached cells were cultured from 4 hours to 6 days. When they re-treated cells, they saw that TRAIL resistance phenotype of attached cells decreased in 6 days. Here, the development of short-term resistance involved the induction of Bcl-xL expression [77].

Similar to our work, TRAIL-resistant ovarian [125], breast [126], or lung cancer cell lines [127,128] were generated through long-time exposure to TRAIL but these cells were then maintained in the presence of TRAIL. In our work, the "persistent resistant" cells could be maintained in conditions devoid of TRAIL, suggesting heritable molecular alterations causing resistance.

2 MATERIALS AND METHODS

2.1 Cell Culture

A172, LN18, T98G, and U87MG GBM cell lines and 293T human embryonic kidney cells were purchased from American Tissue Type Culture Collection (USA). All cells were cultured in DMEM medium (Gibco, USA) with %10 fatal bovine serum (Gibco, USA) and %1 Penicillin-Streptomycin (Gibco, USA) in a 37ºC humidified incubator with 5% CO2.

2.2 Production of TRAIL protein

In order to produce TRAIL, 293T cells were seeded as 2,5 $X10^6$ cells/10 cm plate. Following day, cells were transfected with TRAIL vector expressing a secretable form of TRAIL protein. For trasnfection, Fugene mixture containing 20 ul Fugene Transfection Reagent (Promega, USA) and 180 ul OptiMEM (Promega, USA) and DNA mixture containing 5 ug TRAIL vector in 200 ul OptiMEM were prepared for each plate. DNA and Fugene mixtures were mixed and incubated for 30 minutes at room temperature, then added to plates as drop by drop. Next day morning, medium was changed with 8 ml serum-free medium. The following two days, culture mediums were collected and replaced with 8 ml serum-free medium. After the 2^{nd} collection, TRAIL was concentrated using spin filter columns (Millipore, USA) at 4^o C, 3750 rpm for 20 min. Concentrated TRAIL was stored at -80^o C and measured by using TRAIL Human ELISA Kit (Abcam, USA).

2.3 Cell viability

Cell viability was tested by Cell Titer-Glo® (CTG) Luminescent Cell Viability Assay (Promega, USA). CTG is an ATP based assay and measures the number of viable cells via luciferase reaction by using ATP. CTG assays were performed in the 96 well black plates. Cells were seeded as 10.000 cells/well. Next day, cells were treated with TRAIL and/or other drugs for defined time points. After the treatment, medium was removed and, and CTG mixture (1:10 with medium) was added into the wells. The plate was read at 560 nm wavelength by Synergy H1 Reader (Biotek, USA). Survival was

described as the percentage of viable cells in the treated sample compared to untreated control samples. All experiments were performed in triplicates.

2.4 Caspase 3/7 Activity and Caspase Inhibition Assay

Caspase 3/7 Activity was measured by using Caspase 3/7 Activity Assay Kit (Promega, USA). Cells were seeded into black 96 well plate as 10.000 cells/well. Next day, cells were treated with TRAIL and/or drugs in 40 ul medium/well. After the 3 hours incubation, 17 ul of the Caspase-Glo® 3/7 reagent was added to each well and caspase activity was measured at 560 nm by Synergy H1 Reader (Biotek, USA). For caspase inhibition assay, cells were pre-treated with Z-FA-FMK (Negative Control for Caspase Inhibitors) or Z-VAD-FMK (General Caspase Inhibitor) at 20 μM final concentration for 24h before following drug treatments. All experiments were performed in triplicates.

2.5 Real-time Cell Growth Analysis

xCELLigence RTCA SP Station and Analyzer (ACEA Biosciences, San Diego, CA, USA) was used for real-time cell growth analysis. E-plate 96, electrode array covered special plates was used in this system. 100 ul culture medium was loaded into each well of E-plate 96 and the plate put into the RTCS SP Station for background impedance measurement. Then, all cells were seeded as 2500 cells in 100 ul medium per well on E-plate 96, and plate was incubated for 30 minutes for settlement of cells. Following the incubation, plate was put again in the station and impedance of the wells were measured with 30 min intervals for 100 h. After 24 h cell seeding TRAIL was added into the wells. The cell growth was analyzed using the RTCA Software (ACEA Biosciences).

2.6 Live Cell Imaging

Live-cell imaging experiments were performed by Olympus Xcellence Pro inverted microscope (Center Valley, PA, USA) with a x10 air objective in a chamber at 37°C, supplied with 5% CO_2. Cells were seeded as 25.000 cells/well on 24-well plates and treated with TRAIL and Bortezomib. Time-lapse images were captured after drug treatments with certain time intervals (5 mins). Random positions were recorded from each well and live cells in each image were counted using the ImageJ Software (NIH

Image, Bethesda, MD, USA). Quantifications were performed by counting 9 different image fields for each condition for selected time points. Live cell imaging was performed in collaboration with Fidan Şeker.

2.7 YO-PRO-1/PI Staining

Cells were seeded as 50.000 cells/well on 12-well plates. TRAIL treatments (50 ng/ml) were performed for 3hr. Wells are rinsed once with PBS followed by incubation in 300 µl staining solution (1µM YO-PRO-1 by Invitrogen Cat. No: Y3603, Thermo Fisher, USA and 1:1000 PI (1mg/ml) in PBS) for 15 min at 37^0C in dark. Each well was imaged by Nikon Eclipse TS100 Inverted Fluorescence Microscope (Nikon Instruments Inc.,NY,USA). Quantification of images was done with ImageJ software (NIH Image, NIH Bethesda, USA). Yo-Pro1/PI staining was performed in collaboration with Ezgi Özyerli-Göknar.

2.8 Cell Cycle Assay

For cell cycle measurement, cells were harvested from 6-well plates (300.000 cell/well) and pellets were washed in cold PBS. Pellets were resuspended with cold EtOH (70%) and incubated at 4°C for 30 min following by fixation. Samples were centrifuged and washed with PBS for 2 times, then resuspended in 50 ul PBS containing RNase A (100 ul/ml), and incubated at room temperature for 15 min. PI (50 ul/ml) was added in 200 ul PBS, and incubated at room temperature for 30 min. Stained cells were analyzed by BD Accuri C6 (BD Biosciences, USA) flow cytometer and 10.000 events were recorded for each sample.

2.9 Cloning

2.9.1 shRNA Cloning

shRNAs were designed using RNAiCodex program [129], and oligo sequences are listed below. Oligos were PCR-amplified by using following primers having compatible restriction ends with backbone vector, pSMP. F: 5'GATGGCTGCTCGAGAAGGTATATTGCTGTTGACAGTGAGCG-3', R: 5'-CCCTTGAACCTCCTCGTTCGACC-3'. PCR products were cloned into pSMP retro-viral backbone as described [130]. All vectors were verified by sequencing. Firefly luciferase was used for shRNA control.

sh-Bcl-XL:
TGCTGTTGACAGTGAGCGAGCTCACTCTTCAGTCGGAAATTAGTGAAGCCA
CAGATGTAATTTCCGACTGAAGAGTGAGCCTGCCTACTGCCTCGGA

sh-Bcl-2:
TGCTGTTGACAGTGAGCGAGGAGATAGTGATGAAGTACATTAGTGAAGCCA
CAGATGTAATGTACTTCATCACTATCTCCCTGCCTACTGCCTCGGA

sh-IGFBP-2:
TGCTGTTGACAGTGAGCGCGCAGACAATGGCGATGACCACTAGTGAAGCCA
CAGATGTAGTGGTCATCGCCATTGTCTGCATGCCTACTGCCTCGGA

2.9.2 Overexpression vectors:

pLEX307-HES1 vector cloning:

Gateway cloning was performed from pDONR221_HES1 (DNASU Plasmid #HsCD00043345) to take pLEX_307 lentiviral expression vector (Addgene plasmid #41392). Vector was verified by sequencing.

2.9.3 gRNA cloning

In order to deplete the expression of desired genes with CRISPR/Cas9 method, gRNAs were either derived from Gecko v2 library [131] or designed against functional domains of genes using CCtop tool [132]. All gRNA sequences are presented in **table 2.1.** For cloning, top and bottom strands of gRNA against target genes were annealed and used for ligation into pLenti-CRISPR-V2 vector, which was digested by BsmB1 followed by Antarctic phosphatase treatment. Ligation was performed at RT for 15 minutes using Quick Ligase Kit (Roche, Switzerland) and ligation product was heat shock transformed to competent bacteria Stbl3. After growing and selecting in LB, plasmid isolation and diagnostic digestion was performed by MN miniprep kit, and plasmids were sent for sequencing. The efficiency of gRNAs was verified with western blotting. gRNA cloning was performed in collaboration with Ezgi Özyerli-Göknar.

Gene	Sequence	
gDR5-1	F	CACCGTTCCAGAGCTCACAACGACC
	R	AAACGGTCGTTGTGAGCTCTGGAAC
gDR5-3	F	CACCGAGATACTCACGATCTCATTG
	R	AAACCAATGAGATCGTGAGTATCTC
g-NT1	F	CACCGACGGAGGCTAAGCGTCGCAA
	R	AAACTTGCGACGCTTAGCCTCCGTC
PPARGC1A-1	F	CACCGTGAACTAGATGTGAACGACT
	R	AAACAGTCGTTCACATCTAGTTCAC
PPARGC1A-2	F	CACCGGCTTTCTGGGTGGACTCAAG
	R	AAACCTTGAGTCCACCCAGAAAGCC
MEST-1	F	CACCGCTTTGGCTTCAGTGACAAAC
	R	AAACGTTTGTCACTGAAGCCAAAGC
MEST-2	F	CACCGGAAGTTCAGAAGGCGCTGGG
	R	AAACCCCAGCGCCTTCTGAACTTCC
DAAM2-1	F	CACCGCATCGACCGCATCAATTCCA
	R	AAACTGGAATTGATGCGGTCGATGC
DAAM2-2	F	CACCGGAGTCTGTACGCGTTTGATG
	R	AAACCATCAAACGCGTACAGACTCC
CXCL14-1	F	CACCGGCACCAAGCGCTTCATCAAG
	R	AAACCTTGATGAAGCGCTTGGTGCC
CXCL14-2	F	CACCGGCCAAAGTACCCGCACTGCG
	R	AAACCGCAGTGCGGGTACTTTGGCC

Table 2.1. List and DNA sequences of gRNAs used in CRISPR/Cas9 experiments.

2.10 Viral Packaging and Transduction

All viral packaging was performed as described [87,130]. Briefly, 2.5x10^6 293T cells were seeded on 10 cm culture dish with DMEM supplemented with 10% FBS and 1% Pen/Strep on day 0. Next day, viral plasmid DNA (2,5 µg) and packaging plasmids (8.2Dvpr and VSVG) (2,5 µg) were mixed and transfected to cells using Fugene HD reagent (Promega, USA). Next day, medium was changed. 48- and 72-hours post transfection, virus containing medium was collected and filtrated by 0.45 µm filters. Filtered viral containing media was aliquoted and stored at -80°C freezers.

For viral transduction, cells were seeded at desired density to tissue culture plates and next day were transduced with virus containing media supplemented with protamine sulfate (10µg/ml). 16 hours post-transduction, viral medium was replaced by fresh media. Next day, transduced cells were selected by Puromycin (2 µg/ml) for 3 days. All lentiviral or retroviral vectors used in this study are listed in **table 2.2.**

Vectors	**Cat. No**
pUMVC	Addgene Plasmid #8449
pCMV-dR8.2 dvpr	Addgene Plasmid #8455
pCMV-VSV-G	Addgene Plasmid #8454
3544 pMIG Bcl-2	Addgene Plasmid #8793
3541 pMIG Bcl-XL	Addgene Plasmid #8790
pBABE GFP-puro	Addgene Plasmid #10668
MSCV	Addgene Plasmid #24828
Pico2-Fluc.mCherry	Gift from Dr. Andrew Kung (Dana Farber Cancer Institute)

Table 2.2. List of vectors used in experiments.

2.11 Quantitative Real Time-PCR

RNA was extracted by NucleoSpin RNA isolation kit (Macherey-Nagel, Germany) and RNA concentration was measured by NanoDrop based on the absorbance. 500 ng or 1000 ng total RNA was used for cDNA synthesis. For each sample, required amount of RNA, 2,5 ul of 2 mM dNTPs (Life Technologies, USA), 1 ul of Hexanucleotide mix (Invitrogen, USA) were mixed and nuclease-free dH_2O was added up to 16,5 ul. Reaction mixture was incubated at 65^oC for 5 min. After the incubation, tubes were quickly put on ice. The RT mix consisting of 5ul 5x First Strand Buffer (Invitrogen, USA), 2ul of 0,1 M DTT (Invitrogen, USA) and 0,5 ul of RNasin (Promega, USA) were prepared. 7,5 ul of the mixture was added to each tube and incubated for 10 minutes at room temperature. Then, 1 ul of MMLV-RT enzyme (Invitrogen, USA) was added to each tube and incubated at 37^oC for 1 hour and 70^oC for 15 minutes. After the incubaitons, 75 ul of RNase-free dH_2O was added to each reaction.

For quantitative real time-PCR reaction, 10 ul of 2X LightCycler® 480 SYBR Green I Master Mix (Roche, Switzerland), 1ul of 5 uM primer mix, 7 ul of RT-PCR grade dH_2O and 2 ul of cDNA was mixed per each reaction and loaded to the 96 well opaque white plate (Roche, Switzerland). Roche's LightCycler 480 Instrument II was used to detect delta CT values of each reaction. Quantitative RT-PCR was performed with 40 cycles using the following primer pairs:

Gene	**Sequence**	
CASP9	F	CTTCGTTTCTGCGAACTAACAGG
	R	GCACCACTGGGGTAAGGTTT
Bad	F	CCCAGAGTTTGAGCCGAGTG
	R	CCCATCCCTTCGTCGTCCT
Bcl2	F	CAGGGCGATGTTGTCCACC
	R	GGGGAGGATTGTGGCCTTC
Bcl-XL	F	GGTCGCATTGTGGCCTTTTTC
	R	TGCTGCATTGTTCCCATAGAG
BIRC2 (CIAP1)	F	AGCACGATCTTGTCAGATTGG
	R	GGCGGGGAAAGTTGAATATGTA
BIRC3 (CIAP2)	F	CAGGGCTCCTGGGTAGAACT
	R	CTACTCCGTCCAGACTCATGC
FADD	F	GCTGGCTCGTCAGCTCAAA
	R	ACTGTTGCGTTCTCCTTCTCT

Hrk	F	AGGTTGGTGAAAACCCTGTG
	R	GCATTGGGGTGTCTGTTTCT
Mcl1	F	TGCTTCGGAAACTGGACATCA
	R	TAGCCACAAAGGCACCAAAAG
Noxa	F	ACCAAGCCGGATTTGCGATT
	R	ACTTGCACTTGTTCCTCGTGG
Puma	F	GACCTCAACGCACAGTACGAG
	R	AGGAGTCCCATGATGAGATTGT
DR4	F	ACCTTCAAGTTTGTCGTCGTC
	R	AACTCTCCCAAAGGGCTATGT
DR5	F	AAGACCCTTGTGCTCGTTGT
	R	AGGTGGACACAATCCCTCTG
Bid	F	CCTACCCTAGAGACATGGAGAAG
	R	TTTCTGGCTAAGCTCCTCACG
Bik	F	AGACCCTCCTGTATGAGCAG
	R	GCATTCCAAAGAATCGAAGTCCT
Bad	F	CCCAGAGTTTGAGCCGAGTG
	R	CCCATCCCTTCGTCGTCCT
Bax	F	CAAACTGGTGCTCAAGGCCC
	R	GAGACAGGGACATCAGTCGC
BNIP1	F	TCTAGTCACTTCTTCACGAACGA
	R	CCCGGCGATTGTATTTTGTGAT
BNIP2	F	GGAGGTCGGGATGTTATCACT
	R	CCAGGTCGCAAAAAGCAGG
BNIP3	F	CAGGGCTCCTGGGTAGAACT
	R	CTACTCCGTCCAGACTCATGC
DcR1	F	GCTGCCAGTCCTAGCTTACTCTG
	R	CCCTCTGTGCACGGGTTACA
XIAP (BIRC4)	F	TGTCCTGGCGCGAAAAG
	R	TGCCAGTGTTGATGCTGAAAC
Survivin (BIRC5)	F	GGACCACCGCATCTCTACAT
	R	GACAGAAAGGAAAGCGCAAC
PPARGC1A	F	TGAAGGGTACTTTTCTGCCCC
	R	ATGCTGCTTGCACAAACTGG
DAAM2	F	TGGCTCCTGGACCCCAAGAT
	R	ATGAGATCCTGCTGGACACTCCTC
CXCL14	F	CCGCTACAGCGACGTGAAGA
	R	TTCGTAGACCCTGCGCTTCT
MEST	F	AGATCGCCTCCGCAGGAT
	R	CACACCCACAGAGTCTTGGTA
HES1	F	TGCTACCCCAGCCAGTGTCA
	R	TGGAATGCCGCGAGCTATCTT
TLR3	F	AAGGCTAGCAGTCATCCAACAGA
	R	GGTGGTGGAGGATGCACACA
TMEM150C	F	AGAGCAGTGGTACAGGCATGG
	R	GGTGCATGCTTCACACCAGG
CDYL2	F	CGCGCTGGCCAATGAGATG
	R	AAGCTCCGCACGAGGCATTT
FGF2	F	GGCTTCTTCCTGCGCATCCA
	R	TCCGTAACACATTTAGAAGCCAGT

GLI1	F	TCTCCCCGGAGTGCAGTCAA
	R	CCAGAGATGGGCTCATGGTGC
SLC7A11	F	CATCTGGACGGTGTGTGGGG
	R	GCAGTAGCTGCAGGGCGTAT
KBTBD11	F	CCGCGGCGAGGAACAAG
	R	GGGGATGTTAGGAGAAGCCGC
RelA	F	CCAGACCAACAACAACCCCT
	R	GATCTTGAGCTCGGCAGTGT
RelB	F	TGCATGCTTCGGTCTGGG
	R	CCAATTCATCTGTGCTCCTGG
NFKB1	F	AACAGCAGATGGCCCATACC
	R	AACCTTTGCTGGTCCCACAT
NFKB2	F	GGCCGGGACAAGAGAAAGA
	R	CCAGAATTTTAGACGCCCGC
GAPDH	F	AGCCACATCGCTCAGACAC
	R	GCCCAATACGACCAAATCC
Bcl10	F	GCCAGGTTACGGCAGATTCA
	R	GAAGGTCACGAGCGTCACC
IGFBP2	F	CACTTGTGAGAAGCGCCG
	R	GGTCATCGCCATTGTCTGC

Table 2.3. List of primers used in quantitative real-time PCR experiments.

2.12 Western Blot

Cells were harvested from cell culture plates by trypsinization. For drug treated experiments, medium was also collected. All samples were centrifugated at 1500 rpm for 5 minutes. Supernatants were removed and pellets were lysed with NP-40 lysis buffer for 30 minutes on ice by vortexing at every 10 minutes. NP-40 lysis buffer contained 1% Nonidet P40 (NP-40), 1mM EDTA, 50 mM Tris-HCl (pH 7.4), 250 mM NaCl, 50 mM NaF. 1 mM final concentration of PMSF, 1X phosphatase inhibitor cocktail (PhosSTOP, Roche, Switzerland) and 1X protease inhibitor cocktail (Complete Protease Inhibitor Cocktail Tablets, Roche, Germany) was added to lysis before each use. After the incubation, lysates were centrifuged at 13.000 rpm for 10 min at 4^{o}C and supernatants were collected. Then, protein extracts were mixed with 4x loading dye containing 900 ul of 4X Laemmli sample buffer and 100 ul of beta-mercaptoethanol and boiled at 95^{o} C for 15 minutes. Boiled samples were stored at -20^{o}C. Protein concentration was measured using with BCA Protein Assay kit (Life Technologies).

For immunoblotting, 25-50 ug of proteins were run on 4-15% gradient gel in 1X TGS (Tris-Glycine-SDS) running buffer. Proteins were transferred to PVDF membrane by

semi-dry Trans-Blot Turbo Transfer System (Biorad, USA). Then, membrane was blocked in 5% non-fat dry milk in 1X TBS-T for 1 hour at RT. After the blocking, membrane was incubated with primary antibodies overnight at +4°C. Next day, secondary antibody incubation was performed at RT for 1 hour. After the incubation, membrane was washed with 1X TBS-T. Both chemiluminescence and infrared signals were imaged by Odysses® FC Imaging System (LI-COR, USA) with Image Studio software.

Primary Antibodies	**Purchased from**
Cleaved Caspase-3	Cell Signaling/9664
Caspase-8	Enzo / ALX-804-242
cleaved PARP	Cell Signaling/9541
DR4	ProSci/1139
DR5	ProSci/2019
Bcl-2 (human)	BD Biosciences/551098
Bcl-xL (human)	BD Biosciences/610746
FADD	Abcam/ab24533
H3	Cell Signaling/9715
Alpha tubulin	Abcam /ab15246
Alpha tubulin	Sigma/T9026
Secondary Antibodies	**Purchased from**
Anti-rabbit	Santa Cruz/sc-2054
Anti-mouse	Santa Cruz/sc-2055

Table 2.4. List of antibodies used in western-blot experiments.

2.13 RNA-Sequencing and Analysis

Total RNAs of sensitive and TRAIL-resistant cells were isolated using Qiagen RNAeasy Mini Kit. RNA-seq library was prepared based on protocols of BGISEQ-500 platform for 50 bp single-end reads. Sequenced data were converted to FASTQ files using the BGISEQ-500 platform at the BGI Genome Sequencing Company (Beijing, China). The reads were aligned to human hg19 genome using HISAT [133], and then analyzed. The reads were counted by using Ensembl IDs at the UCSC Genome Browser with GenomicFeatures package of R program [134]. Around 26 million reads were generated from sequencing of each sample, and 93% of those bases were equal or above of 30 Q-score. Bioinformatical analysis and functional pathway analysis were performed in collaboration with Tunç Morova and Dr. Zeynep Hülya Gümüş, respectively.

2.13.1 Statistical and functional analysis of RNA seq data and differentially expressed gene Identification

Differentially expressed genes between sensitive and TRAIL-resistant cells were determined using DESeq [135], which controls for Type I Errors with Negative Binomial distributions. Significant differentially expressed genes were determined by using multiple-testing correction for False Discovery Rate (FDR) at 5%. Expression values of genes that changed by 2-fold were selected as significant.

2.13.2 Functional analysis of RNA seq data

To relate the RNA-sequencing results to mechanisms of cells, the complex biology of cells during the TRAIL-resistant cell generation as compared to their parental cells (TRAIL-sensitive) were determined with Ingenuity Pathways Analysis (IPA), a web-based application. Transcript identifiers were mapped for matching gene object in the IPA data base. Data were searched and categorized statistically enriched in the DEG set and changing of each category was calculated. (www.ingenuity.com).

2.14 Co-culture Experiments

Fluc-mCherry (FMC) expressing A172 and U87MG tumors cells and sTRAIL-GFP expressing bone-marrow derived human mesenchymal stem cells (MSCs) were mixed with different ratios (1:1, 1:3, 2:1, 3:1) and seeded on 96 well black plates. For Firefly luciferase (Fluc) measurement, cells were treated with D-luciferin (10 ug/ml) and Fluc activity was measured by BioTek2s Synergy H1 plate reader and Gen5 analysis software.

2.15 In vivo Studies

All in vivo experiments were approved by the institutional ethical comity of Harvard Medical School, Brigham and Women's Hospital. In vivo experiments were performed in collaboration with Deepak Bheree and Dr. Khalid Shah. A172 sensitive and resistant cells were infected with Firefly luciferace (Fluc)-mCherry (FMC) viruses. Human bone marrow derived mesenchymal stem cells (MSCs) were infected with LV-S-TRAIL viruses. A 6-8-week-old non-obese diabetic/severe combined immunodeficiency (NOD/SCID) mice were used in experiments. Tumor cells and MSCs were mixed and implanted stereotactically [from bregma, AP: -2 mm, ML: 1.5 mm, V (from dura): 2 mm; n=5]. Tumors were visualized by using IVIS Lumina III (Perkin Elmer, USA) under the isoflurane anesthesia following intraperitoneally 150 ug/g body weight of D-Luciferin injection. Quantification of tumor growth was performed with GraphPad PRISM software (San Diego, CA, USA).

3 RESULTS

3.1 Generation of TRAIL-resistant cell populations from GBM cell lines

Glioblastoma multiforme (GBM) cells exhibit different response to TRAIL treatment [136]. To understand this heterogenic response to TRAIL in GBM, TRAIL sensitive GBM cell lines (A172, LN18, T98G) were cultured under gradually increasing TRAIL concentrations for long term. U87MG cells, mid-sensitive to TRAIL, were cultured with fixed TRAIL doses (0, 10, 50 and 250 ng/ml). Mediums of cells were changed every 3 days and TRAIL was added. During the culturing, dead cells were removed and surviving cells were expanded. TRAIL treatment duration was adjusted according to the maximum tolerated TRAIL doses of each cell line. Accordingly, selection and expansion of a highly TRAIL-sensitive line, A172, took the longest (96 days) compared to medium sensitive U87MG cells (30 days) **(Figure 1)**.

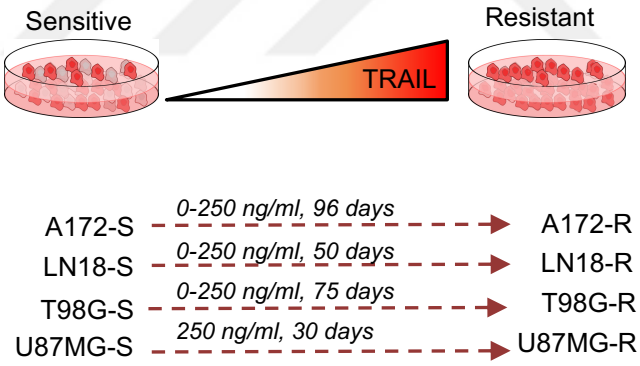


Figure 3.1. Experimental approach to isolation of TRAIL-resistant sub-populations. A172, LN18 and T98G cells were cultured with gradually increasing TRAIL doses (0 to 250 ng/ml). U87MG cells were cultured with fixed TRAIL doses (250 ng/ml).

3.1.1 TRAIL response of TRAIL-resistant sub-populations

After the derivation of surviving TRAIL-resistant cells, treatment was discontinued, and cells were cultured in TRAIL-free conditions. TRAIL response of TRAIL-resistant sub-populations was tested by Cell-Titer-Glo (CTG) viability test. CTG results showed that resistant sub-populations (A172-R, LN18-R, T98G-R, and U87MG-R) were not affected from TRAIL, however control cells (A172-S, LN18-S, T98G-S, and U87G-MG-S) were affected. Cell viability significantly decreased in control cells treated with TRAIL for 24 hours (**Figure 3.2**), but not in resistant cells.

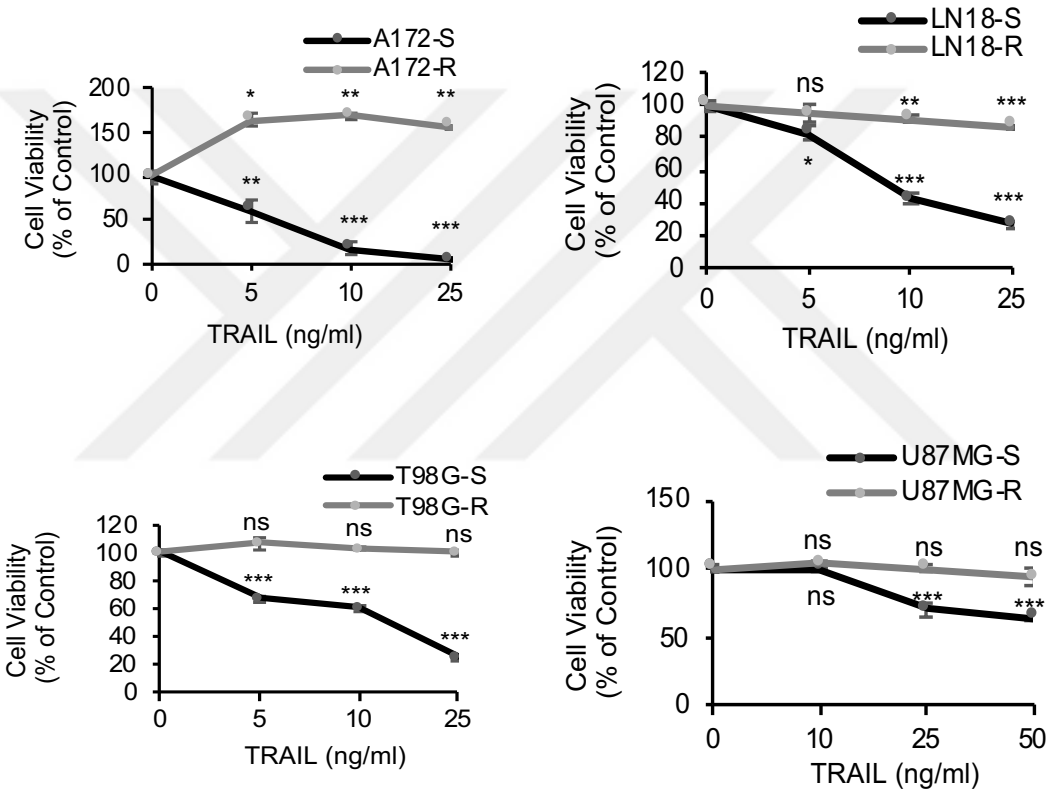


Figure 3.2. Viability of TRAIL-resistant subpopulations in response to 24-hour treatment of different TRAIL doses as measured by CellTiterGlo assay.

Some cells showed morphological changes in their cell shapes during this resistance generating period. For example, A172-R cells created sphere structure (**Figure 3.3)**.

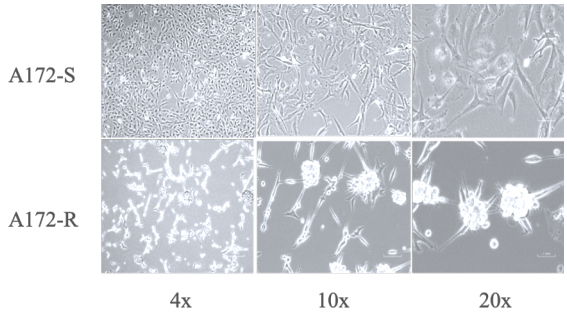


Figure 3.3. Light microscopy snapshots of parental (A172-S) and A172 TRAIL-resistant (A172-R) subpopulations.

3.1.2 Re-generation of TRAIL-resistant sub-populations

To test whether the generation of TRAIL-resistant cells was repeatable, the process was performed again, and TRAIL-resistant cells could be re-isolated.

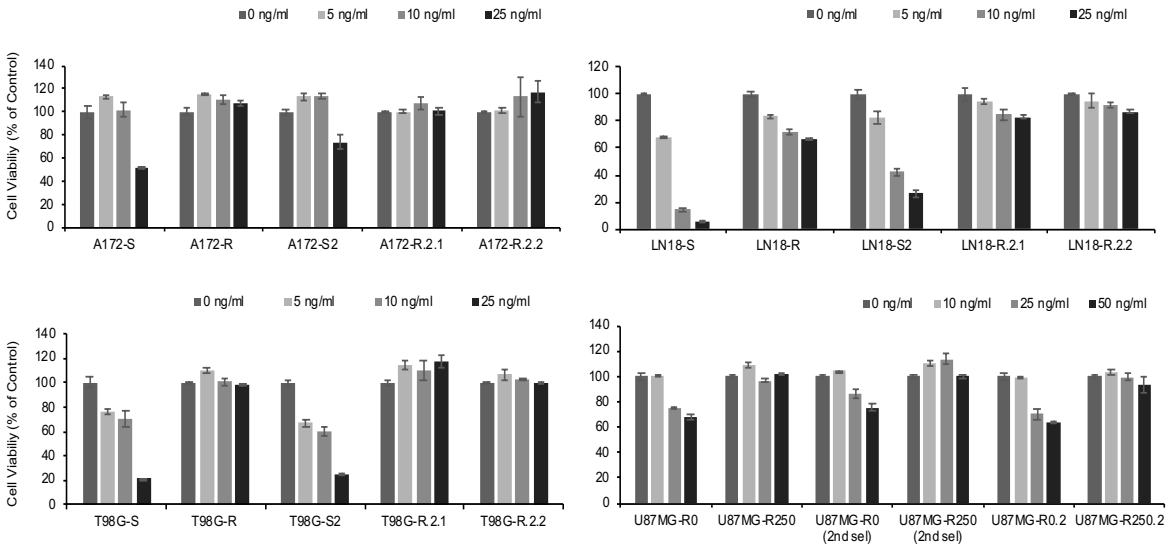


Figure 3.4. Viability results of all resistant subpopulations treated with SuperKiller TRAIL (SKT) for 24 hours.

TRAIL response of TRAIL-resistant sub-populations was tested by CTG viability test. CTG results showed that 2nd generation resistant sub-populations (A172-R, LN18-R, T98G-R and R250 (U87MG) cells) were not affected by TRAIL, however control cells (A172-S, LN18-S, T98G-S and R0 (U87MG)) were affected. This experiment was performed several times and with different TRAIL types. Results showed that approximately more than 90% cell viability was observed in all resistant cells sub-populations, and less than 50% cell viability was observed in control cells treated with Super Killer TRAIL (SKT, Enzo) for 24 hours (**Figure 3.4**). SKT was used in all TRAIL-resistant cell characterization experiments.

We decided to continue with second generation (R2.2) sub-groups of A172, LN18, and T98G cells and with first generation of U87MG (R250) cells for further experiments.

3.1.3 Caspase activity of TRAIL-resistant sub-populations

Caspases play a major role in apoptosis, so we tested caspase-3/7 activity of resistant cells as an apoptotic marker. Accordingly, caspase-3/7 activity of resistant sub-populations was lower than control cells treated with different TRAIL doses for 3 hours (**Figure 3.5**).

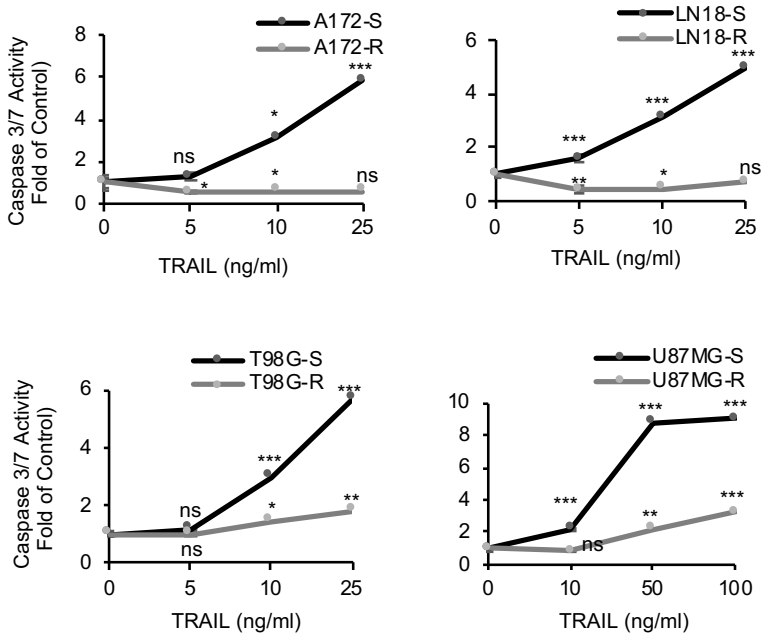


Figure 3.5. Caspase 3/7 activity of TRAIL-resistant subpopulations treated with different TRAIL doses (0, 5, 10, 25 ng/ml for A172, LN18, and T98G cells; and 10, 50, 100 ng/ml for U87MG cells) for 3 hours.

3.1.4 Apoptotic protein levels in TRAIL-resistant sub-populations after TRAIL treatment

We further analyzed the effects of TRAIL on signaling components. For this approach, both sensitive and resistant cells were treated with TRAIL (25 ng/ml for A172, LN18, and T98G cells; and 50 ng/mL for U87MG) for 6 hours. Apoptosis related proteins (Caspase-8, -3 and c-Parp) were elevated in parental groups treated with TRAIL, however they were less or not detected in resistant sub-populations of all cells (**Figure 3.6**). A-tubulin was shown as loading control.

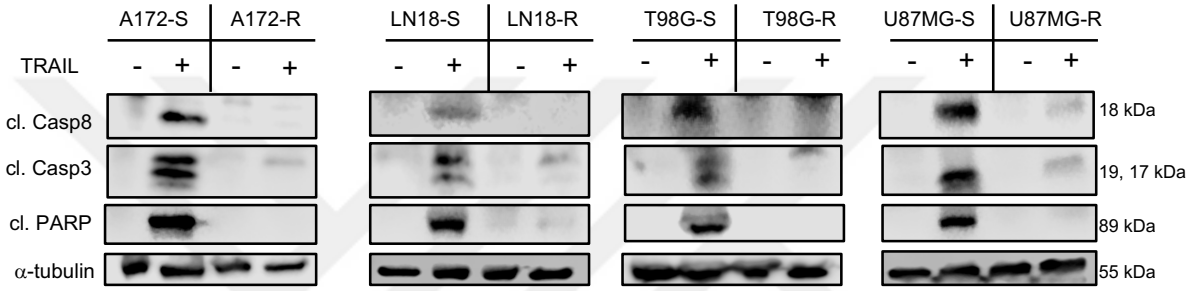


Figure 3.6. Western blotting showing changes in Caspase-8, -3 and PARP cleavage with TRAIL in sensitive and TRAIL-resistant pairs of GBM cell lines.

Similarly, we observed significant increase in the percentage of apoptotic cells upon TRAIL treatment in A172-S cells compared with TRAIL-resistant sub-populations (A172-R) by YO-PRO-1 (YP1) assay, a fluorescence based live/dead assay (**Figure 3.7**).

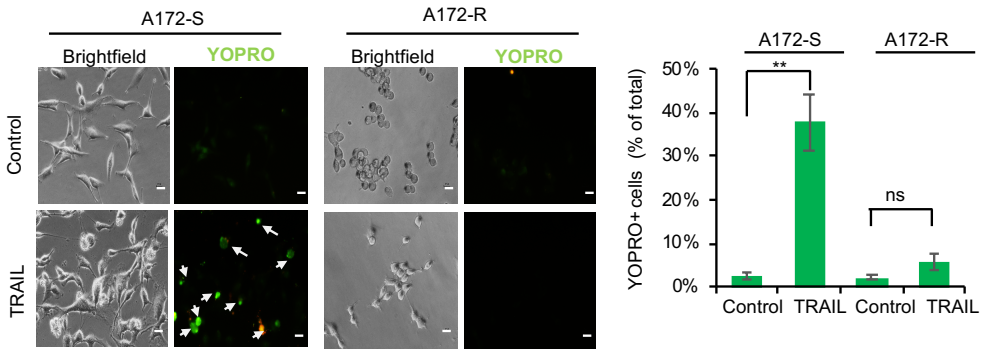


Figure 3.7. Yo-Pro staining of sensitive and TRAIL-resistant subpopulations of A172 cells treated with TRAIL (50 ng/ml) for 3 hours. (Scale bars: 100 um). Graph displaying of number of Yo-pro positive cells.

3.1.5 TRAIL resistance in long term

To assess the long-term effects of TRAIL on isolated sub-populations' growth and proliferation, we performed a real-time cell growth analysis. In this experiment, we seeded all sensitive and resistant cells into a special plate that allows the quantification of cells through measuring cell impedance (xCelligence). 24 hours after cell seeding, TRAIL was added into wells (50 ng/ml (for A172, LN18 and T98G), and 100 ng/ml (for U87MG). Then, cell growth was monitored for 90 hours. This cell growth analysis showed that sensitive cells (red lines) started to die after TRAIL treatment, however resistant cells (green lines) survived under TRAIL for long term **(Figure 3.8)**.

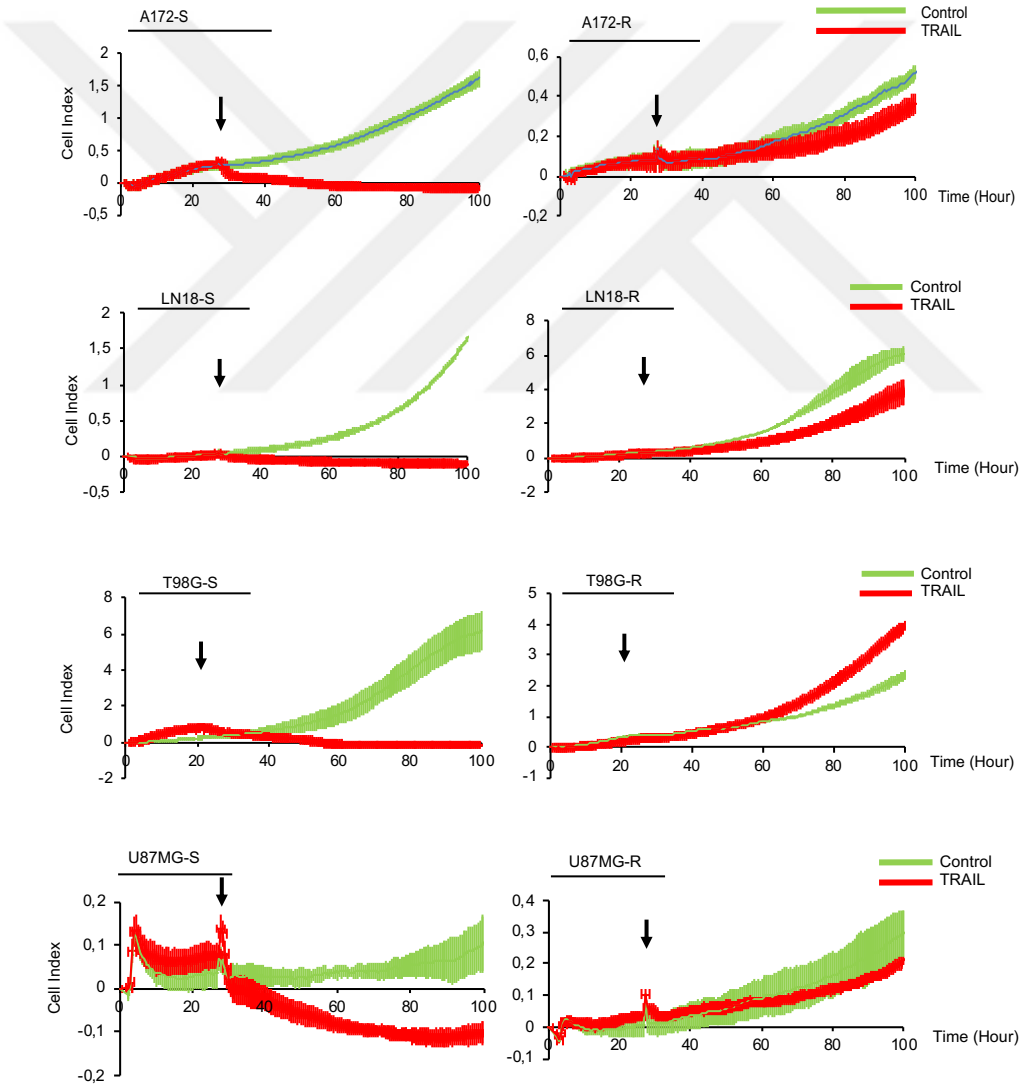


Figure 3.8. Long-term real time cell survival analysis of control cells and TRAIL-resistant subpopulations treated with TRAIL for 90 hours. Arrows indicate the TRAIL addition timepoints.

3.1.5.1 Tumor generation of TRAIL-resistant A172 cells *in vivo*

To confirm the TRAIL resistance of subpopulations, *in vivo* experiment was performed. A172 cells were used in this experiment. To deliver TRAIL on-site, we utilized clinical grade, bone marrow-derived human mesenchymal stem cells (hMSC) that either express GFP or secrete TRAIL [137]. Tumor cells were infected bioluminescent and fluorescent marker (Fluc-mCherry) for imaging.

Before the *in vivo* experiments, tumor cells and hMSCs were cocultured with different ratios and Fluc intensity of live tumor cells were measured after 72 hours of co-culture. Secreted TRAIL from hMSCs affected only sensitive cells, whereas resistant cells were alive **(Figure 3.9)**.

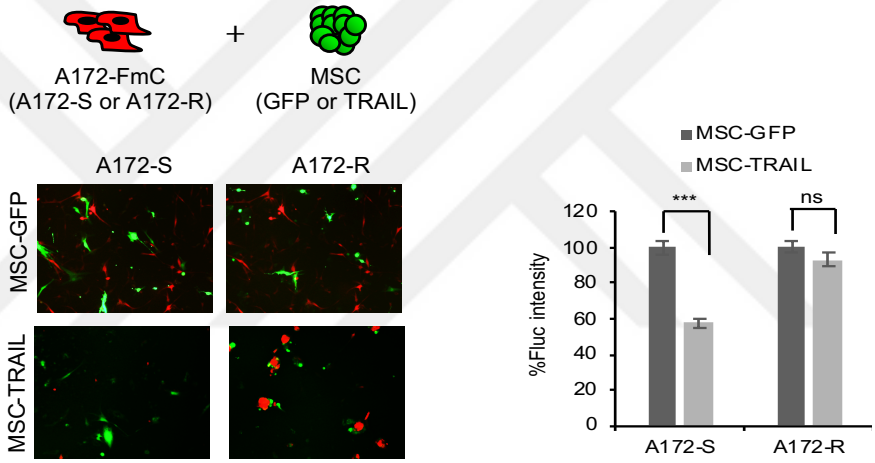


Figure 3.9. Representative snapshots of A172-S and -R cells (red) co-cultured with hMSC-GFP or hMSC-TRAIL (green), and relative tumor cells viability in coculture with hMSCs for 72 hours as determined by measuring Fluc activity.

Similar effect was observed *in vivo*. Both A172-S and –R cells were mixed with hMSCs, and stereotactically implanted into the mice brains **(Figure 3.10)**. Tumor growth was monitored by using IVIS Lumina machine following D-luciferin (10 mg/kg) injection intraperitoneally. Secreted TRAIL from hMSCs markedly reduced growth of TRAIL-sensitive tumors, however resistant cells were largely unaffected and continued to grow **(Figure 3.11)**. *In vivo* experiments were performed at Center for Stem Cell Therapeutics and Imaging, Brigham and Women's Hospital, Harvard Medical School collaborating with Dr. Deepak Bhere and Dr. Khalid Shah.

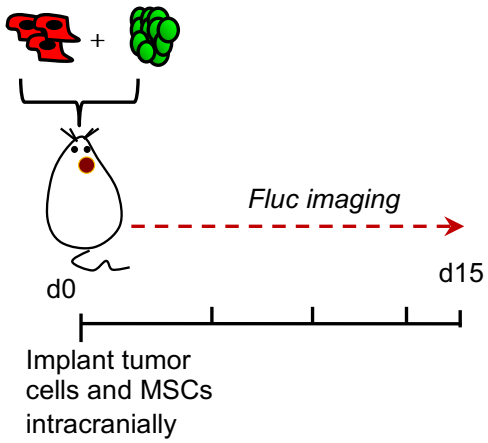


Figure 3.10. Schematic showing of in vivo experiment

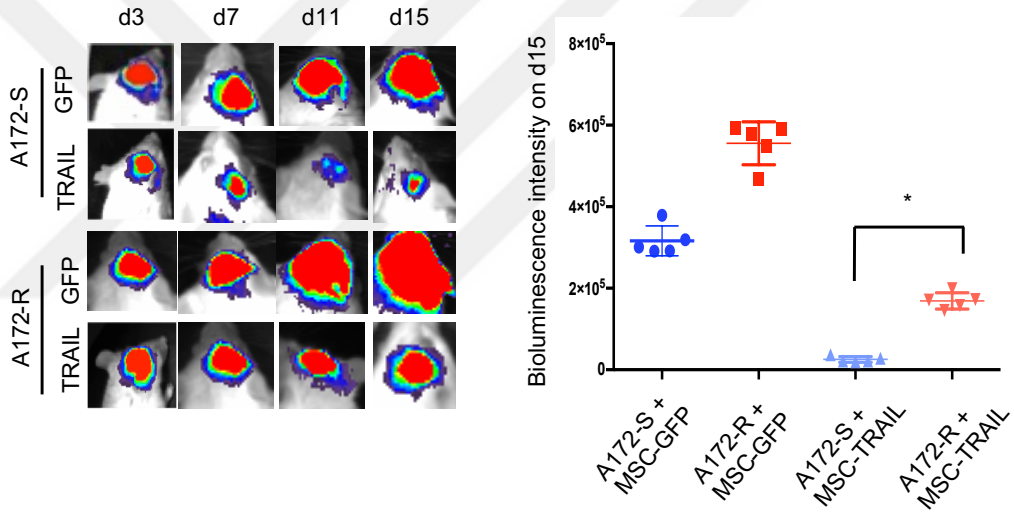


Figure 3.11. Representative snapshots of tumor imaging and quantification of tumor growth.

3.2 TRAIL-resistant cell generation from U87MG cells

In parallel with other experiments; TRAIL resistant cell generation from U87MG cells was started with 3 different TRAIL doses. These doses were 10 ng/ml, 50 ng/ml, and 250 ng/ml, and acquired TRAIL resistant cells were called R10, R50 and R250. R0 is defined control (parental) cells. **(Figure 3.12)**. Similarly, R10 and R50 cells were cultured under fixed TRAIL doses and every 3 days medium of cells was refreshed and new TRAIL was added for 30 days.

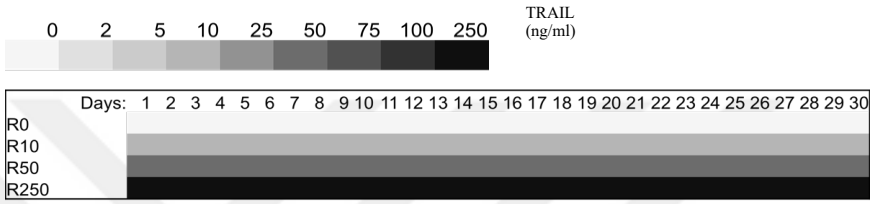


Figure 3.12. Experimental approach to isolation of TRAIL-resistant sub-populations from U87MG cells. U87MG cells were cultured with fixed TRAIL doses (10, 50 and 250 ng/ml).

3.2.1 TRAIL response of TRAIL-resistant U87MG-R10 and R50 Cells

After 30 days, TRAIL was removed, and cells were continued to culture. Besides the R250 cells; R10 and R50 cells also showed resistance against TRAIL after 30 days. TRAIL response of R10, and R50 cells was tested by Cell-Titer-Glo (CTG) viability test. More than 80% cell viability was observed in both R10 and R50 sub-populations, less than 40% cell viability was observed in control cells treated with 250 ng/ml TRAIL for 24 hours **(Figure 3.13)**. This experiment was performed several times.

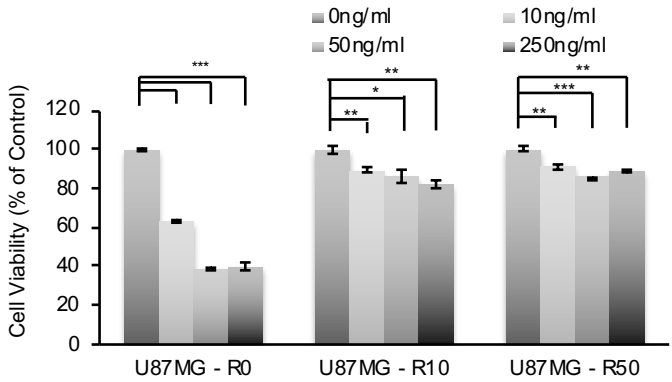


Figure 3.13. Viability of U87MG-R10 and R50 cells treated with TRAIL for 24 hours.

3.2.2 Caspase Activity of TRAIL-resistant U87MG-R10 and R50 Cells

According to Caspase-3/7 Assay results, caspase-3/7 activity of U87MG-R10 and R50 TRAIL resistant sub-populations was lower than control cells treated with different TRAIL doses (0, 10, 50 and 250 ng/ml) for 3 hours **(Figure 3.14)**.

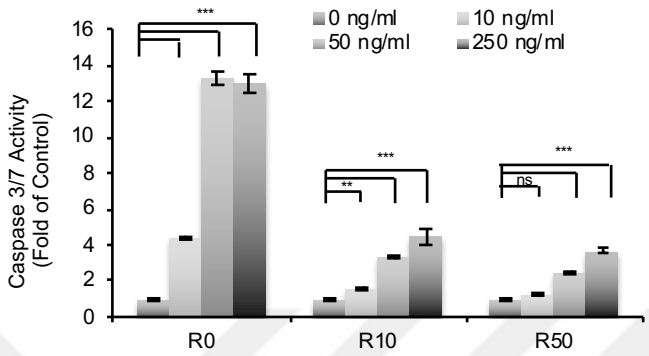


Figure 3.14. Caspase 3/7 activity of U87MG-R10 and R50 TRAIL-resistant subpopulations treated with different TRAIL doses (0, 10, 50, 250 ng/ml) for 3 hours.

3.2.3 Long term effects of TRAIL in U87MG-R10 and R50 Cells

In order to assess the long-term effects of TRAIL on U87MG-R10 and R50 cells, real-time cell survival analysis was performed. In this experiment, cells were treated with 500 ng/ml TRAIL after 24 h cell seeding and cell growth was measured for 90 hours. Data were normalized to TRAIL addition time **(Figure 3.15)**.

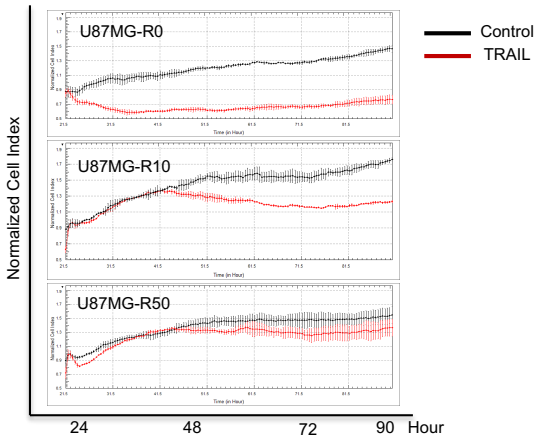


Figure 3.15. Real-time cell survival analysis of U87MG-R10 and R50 cells treated with 500 ng/ml TRAIL for 90 hours.

Long-term cell survival analysis results showed that, the control cells started to die after the TRAIL treatment, however the resistant cells survived for long term. Even though resistant cells were not markedly affected from TRAIL, there was some reduction in growth of TRAIL-treated of R10 cells after 40 hours. R50 cells survived as much as R250 cells.

3.3 Resistance of sub-populations was specific to TRAIL

To test whether the TRAIL-resistant subpopulations were resistant to other drugs besides TRAIL, we tested several drugs with different mechanisms of action. First, cells were treated with Temozolomide (TMZ), which is a first-line clinical drug for GBM [11], with different doses (0, 100, 250 and 500 nM) for 24 hours. Viability results showed that only LN18-R cells were resistant to TMZ. Other three TRAIL-Resistant cells had similar response to TMZ with their parental cells **(Figure 3.16)**.

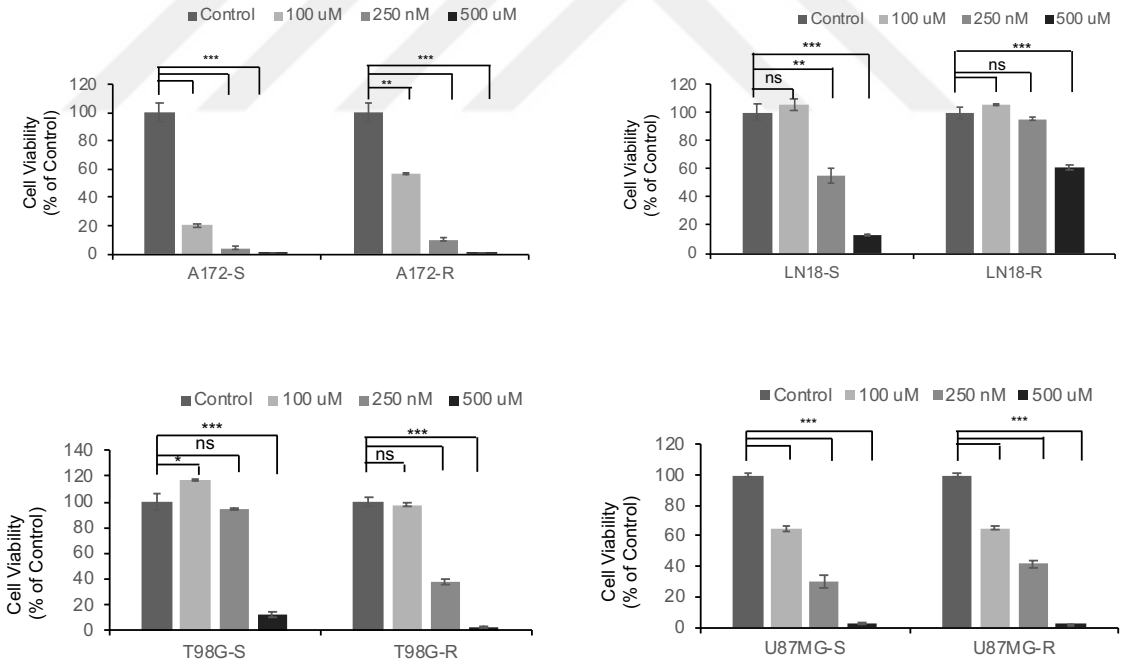


Figure 3.16. Viability of TRAIL-resistant sub-populations treated with Temozolomide for 24 hours.

Second drug was Fas-ligand (FasL) to induce death receptor-mediated extrinsic apoptosis [138]. Cells were treated with FasL (100 ng/ml) for 24 hours. Accordingly, A172-R cells were more sensitive to FasL, however there was not significant different response in all other cells **(Figure 3.17)**.

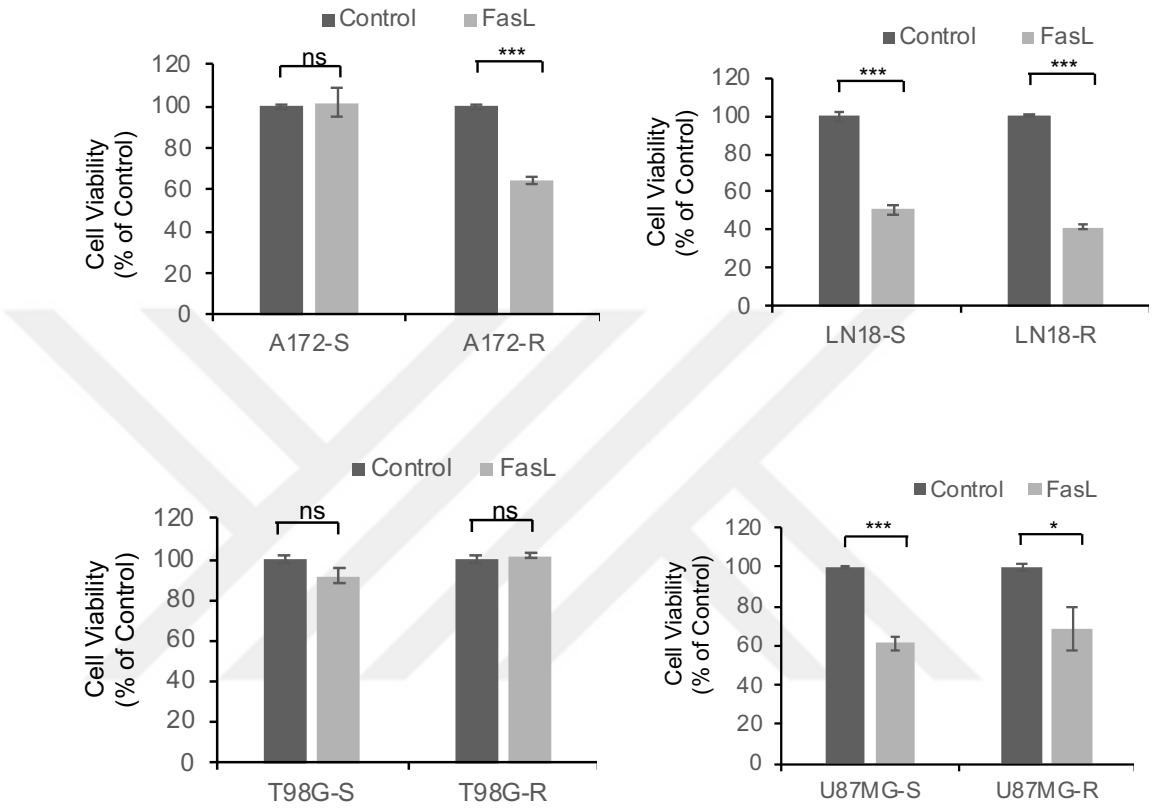


Figure 3.17. Viability of TRAIL-resistant sub-populations treated with Fas-ligand for 24 hours.

Other drug was Staurosporine for inducing the intrinsic pathway of apoptosis [139]. Cells were treated with Stautosporine (10 nM) for 24 hours, then viability test was performed. Viability test results showed that LN18-R, T98G-R and U87MG-R cells exhibited not fully, but partial resistant phenotype to Staurosporine **(Figure 3.18)**.

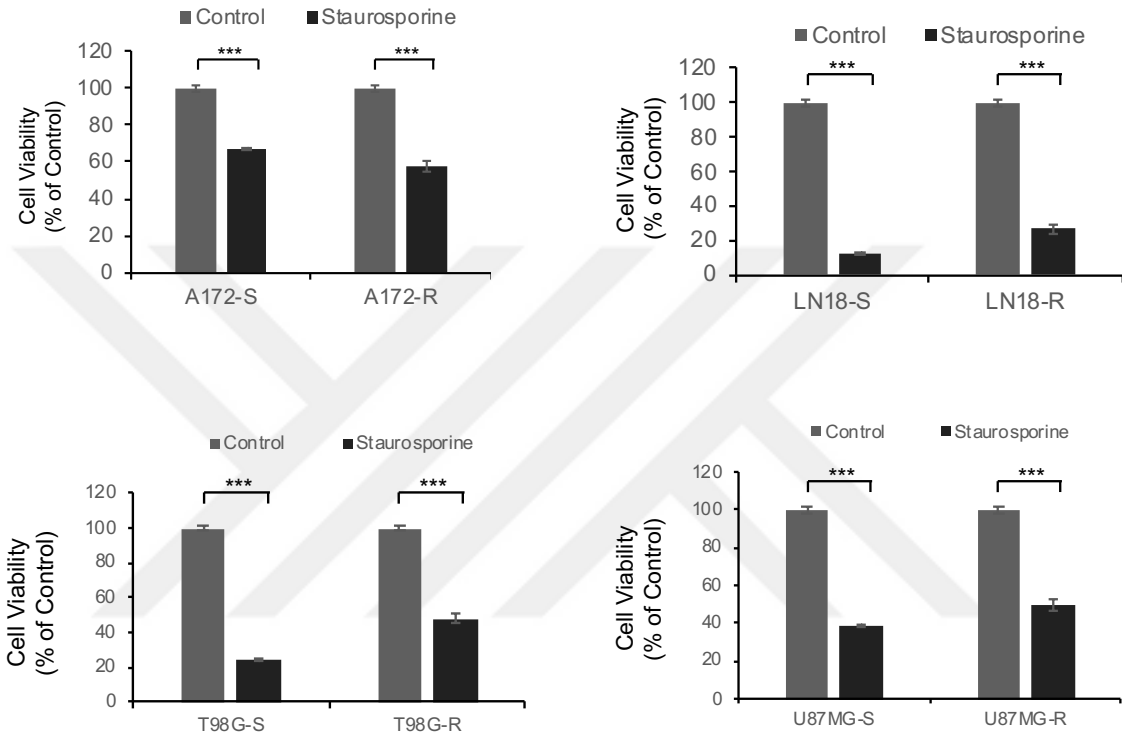


Figure 3.18. Viability of TRAIL-resistant sub-populations treated with Staurosporine for 24 hours.

3.4 Re-sensitization of TRAIL-resistant cells

To address whether the TRAIL-resistant subpopulations were committed resistant cells, or they were re-sensitizable, we tested the efficacy of known TRAIL-sensitizing drugs on the TRAIL-resistant cells. We compared known sensitizers MS-275, a histone deacetylase inhibitor and Bortezomib, a proteasome inhibitor.

3.4.1 MS-275 cannot re-sensitize sub-populations to TRAIL

MS-275, a histone deacetylase inhibitor, is a known TRAIL sensitizer [140–142]. So, we started to test with this drug, and cells were treated with MS-275 (2,5 uM) for 24 hours. After 24 hours, viability test was performed. Accordingly, MS-275 alone did not affect the cell viability in any of the cell lines. Additionally, MS-275 and TRAIL combination did not significantly affect A172-R and T98G-R cells. Although other two cell line was partially affected from combination, TRAIL-resistant cells could not be fully re-sensitizable to TRAIL with MS-275 combination treatment **(Figure 3.19)**.

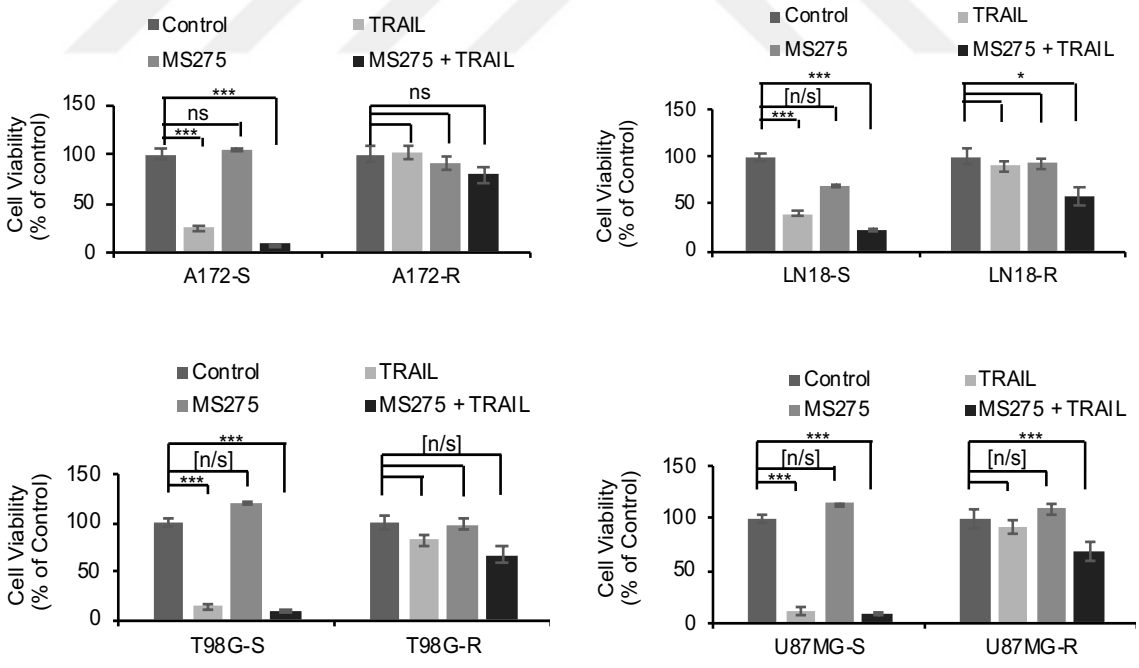


Figure 3.19. Viability of TRAIL-resistant sub-populations treated with MS-275 alone and combination with TRAIL for 24 hours.

3.4.2 Bortezomib re-sensitizes TRAIL-resistant sub-populations to TRAIL

After MS-275 treatment, we tried another known TRAIL sensitizer Bortezomib, a proteasome inhibitor [49]. In contrast with MS-275, Bortezomib re-sensitized to TRAIL in all TRAIL-resistant sub-populations. All GBM cell lines and their resistant sub-populations were treated with Bortezomib (50 nM) alone, TRAIL (50 ng/ml for A172, LN18, and T98G cells; and 100 ng/ml for U87MG cells) alone, and combination of Bortezomib and TRAIL. We observed that cells continued to survive under Bortezomib alone conditions, however combination treatment significantly decreased cell viability in all sensitive cell lines and their TRAIL-resistant subpopulations **(Figure 3.20)**.

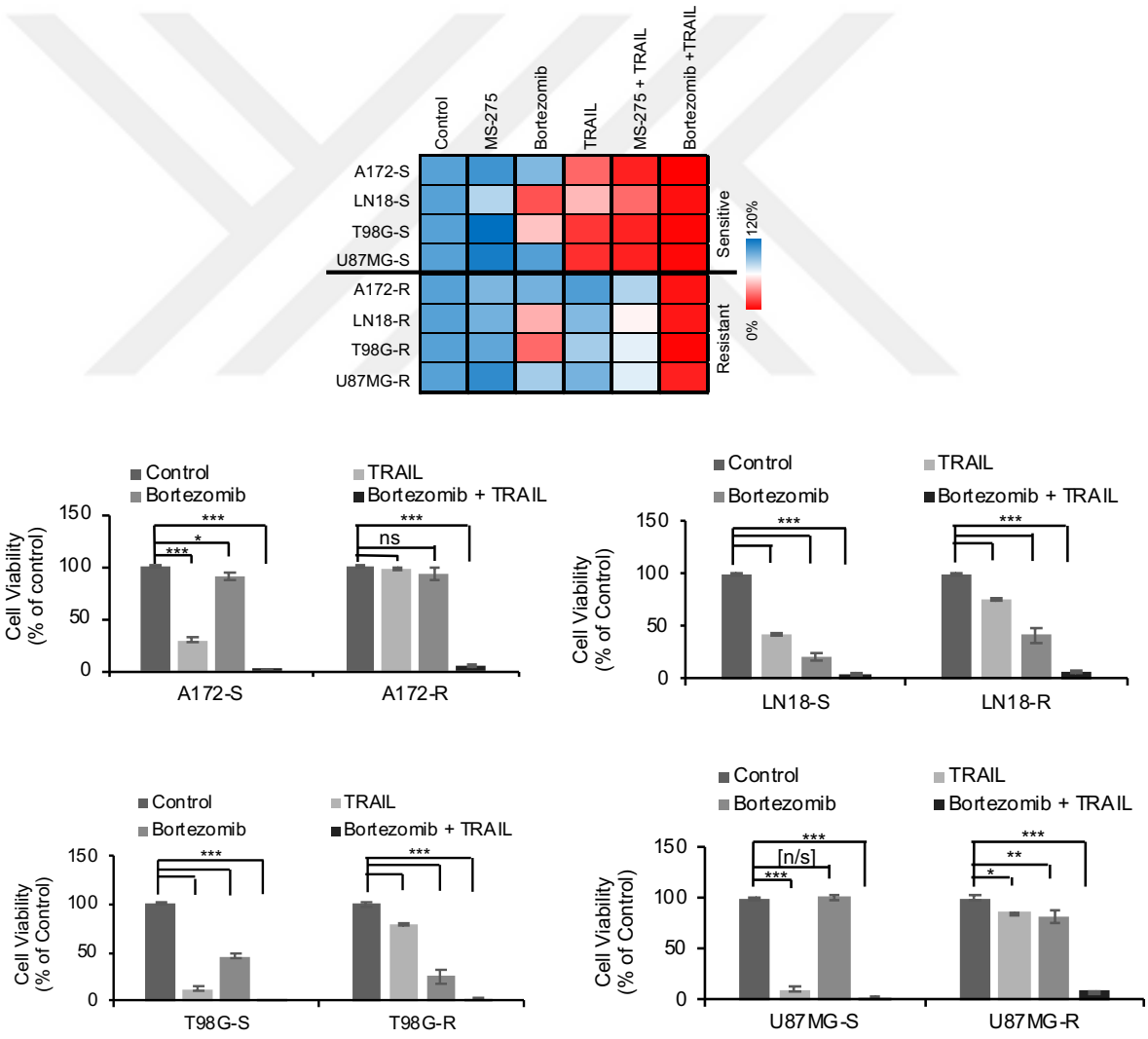


Figure 3.20. Heatmap and bar graph showing of viability results of TRAIL-resistant sub-populations treated with Bortezomib alone and combination with TRAIL for 24 hours.

Live cell experiments confirmed the viability results **(Figure 3.21)**. Live cell quantification was performed by ImageJ software through counting live cell percentage at every two hours. Interestingly, analysis showed that viability of sensitive cells decreased less than 20% after 3 hours however, resistant cells reached this level 9 hours later.

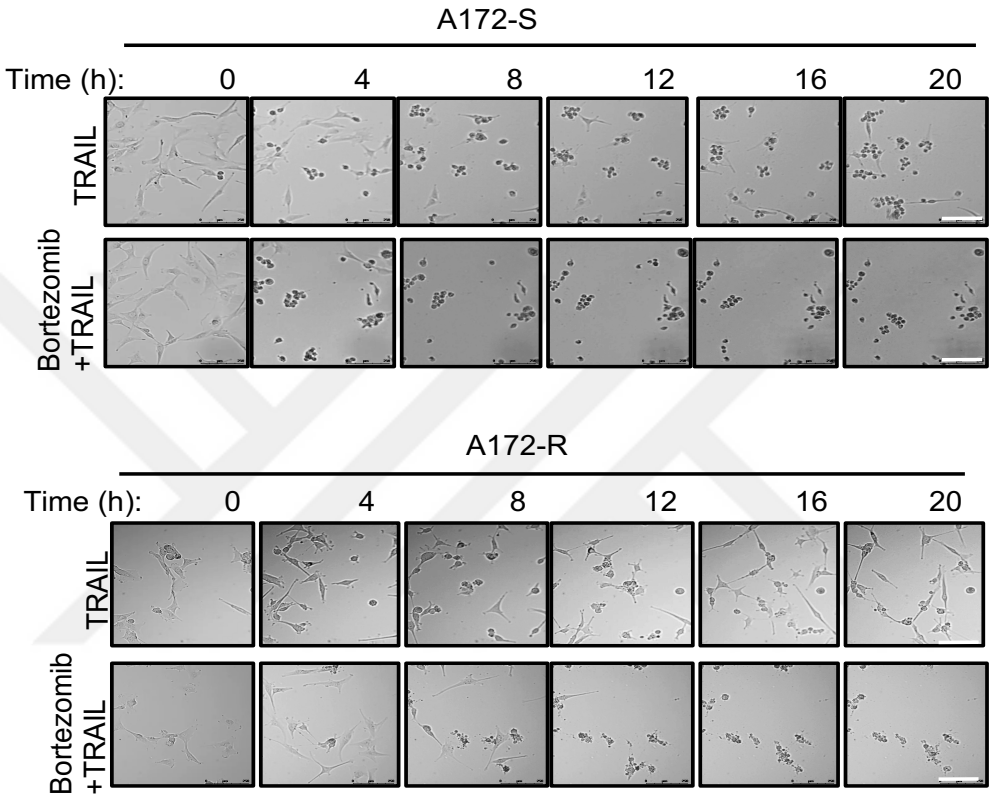


Figure 3.22. Representative snapshots from live cell imaging of A172 control cells and TRAIL resistant subpopulations upon Bortezomib (50 nM) and TRAIL (50 ng/ml) combinational treatment for 20h. (Scale bars: 250 um).

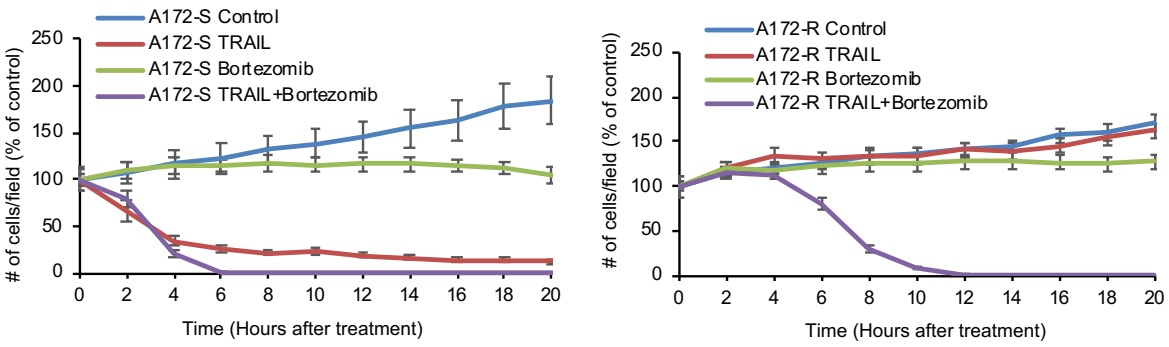


Figure 3.21. Quantification of live cell imaging data.

3.5 Regulation of apoptotic cell death pathway by Bortezomib

To test the cell death mechanisms of Bortezomib and TRAIL combination, first we measured the caspase 3/7 levels of cells. Cells were treated with Bortezomib and TRAIL alone or with combination for 3 hours, then caspase 3/7 activity was measured and observed that Bortezomib alone did not increase the caspase 3/7 levels. However, combination with Bortezomib and TRAIL significantly increased the caspase 3/7 activity in all cell lines **(Figure 3.23)**.

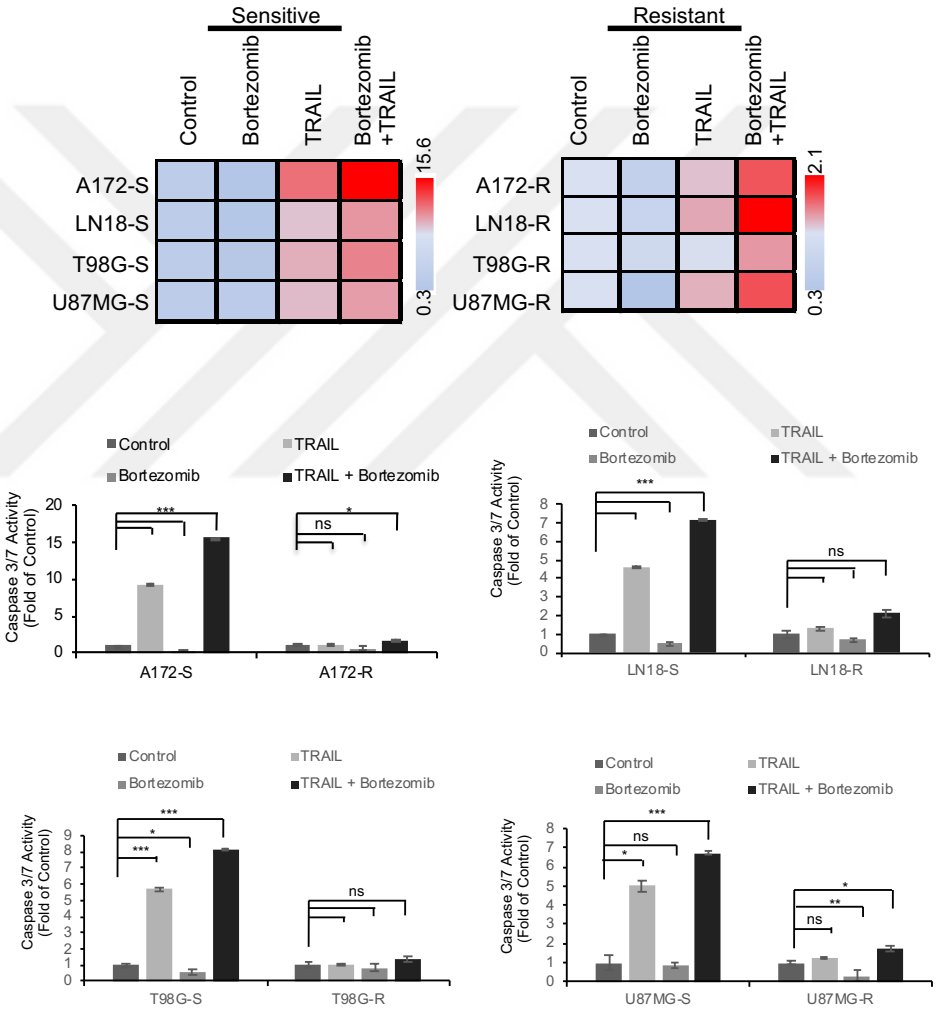


Figure 3.23. Heatmap and bar graph showing of caspase 3/7 activity of TRAIL-resistant subpopulations treated with Bortezomib alone (50 nM) or with TRAIL (50 ng/ml) for 3 hours.

Then, we inhibited caspases with general caspase inhibitor, Z-VAD-FMK (20 uM), and Z-VA-FMK was used as the negative caspase inhibitor. First, cells were pre-treated with inhibitors for 24 hours, then, drugs were applied, and inhibitors were refreshed. After the 24 hours incubation viability tests were performed. When we inhibit the caspases with general caspase inhibitor, all cells significantly escaped the apoptosis **(Figure 3.24)**.

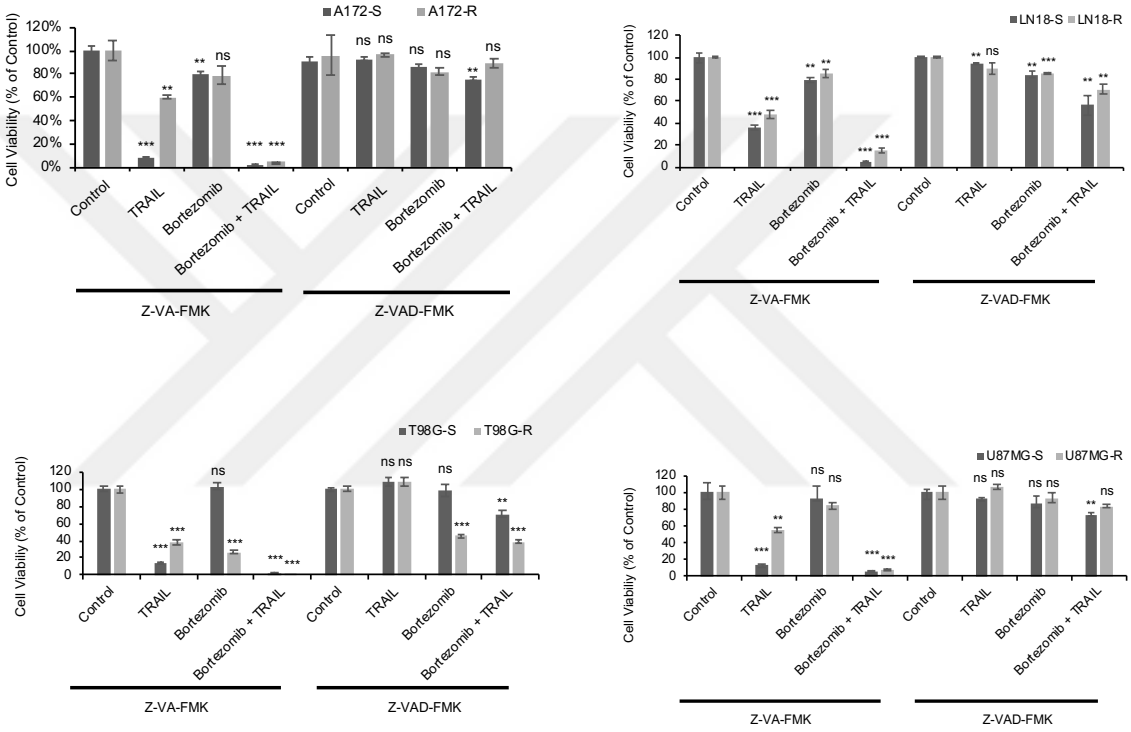


Figure 3.24. Viability analysis A172-S and –R cells pretreated with caspase inhibitors (20 uM for 24h) followed by TRAIL (50ng/ml) and Bortezomib (50 nM) treatment for 24h. Z-FA-FMK: negative control, Z-VAD-FMK: general caspase inhibitor.

Additionally, we checked important proteins in apoptosis by western blot. We observed that combination treatment (6 hours) increased the truncated-Bid (tBid), cleaved Caspase-9, cleaved Caspase-3, and cleaved PARP levels in A172-R cells compared with TRAIL and Bortezomib alone conditions **(Figure 3.25)**.

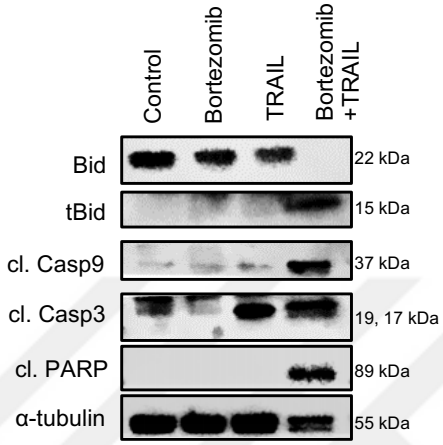


Figure 3.25. Western blotting showing changes in PARP cleavage with Bortezomib alone (50 nM) or with TRAIL (50 ng/ml) in A172-S and -R cells for 6 hours. A-tubulin was shown as loading control.

3.6 Maintenance of DR5 expression for TRAIL resistance

TRAIL binds to Death Receptors, DR4 and DR5, on cell surface and these receptors play a major role in TRAIL resistance [143]. Therefore, we checked DR4 and DR5 levels between sensitive and TRAIL-resistant cell groups; and observed that DR5 expression levels were markedly lower in all resistant cells compared with their controls. DR4 expression levels also decreased in LN18-R and U87MG-R cells, but endogenous expressions could not be detected in A172-R and T98G cells by qRT-PCR **(Figure 3.26)**.

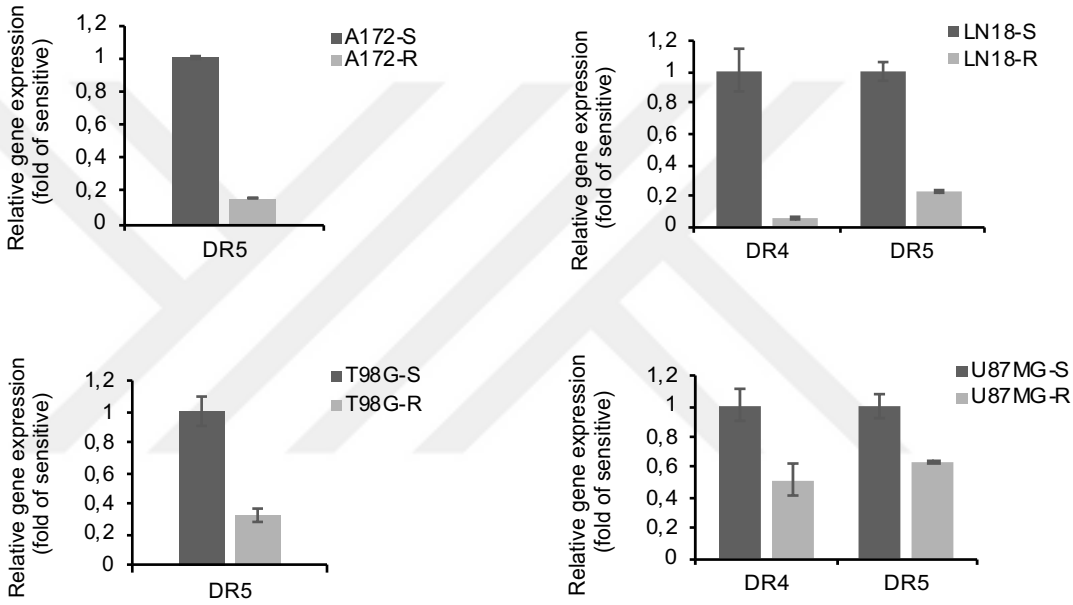


Figure 3.26. qPCR analysis showing that endogenous DR4 and DR5 expression levels of sensitive and TRAIL-resistant sub-populations of GBM cell lines. Data were normalized to sensitive conditions.

We further analyzed the effects of Bortezomib on apoptosis related gene levels, particularly focusing on *DR4* and *DR5* expressions. qRT-PCR analysis showed that Bortezomib treatment upregulated *DR4* and *DR5* expression levels in all resistant cells. We also noted that *Bid, Bik, Bak, Noxa, HRK, BNIP1, BNIP2* pro-apoptotic genes were up-regulated; *DcR1, Mcl1, cIAP1, cIAP2, Survivin and Bcl-2* anti-apoptotic genes were downregulated upon Bortezomib treatment in A172-R cells. *Bcl-xL* gene expression was markedly downregulated in all resistant sub-populations treated with Bortezomib for 24 hours **(Figure 3.27)**.

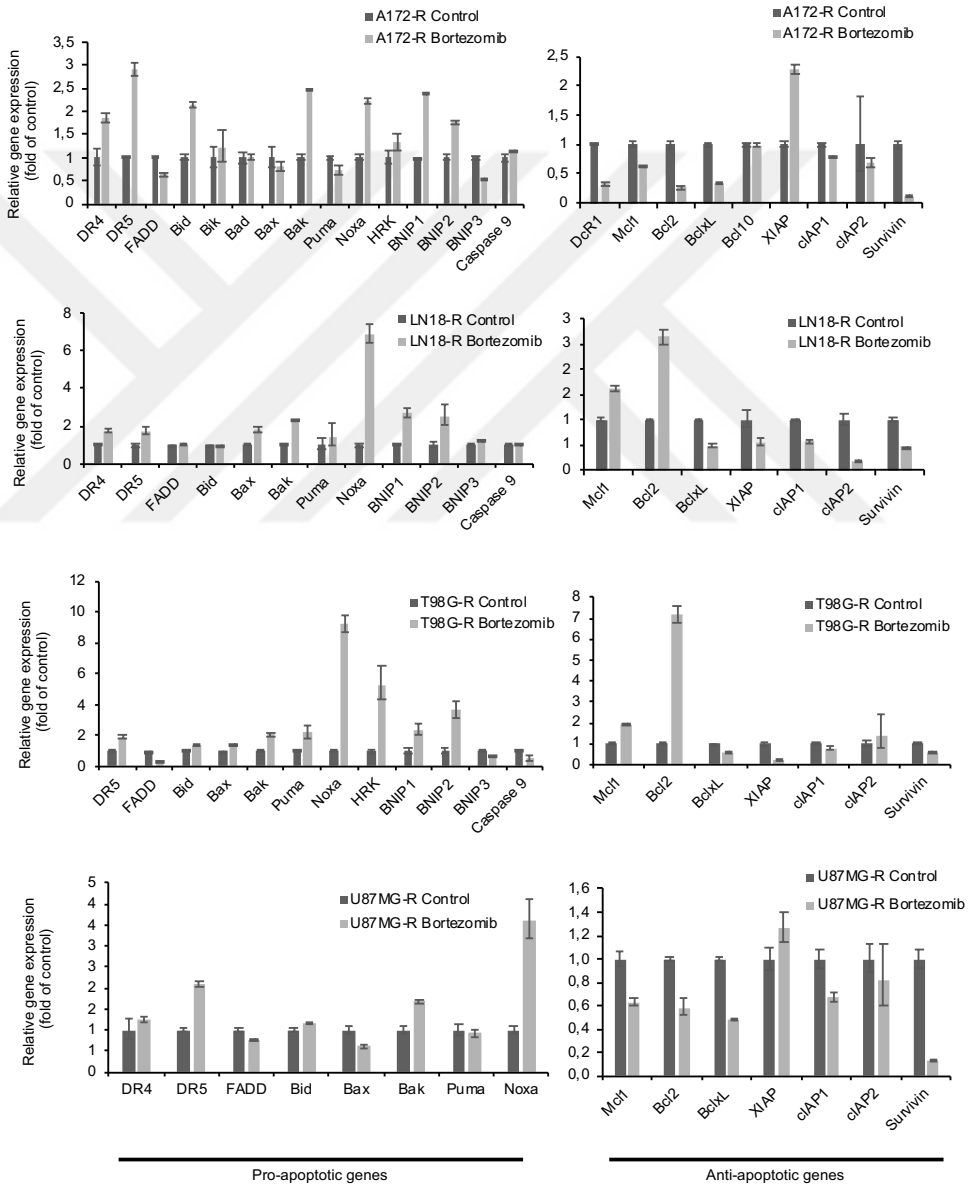


Figure 3.27. qRT-PCR analysis showing that pro-apoptotic and anti-apoptotic gene expression levels of TRAIL pathway in Bortezomib treated TRAIL-resistant cells.

Bortezomib induced changes in protein levels of DR5, Bcl-2 and Bcl-xL levels were consistent with the gene expression level changes in A172-R cells **(Figure 3.28)**.

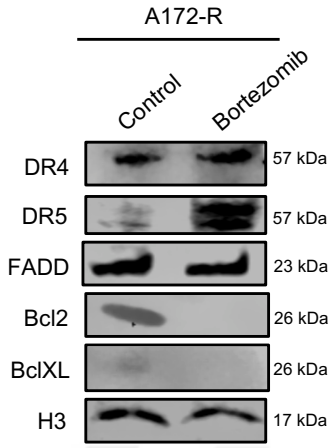


Figure 3.28. Western blot showing of major TRAIL pathway related proteins in Bortezomib treated A172-R cells.

Given the marked regulation of DR5 by Bortezomib, we wanted to test the functional role of DR5 on TRAIL and Bortezomib combination and undertook CRIPSR/Cas9 mediated loss of function of DR5 **(Figure 3.29)**.

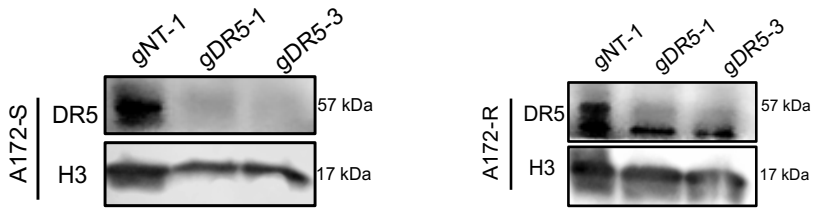


Figure 3.29. Western Blot showing the CRISPR knockouts of DR5 protein levels in A172-S and –R cells. H3 was shown as protein equal loading control.

After the knock-out of DR5 in A172 cells, TRAIL and Bortezomib combination was tested. Ablation of DR5 partly blocked the TRAIL-induced apoptosis in A172-S cells and re-sensitization of TRAIL in both A172-S and R cells **(Figure 3.30)**.

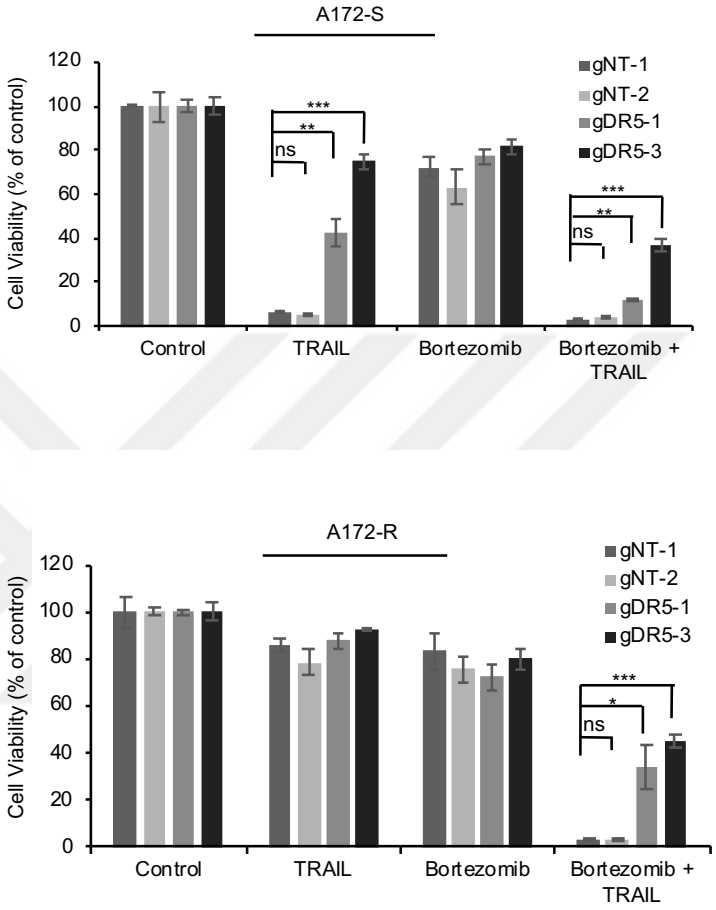


Figure 3.30. Viability analysis of DR5 knockout A172-S and -R cells upon TRAIL alone (50 ng/ml), Bortezomib alone (50 nM), and combination treatment for 24h.

Together, these results demonstrate that DR5 expression is critical for TRAIL sensitivity and re-sensitization of GBM cells.

3.7 Regulation of TRAIL response in GBM cells by Bcl-2 And Bcl-xL expression

Anti-, and pro-apoptotic Bcl-2 family members play a critical role in apoptotic balance in tumor cells [57]. To understand the effect of anti-apoptotic Bcl-2 family members on TRAIL resistance in GBM cells, first, we overexpressed Bcl-2 and Bcl-xL genes in A172 **(Figure 3.31)**, LN18 **(Figure 3.32)**, T98G **(Figure 3.33)**, and U87MG **(Figure 3.34)** -S and -R GBM cell lines.

A172:

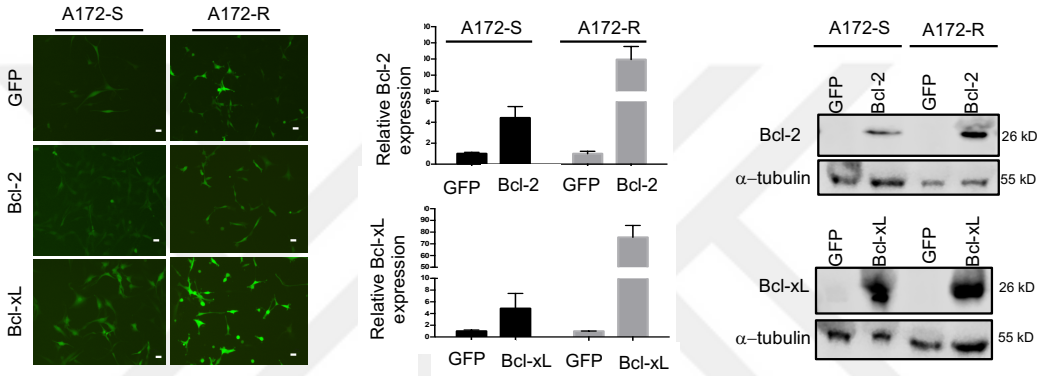


Figure 3.31. Representative snapshots and confirmation of overexpression of Bcl-2 and Bcl-xL genes by qRT-PCR and western blot in A172-S and -R cells.

LN18:

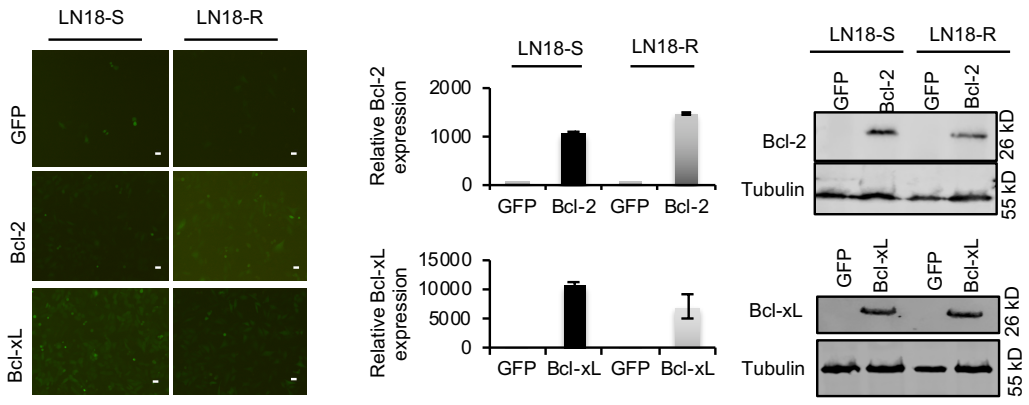


Figure 3.32. Representative snapshots and confirmation of overexpression of Bcl-2 and Bcl-xL genes by qRT-PCR and western blot in LN18-S and -R cells.

T98G:

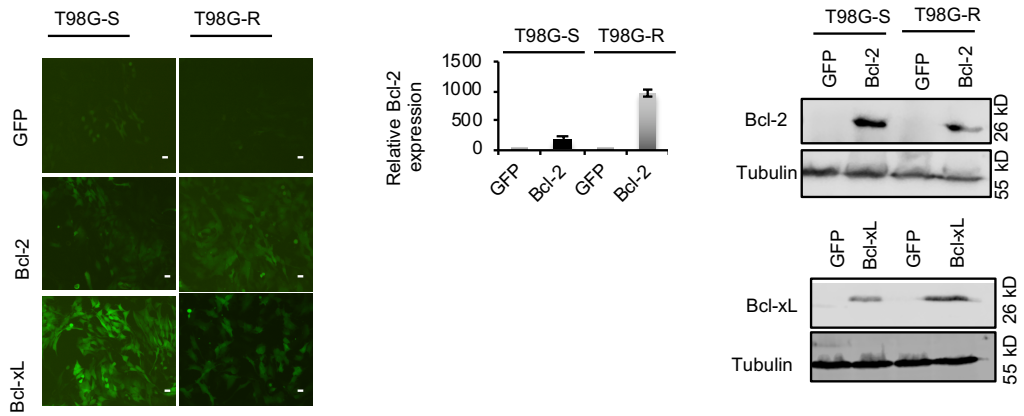


Figure 3.33. Representative snapshots and confirmation of overexpression of Bcl-2 and Bcl-xL genes by qRT-PCR and western blot in T98G-S and -R cells.

U87MG:

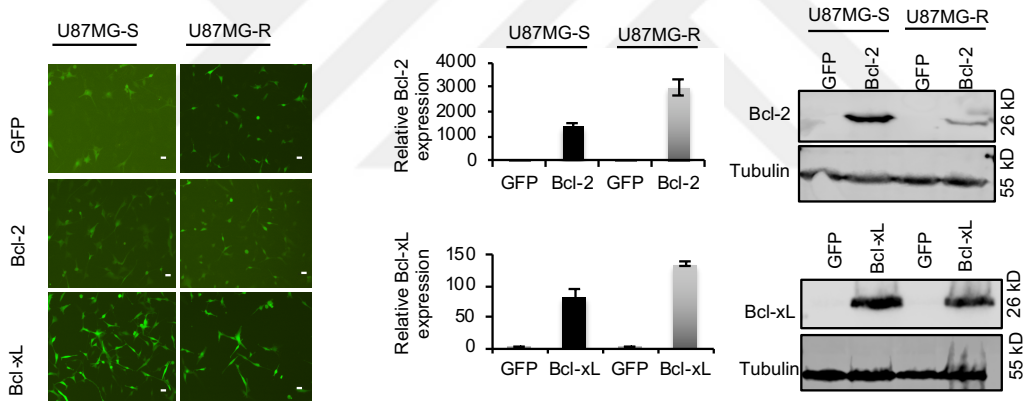


Figure 3.34. Representative snapshots and confirmation of overexpression of Bcl-2 and Bcl-xL genes by qRT-PCR and western blot in U87MG-S and -R cells.

After the confirmation of overexpression in all cell lines, TRAIL response was tested. Cells were treated with TRAIL (50 ng/ml for A172, LN18, and T98G cells; 100 ng/ml for U87MG cells) for 24 hours. Then, viability test was performed, and results showed that Bcl-2 or Bcl-xL overexpression increased resistance to TRAIL in sensitive cells, had no effect on TRAIL-resistant cells as they were already fully resistant (**Figure 3.35**).

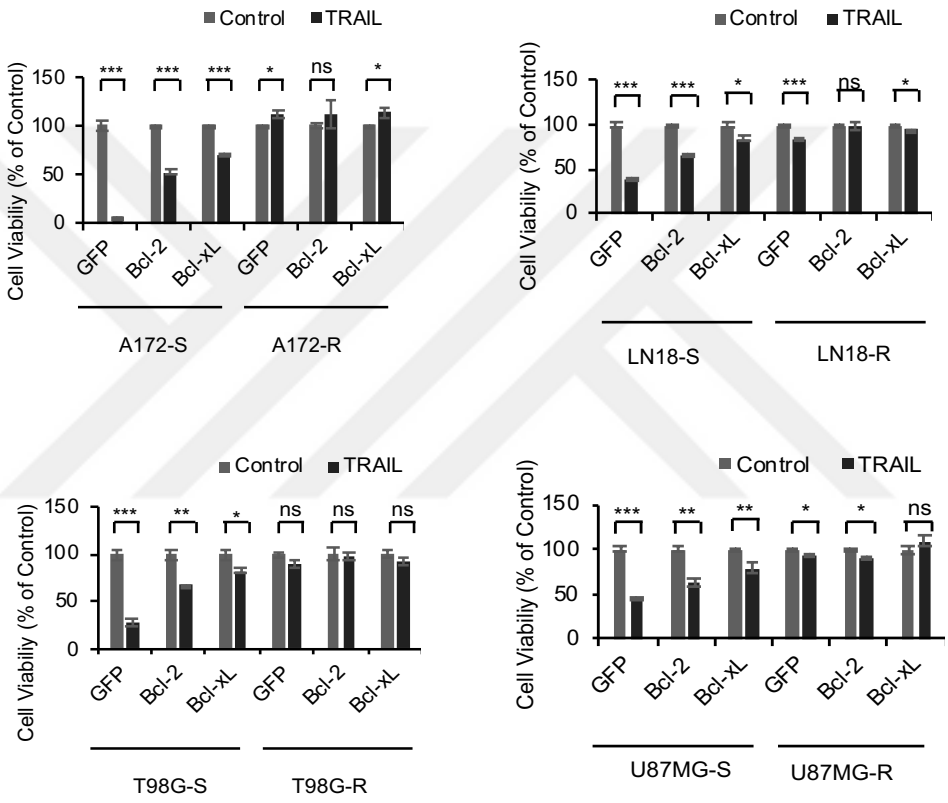


Figure 3.35. Viability of Bcl-2 and Bcl-xL overexpressed A172, LN18, T98G, and U87MG cells treated with TRAIL for 24 hours.

3.7.1 The effects of Bcl-2 and Bcl-xL overexpression on Bortezomib-mediated re-Sensitization

Bcl-2 or Bcl-xL overexpression conferred resistance to TRAIL in sensitive cells; however, neither Bcl-2 nor Bcl-xL overexpression was enough to override Bortezomib-induced re-sensitization **(Figure 3.36)**.

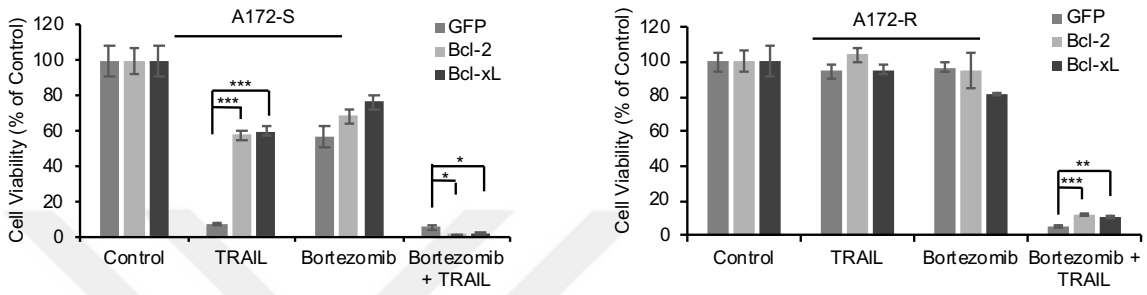
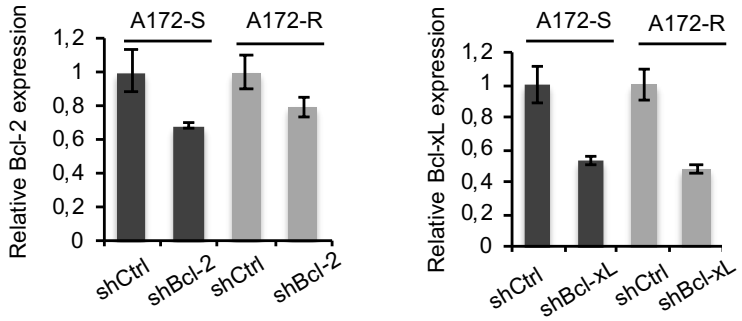


Figure 3.36. Viability analysis of A172-S and A172-R cells overexpressing Bcl-2 and Bcl-xL proteins upon TRAIL (50 ng/ml), Bortezomib (50 nM) and combinational treatment.

3.7.2 The Effects of Bcl-2 And Bcl-xL Downregulation on TRAIL-resistance

To complement of Bcl-2 and Bcl-xL expression on TRAIL resistance, we undertook loss-of-function approach and knocked-down Bcl-2 or Bcl-xL by shRNA in all S and R cells. Knockdown was confirmed by qRT-PCR (**Figure 3.37)**.



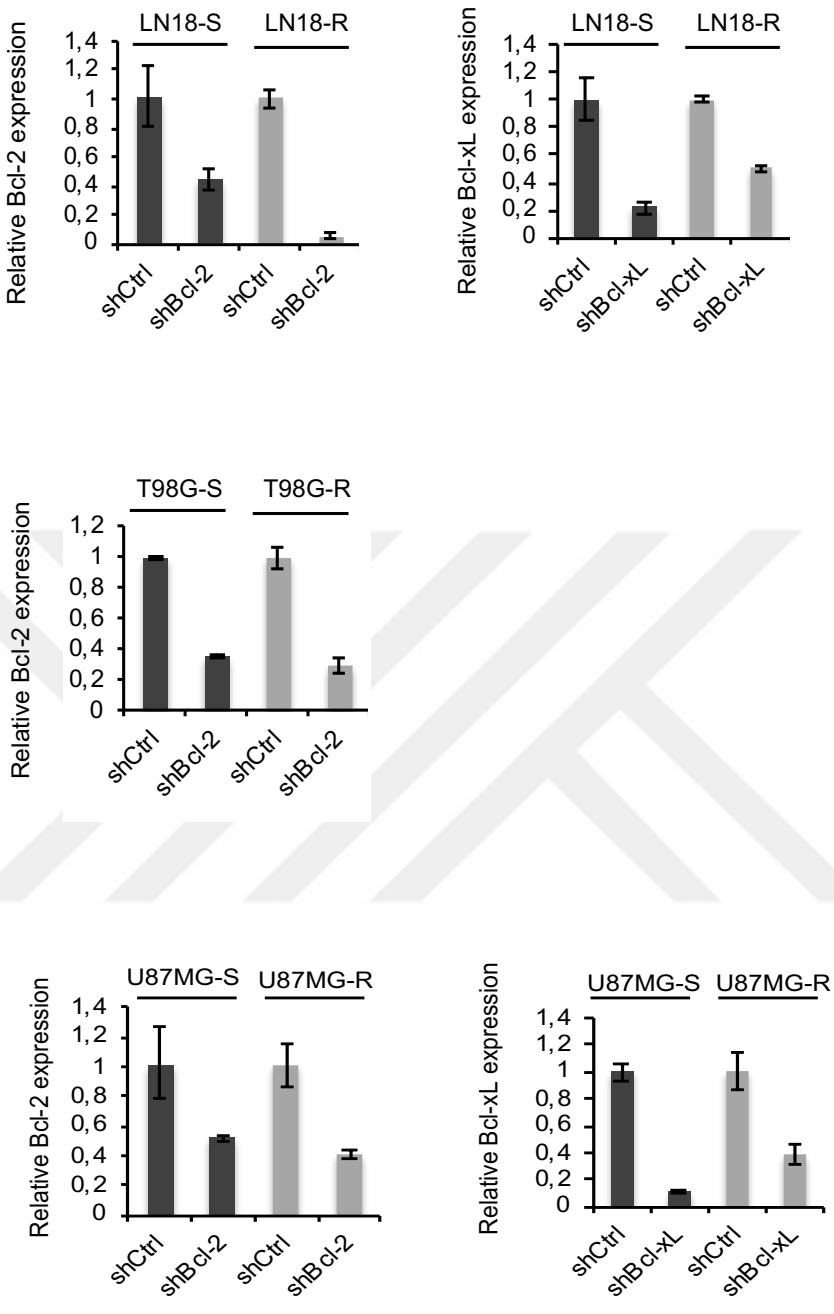


Figure 3.37. qPCR analysis showing shRNA mediated knockdown of Bcl-2 and Bcl-xL in A172, LN18, T98G and U87MG-S and -R cells.

Bcl-2 and Bcl-xL knock-down cells were treated with TRAIL (50 ng/ml for A172, LN18, and T98G cells; 100 ng/ml for U87MG cells) for 24 hours. According to viability results, we did not observe a functional outcome on TRAIL response with partial silencing of Bcl-2 or Bcl-xL expression **(Figure 3.38)**.

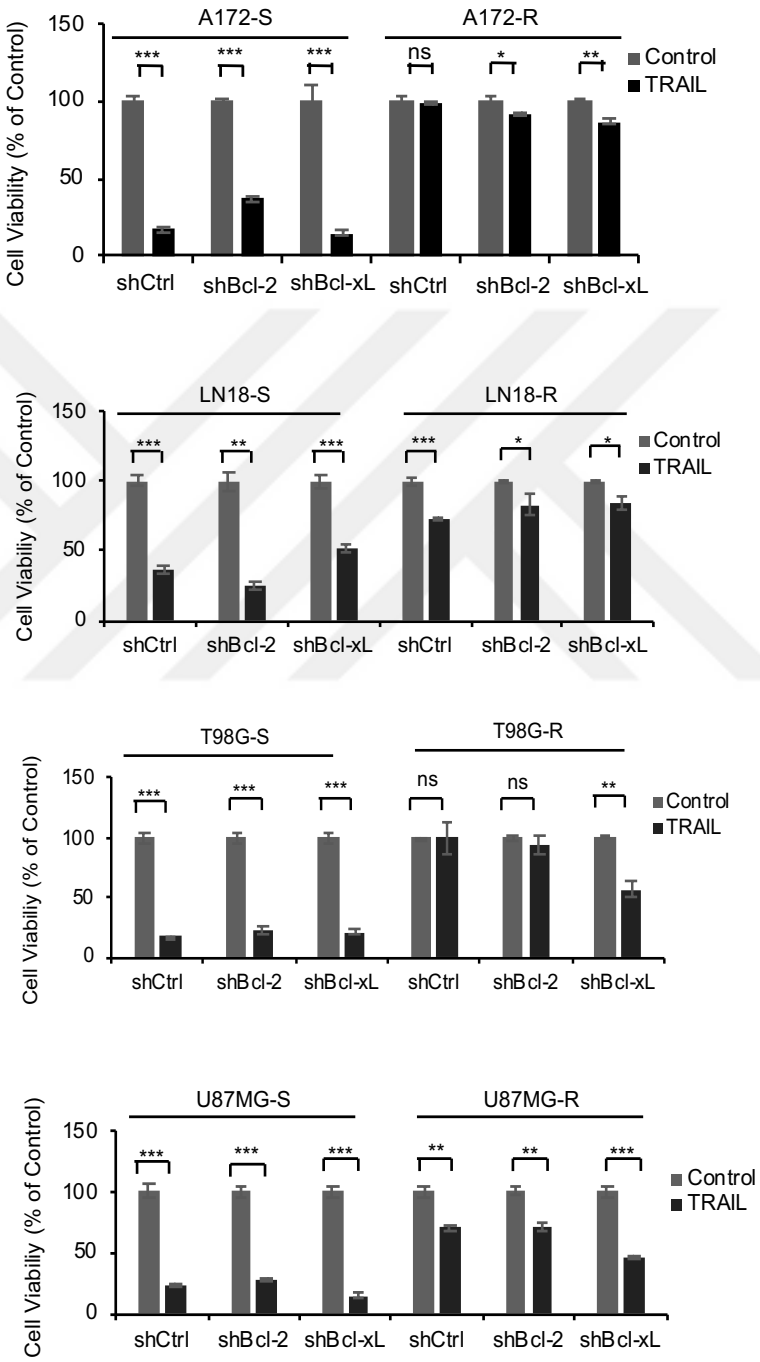


Figure 3.38. Viability analysis of A172, LN18, T98G, and U87MG-S and -R cells treated with TRAIL (50 ng/ml for A172, LN18, and T98G cells; 100 ng/ml for U87MG cells) upon Bcl-2 and Bcl-xL knockdown.

3.8 Re-sensitization of TRAIL-resistant cells by BH3 mimetics

In contrast to Bcl-2 and Bcl-xL knock-down, pharmacological inhibition of Bcl-2 family with BH3 mimetics re-sensitized cells to TRAIL. The combination of BH3 mimetics with TRAIL phenocopied Bortezomib and TRAIL effect. ABT-263 alone did not considerably decrease cell viability, however combination of ABT-263 with TRAIL significantly decreased viability in both A172–S and A172–R cells. Another Bcl-2 family inhibitor, ABT-737, showed a similar effect, and the TRAIL resistance was overcome with combination treatment in TRAIL- resistant cells. Together these results showed that Bcl-2 or Bcl-xL overexpression cannot block Bortezomib mediated re-sensitization; however, their inhibition and TRAIL can cooperate to induce apoptosis in TRAIL-resistant cells **(Figure 3.39)**.

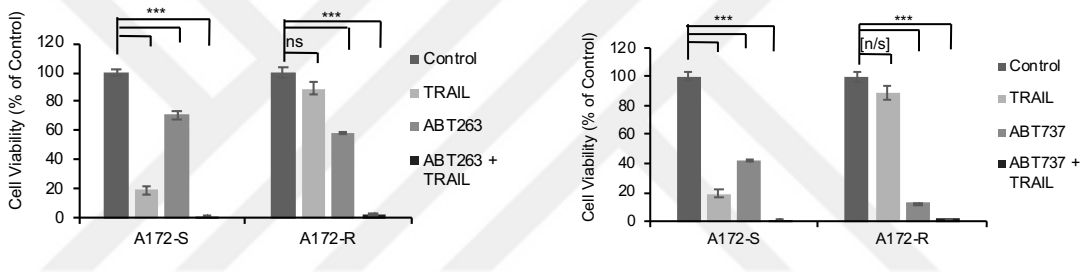


Figure 3.39. Viability results of A172-S and A172–R cells showing significantly reduced viability upon TRAIL (50 ng/ml) and ABT263 and ABT737 (1 uM) treatment for 24h.

3.9 RNA-sequencing of TRAIL-sensitive and -resistant cells

To investigate the molecular mechanisms of acquired TRAIL resistance in this heterogenous tumor cell subpopulations, we conducted RNA-sequencing analysis on all cell lines and their resistant subpopulations (A172-S/R, LN18-S/R, T98G-S/R, and U87MG-S/R). High quality total RNA samples were isolated from two biological replicates of each cell lines and RNA samples were sent to BGI Genome Sequencing Company (Beijing, China). Quality control was performed by Agilent 2100 Bio analyzer (Agilent RNA 6000 Nano Kit). Samples were sequenced at BGISEQ-500 platform to generate 50 bp single-end reads, and about 26.02 M reads per sample were generated. The reads that passed the quality control were aligned to human genome assembly hg19 using HISAT [133], which uses ultra-high-throughput short read aligner Bowtie as its core alignment engine and then analyzes the results to identify splice junctions between exons. The average mapping ratio with reference genome is 95.56%, the average mapping ratio with gene is 84.13%; and total 23,594 genes were detected **(Table 3.1)**. Bioinformatic analysis were performed by Tunç Morova, Koç University School of Medicine.

Sample	Total Raw Reads(Mb)	Total Clean Reads(Mb)	Total Clean Bases(Gb)	Clean Reads Q20(%)	Clean Reads Q30(%)	Clean Reads Ratio(%)
AC1	26.33	26.03	1.30	98.17	90.87	98.87
AC10	25.86	25.74	1.29	98.53	92.35	99.55
AC11	26.13	26.08	1.30	98.44	92.21	99.81
AC12	25.77	25.68	1.28	97.99	90.31	99.66
AC2	26.33	25.84	1.29	98.40	91.73	98.12
AC3	26.33	25.64	1.28	98.50	92.29	97.39
AC4	26.33	26.13	1.31	98.21	90.94	99.24
AC5	26.33	26.29	1.31	98.51	92.26	99.83
AC6	26.33	26.23	1.31	98.64	92.72	99.62
AC7	26.33	26.29	1.31	97.45	88.41	99.85
AC8	26.33	26.26	1.31	98.42	91.82	99.75
AC9	26.11	25.97	1.30	98.47	92.31	99.46

Samples: Sample names
Total Raw Reads(Mb): The reads amount before filtering, Unit: Mb
Total Clean Reads(Mb): The reads amount after filtering, Unit: Mb

Table 3.1. Clean reads quality metrics of sequenced samples.

Hierarchical clustering analyses revealed that biological replicates significantly correlated with each other and the most gene expression changes was observed for A172 cells. Indeed, A172-R cells were the most distant from A172-S cells **(Figure 3.40)**.

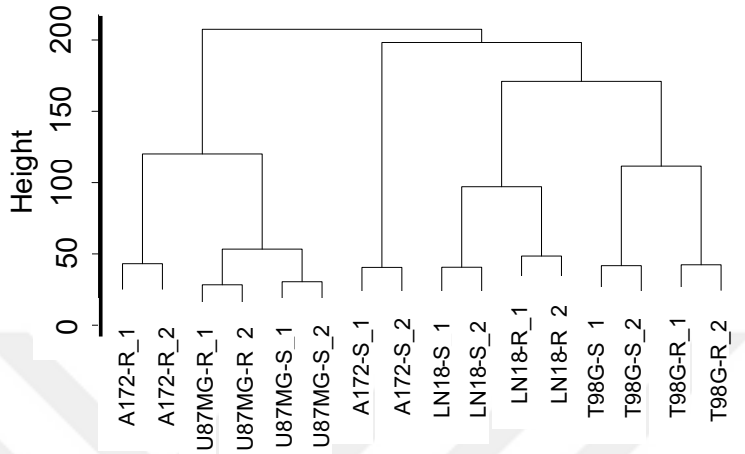


Figure 3.40. Hierarchical clustering between samples.

Differentially expressed genes were identified based on negative binomial distribution using DESeq2 algorithms. Number of differentially expressed genes (DEGs) correlated with these separations. The highest number of DEGs were in A172 cells (3681 upregulated, 3485 downregulated), the least changes were seen in U87MG cells (297 upregulated, 338 downregulated) as shown by bar graph **(Figure 3.41)** and volcano plots **(Figure 3.42)**.

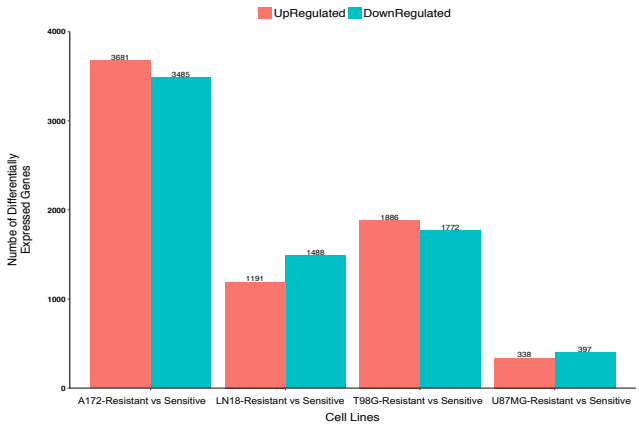


Figure 3.41. Bar graph showing differentially expressed genes (DEGs) in each cell line pair.

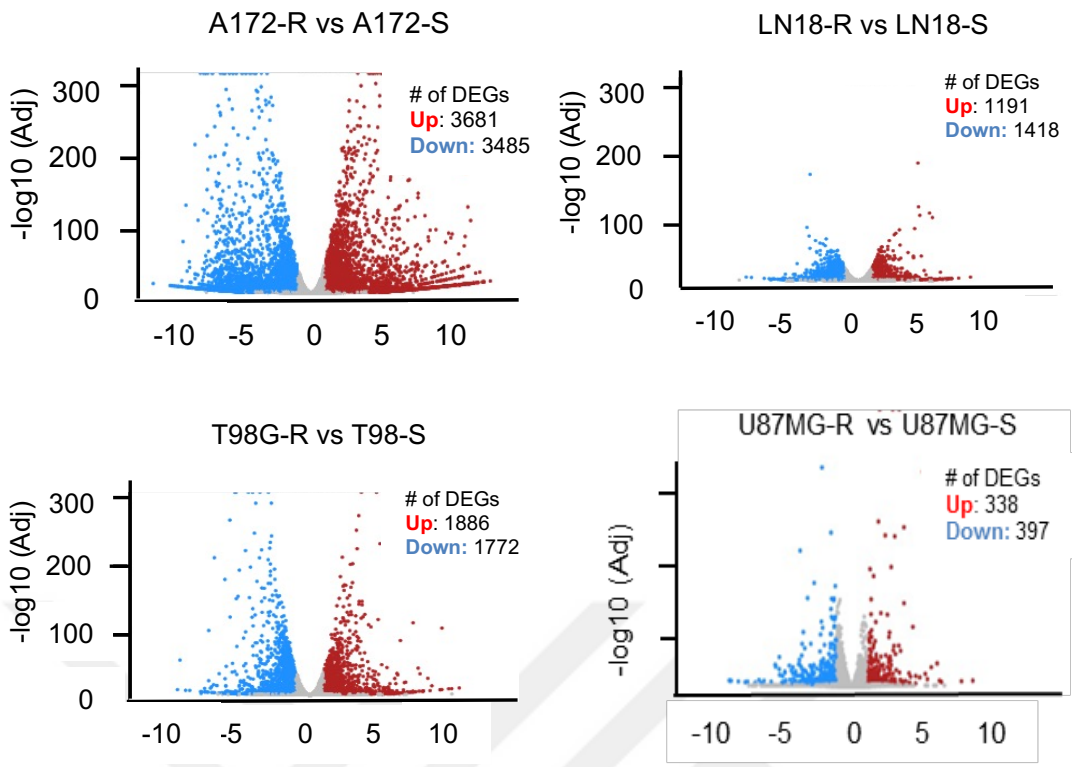


Figure 3.42. Volcano plots showing differentially expressed genes (DEGs) in each cell line pair.

Differentially expressed genes (DEGs) of cell lines were combined and four common upregulated *(PPARGC1A, DAAM2, CXCL14,* and *MEST*), and 8 common downregulated (*HES1, TLR3, TMEM150C, CDYL2, FGF2, GLI1, SLC7A11, KBTBD11*) genes were found (**Figure 3.43**).

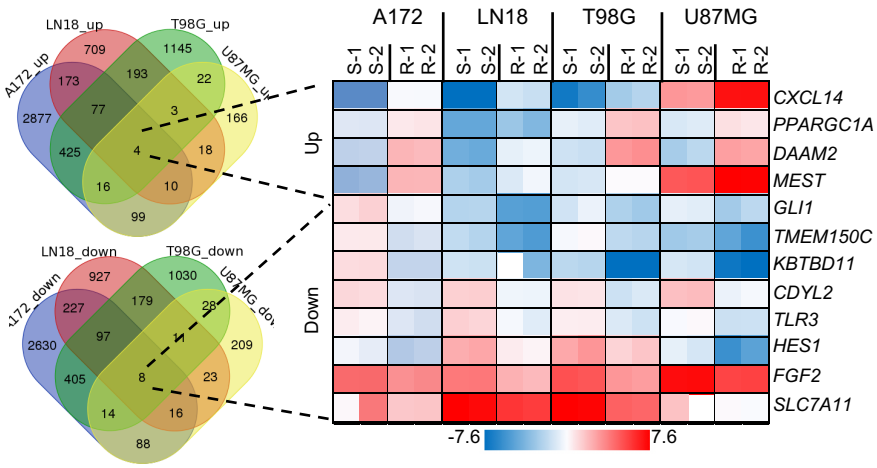


Figure 3.43. Venn diagram and heatmap showing common upregulated and downregulated DEGs in all cell lines.

These common up- and down-regulated genes were listed in **Table 3.2** with expression levels.

Up-regulated

	A172	LN18	T98G	U87MG
PPARGC1A	4,82	2,02	4,02	2,31
DAAM2	41,57	7,18	13,78	10,83
CXCL14	267,56	28,88	11,11	7,13
MEST	203,12	2,75	20,02	3,39

Down-regulated

	A172	LN18	T98G	U87MG
HES1	0,15	0,35	0,45	0,11
TLR3	0,20	0,41	0,39	0,49
TMEM150C	0,16	0,22	0,33	0,29
CDYL2	0,14	0,41	0,33	0,33
FGF2	0,46	0,40	0,30	0,44
GLI1	0,30	0,23	0,39	0,48
SLC7A11	0,16	0,46	0,19	0,40
KBTBD11	0,06	0,40	0,04	0,04

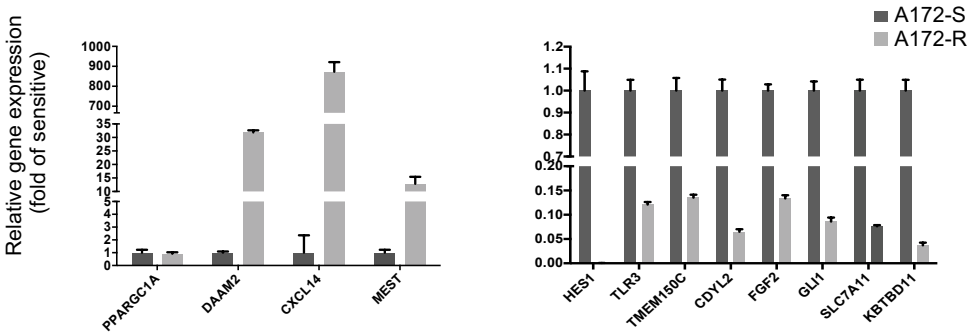
Fold Change

Table 3.2. Common up- and down-regulated gene list.

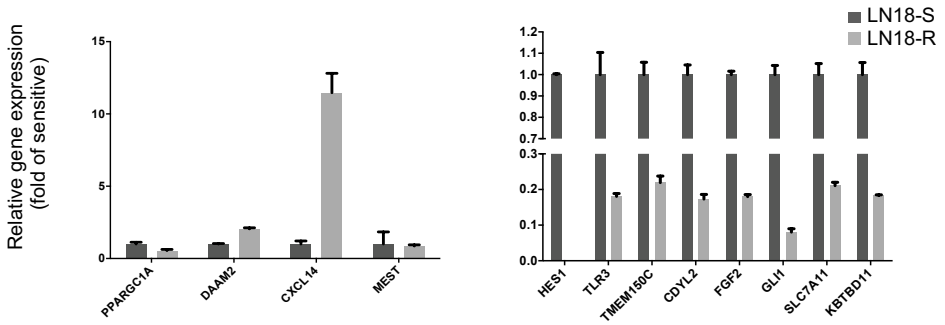
3.9.1 qRT-PCR confirmation of common gene expressions

qRT-PCR analysis confirmed the common gene expression differences obtained from the RNA-sequencing in all cell line pairs (**Figure 3.44**).

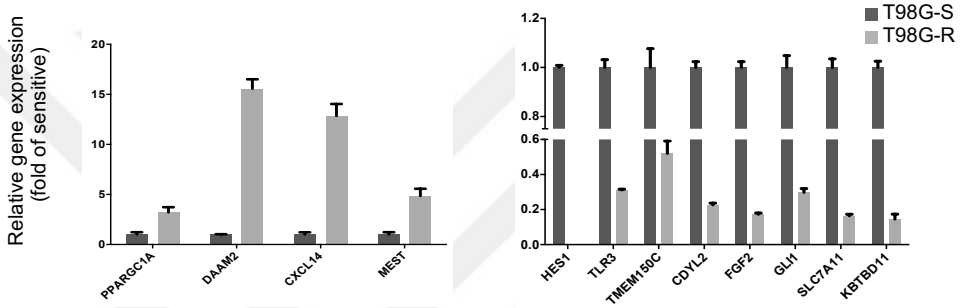
A172:



LN18:



T98G:



U87MG:

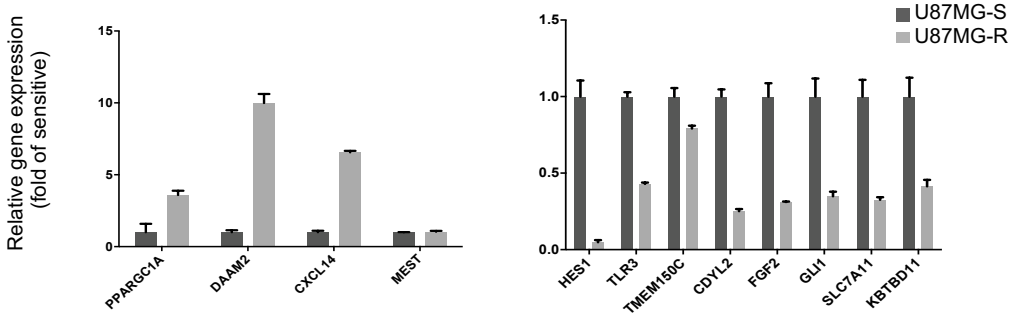


Figure 3.44. qRT-PCR confirmation of common genes.

3.9.2 The effects of Bortezomib on RNA-sequencing related common gene expressions

We tested these common gene expression levels in Bortezomib treated A172-R cells, and we found that *PPARGC1A* and *DAAM2* expression was decreased, *TMEM150C* and *SLC7A11* expression was increased compared with control **(Figure 3.45)**.

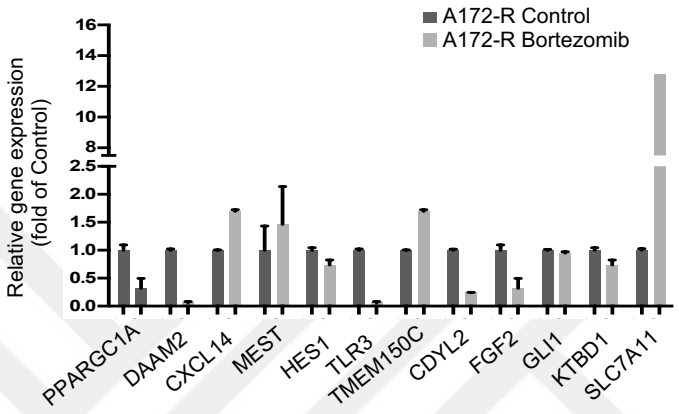


Figure 3.45. qRT-PCR analysis of common genes obtained from RNAseq analysis in A172-R cells treated with Bortezomib.

3.9.3 Functional analysis of RNA sequencing data

To relate the RNA-sequencing results to cell physiologic mechanisms, the complex biological processes during the TRAIL-resistant cell generation as compared to their parental cells (TRAIL-sensitive) were examined in the context of functional groups with Ingenuity Pathways Analysis (IPA), a web-delivered commercial application. Differentially expressed genes (DEGs) data were uploaded to IPA, and each identifier was mapped to its corresponding gene object in the IPA Knowledgebase (www.ingenuity.com). Data were searched and categorized statistically enriched in the differentially expressed gene set, and the likelihood of perturbations in each category was scored. IPA analysis were performed by Dr. Zeynep Hülya Gümüş, Mount Sinai School of Medicine, NY.

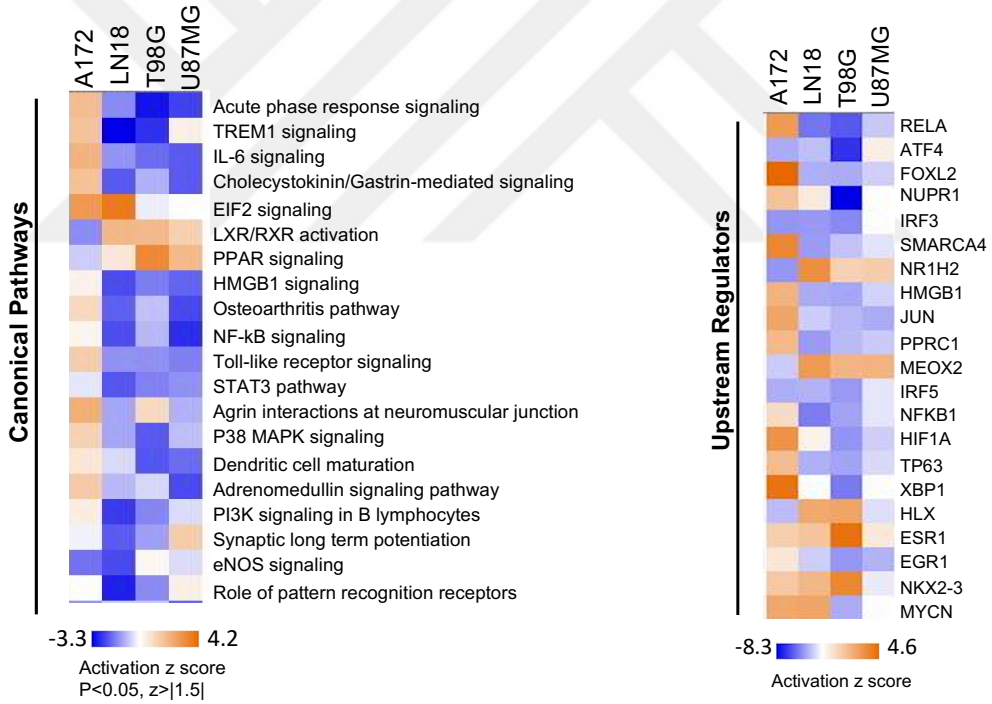
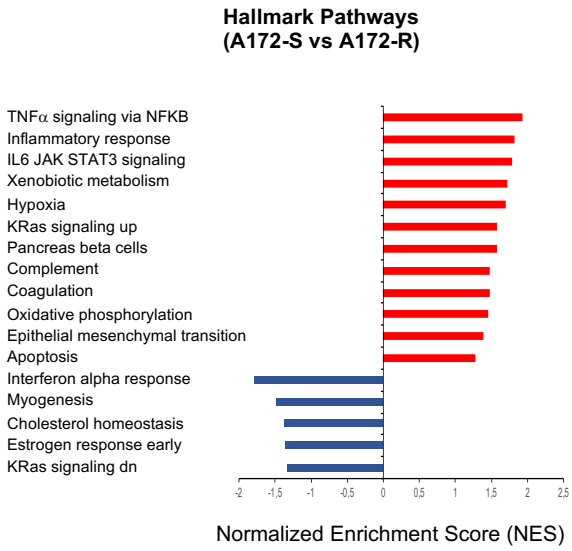


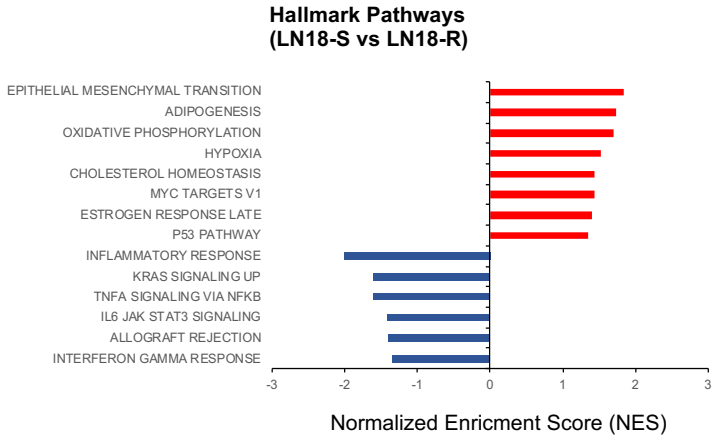
Figure 3.46. Ingenutiy pathway analysis of DEGs showing activation or inhibition of canonical pathways (left) and upstream regulators (right) in each cell line pair.

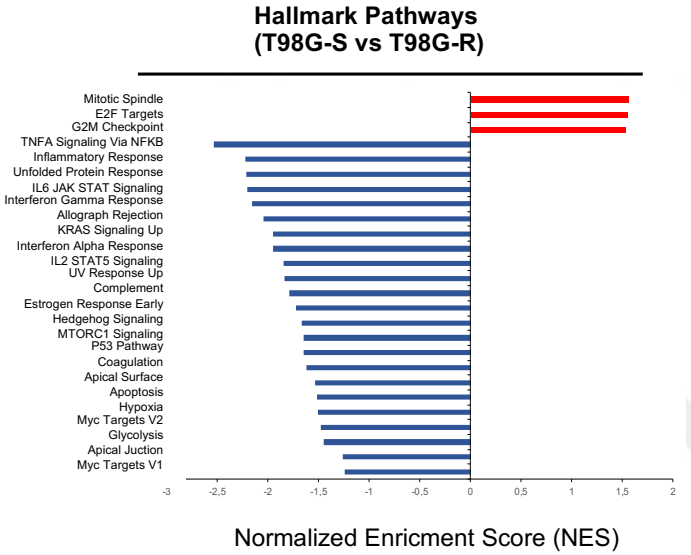
IPA analysis of DEGs revealed major alterations in canonical pathways upon acquired TRAIL resistance. Specifically, inflammation and immune activation related pathways were involved in top 20 of list, such as acute phase response signaling, TREM1 signaling, IL-6 signaling, HMGB1 signaling and NF-κB signaling were activated in A172 TRAIL-resistant cells compared to TRAIL-sensitive cells. On the contrary, these pathways were inhibited in the LN18, T98 and U87MG TRAIL-resistant cells (with negative activation z-scores). These results suggest that acquired TRAIL resistance was caused by different roots in GBM lines. In addition, upstream regulators of transcription factors were analyzed by "upstream regulator analysis" in IPA, and results supported to altered pathways. For example, RelA, NF-κb, or HMGB1 were among activated upstream regulators in A172-R cells **(Figure 3.46)**.

3.9.4 Gene Set Enrichment Analysis (GSEA)

In parallel, we performed the gene set enrichment analysis (GSEA) in RNA-seq data and confirmed the altered pathways in TRAIL-resistant cells compared with -sensitives. Graphs represent the Gene Set Enrichment Analysis (GSEA) results pointing out TRAIL-resistance mediated positively, and negatively enriched hallmark pathways based on their Normalized Enrichment Score (NES) **(Figure 3.47)**.







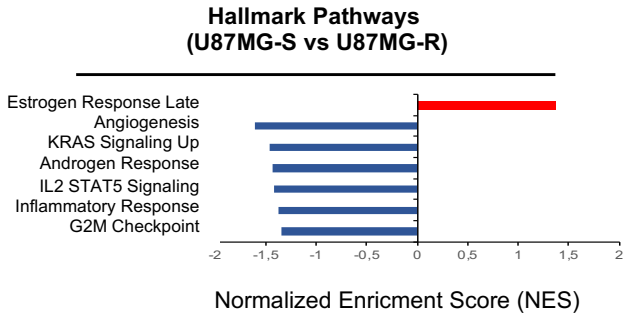


Figure 3.47. Gene Set Enrichment Analysis (GSEA) of A172, LN18, T98G, and U87MG cells.

GSEA confirmed that NF-κB pathway was markedly changed in all GBM cell lines. NF-κB pathway positively enriched in A172 cells (normalized enrichment score (NES): 1,92), and negatively enriched in LN18 (NES: -1,60), T98G cells (NES: -2,53), and U87MG cells (NES: -1,271) **(Figure 3.48)**.

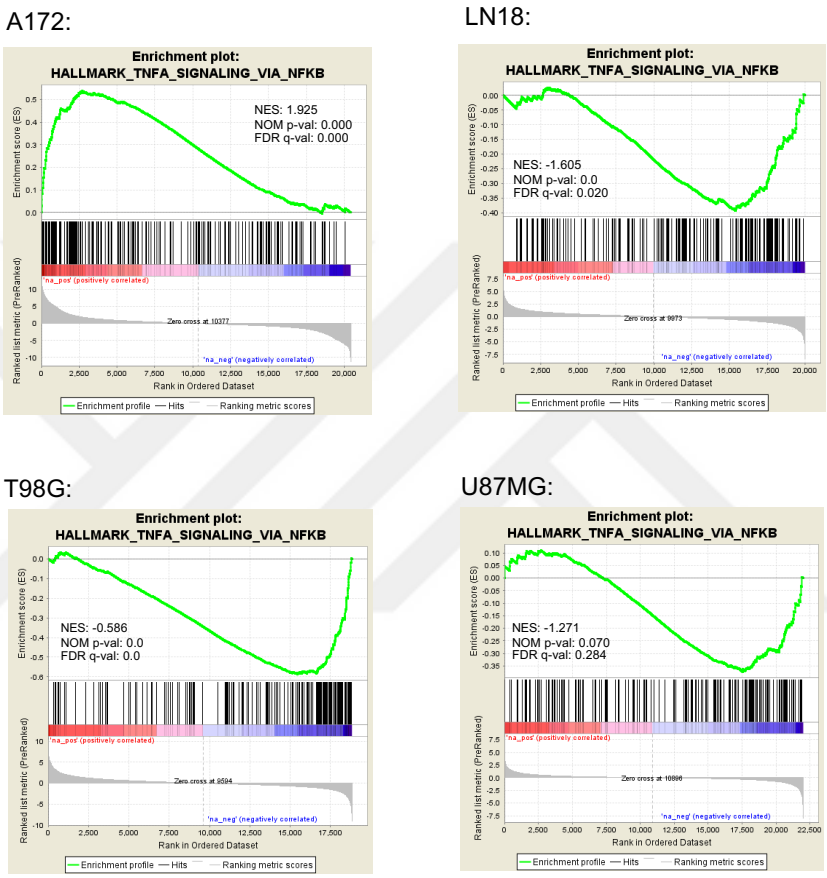


Figure 3.48. Representative enrichment plots for hallmark NF-kB pathway in A172, LN18, T98G and U87MG cells.

To detect the endogenous expression levels of NF-κB, qRT-PCR was performed and demonstrated that *RelA, RelB, NFKB1* and *NFKB2* gene expressions were downregulated in LN18-R, T98G-R and U87MG-R cells. These results supported the inhibited state of the NF-κB pathway in these cells. However, *NFKB2* expression was markedly elevated in A172-R cells, possibly explaining to the activated state in A172-R cells **(Figure 3.49)**.

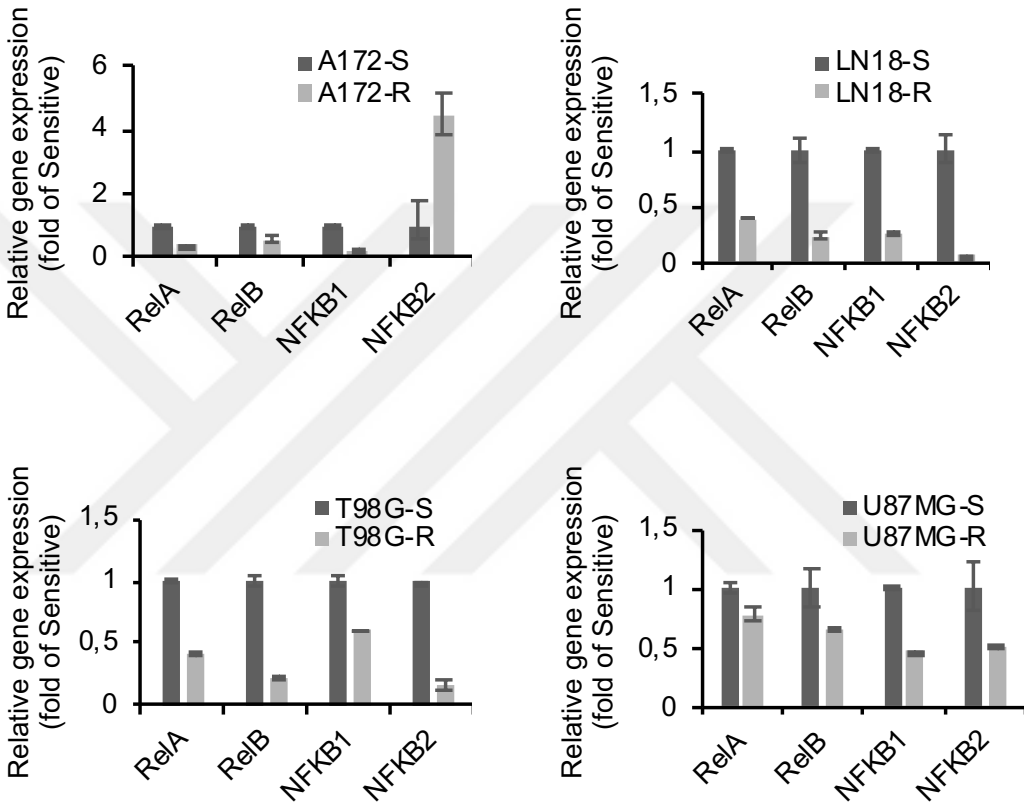


Figure 3.49. qPCR validation of NF-kB related genes (RelA, RelB, NFKB1, NFKB2) in all TRAIL resistant cell lines. Data were normalized to sensitives.

3.9.5 Functional analysis of NF- κB pathway

To functionally test the effects of NF-κB pathway on TRAIL sensitivity, we applied NF-κB inhibitor, QNZ, on A172 cell line pair. Accordingly, A172-R cells were more vulnerable to NF-κB inhibition than A172-S cells as their viability decreased more with QNZ treatment **(Figure 3.50)**.

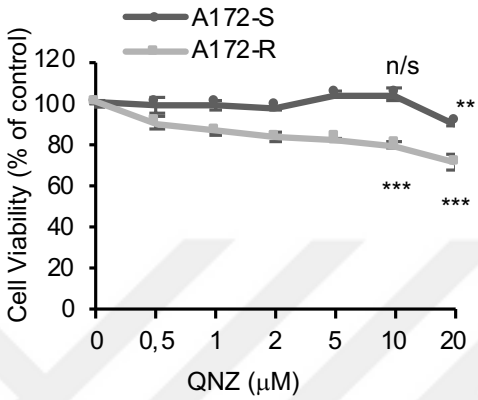


Figure 3.50. Viability of A172-S and -R cells treated with QNZ for 24 h.

Then, we combined the QNZ (20 uM) and TRAIL (50 ng/ml), and QNZ treatment increased the sensitivity of A172 both the A172-S and A172-R cells to TRAIL **(Figure 3.51)**.

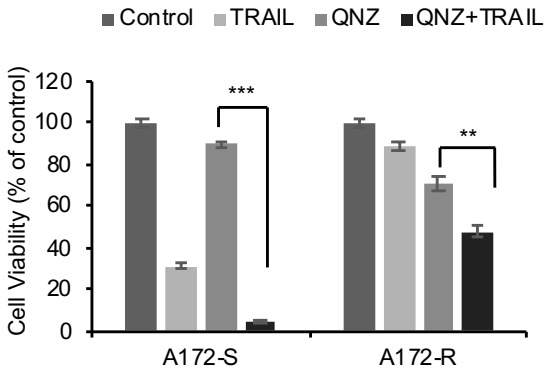


Figure 3.51. Viability analysis of A172-S and A172–R cells treated with QNZ (20 uM) and TRAIL (50 ng/ml) combination for 24h.

3.9.6 Functional analysis of PI3K pathway

The PI3K/Akt pathway is a well-known pro-survival pathway and it was among activated networks in A172-R cells. Also, we tested the ability of the well-known PI3K inhibitor, LY294002, to re-sensitize TRAIL-resistant cells. In contrast of NF-κB inhibition, PI3K inhibition was not sufficient to override acquired TRAIL-resistance **(Figure 3.52)**.

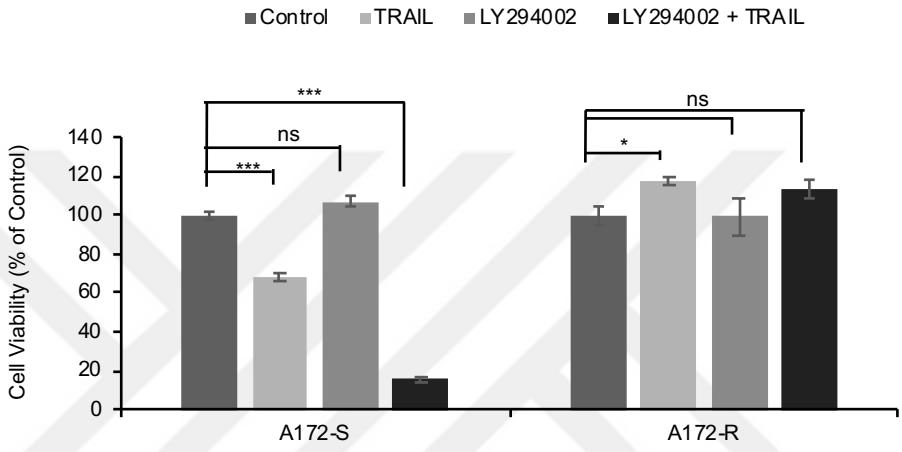


Figure 3.52. Viability analyses of A172-S and –R cells and their treated with PI3K inhibitor (LY294002, 10 uM) and TRAIL combination (50 ng/ml) for 24h.

4 DISCUSSION

In this thesis, we generated acquired TRAIL resistance models using multiple Glioblastoma Multiforme cell lines. We showed that selection of persistent resistant cells was possible through long-term TRAIL exposure. We also demonstrated that TRAIL-resistance of these persistent cells can be overcome by Bortezomib and cells underwent apoptosis upon combination treatment. DR4 and DR5 are important components in TRAIL-induced apoptosis and they were among majorly silenced in our all TRAIL-resistant cells. Additionally, DR4 and DR5 expression was partly restored with Bortezomib treatment; and CRISPR/Cas9 mediated silencing of DR5 could block Bortezomib-mediated re-sensitization; suggesting their adaptive role in acquired TRAIL resistance. Other major apoptosis pathway components in TRAIL resistance were anti-apoptotic Bcl-2 and Bcl-xL proteins. While their functional inhibition could cooperate with TRAIL and promote apoptosis, their overexpression could not override the Bortezomib-mediated re-sensitization. Finally, genome-wide RNA sequencing analysis revealed major alterations during the transition from TRAIL-sensitive to TRAIL-resistant state and identified NF-κB pathway to be markedly changed in all TRAIL-resistant models.

TRAIL resistant cell populations can be derived from GBM cell lines

In TRAIL-resistant cell generation, we described two different methods. We utilized dose-escalation method for the highly TRAIL sensitive cells GBM cells (A172, LN18 and T98) by gradually increasing TRAIL concentration for long term period, which encompassed more than 30 passages. On the other hand, in U87MG cells, mid-sensitive to TRAIL, we applied 3 different TRAIL doses (10, 50, and 250 ng/ml) and selected survivors in a short period. These selection periods varied depending on the cell type. With both approaches, cells were grown in TRAIL-free conditions after the selection period, and cell maintained their resistance, showing a “persistent resistance” phenotype. Their resistance was validated with several in vitro and in vivo experiments. Earlier work for TRAIL-resistance model examined the cause of fractional killing to TRAIL-induced apoptosis. There, cells were exposed to TRAIL for 6 hours, surviving tumor cells exhibited transient refractory phase for 1 day, but then reset to the naïve state within several days [144]. In another study, researchers generated acquired TRAIL resistance in prostate and pancreatic carcinoma cells within 1

day. They removed the undetached cells after 4 hours TRAIL treatment, then cultured the survivors, and following 1-6 days, they re-treated cells with TRAIL and showed the reduced viability and increasing PARP cleavage. In this study, the development of short-term resistance involved the induction of Bcl-xL expression [145]. Similar to our work, TRAIL-resistant ovarian [125], breast [126], or lung cancer cell lines [127,128] were generated through long-time exposure to TRAIL but these cells maintained their resistance in the presence of TRAIL. In our work, the "persistent resistant" cells could be maintained in conditions devoid of TRAIL, suggesting heritable molecular alterations causing resistance. Additionally, resistant phenotype of our cells was not lost under long term TRAIL treatment in both in vitro and in vivo conditions.

In our TRAIL-resistant models, we did not observe major differences in their responses to other apoptosis-inducers such as Fas-ligand (FasL) and Staurosporine. Whereas, FasL binds to their receptors and starts the apoptosis similar the TRAIL pathway [138] and Staurosporine induces apoptosis via intrinsic pathway [139], in contrast with reported cross-resistance of ovarian carcinoma cells to Fas-ligand [125]. When tested for Temozolomide (TMZ), two of the four TRAIL-resistant models exhibited slightly less sensitivity to TMZ, suggesting possible DNA-repair pathway alterations in these models. Known acquired TRAIL-resistant cell models show that the different resistant mechanisms have been occurred during the resistance generation. These findings suggest that our resistant cell models exhibited resistance towards only TRAIL.

Bortezomib re-sensitizes TRAIL-resistant subpopulations to TRAIL

To overcome TRAIL resistance, we applied known TRAIL sensitizers. We showed that the persistent TRAIL-resistant cells were not re-sensitized with known TRAIL sensitizer, MS-275, an HDAC inhibitor, which was previously shown to increase TRAIL response by upregulating DR4/5 levels in GBM cells, and repressing the tumor generation in vivo [87]. The viability of our resistant cells was on the 60% with MS-275 and TRAIL combination. This might suggest that HDAC inhibition might not be the best combination approach in tumors that evolve to a TRAIL-resistant state. However, all of our resistant cells were markedly re-sensitized to TRAIL by the proteasome inhibitor, Bortezomib. Previously reports showed that proteasome inhibitors such as Clasto-lactacystin, could sensitize TRAIL-resistant cells via increased XIAP degradation [126]. Additionally, Bortezomib was

shown to stabilize the pro-apoptotic proteins Caspase-3, t-Bid, Bik and Bim [121,146–148] and made tumors more prone to apoptosis. Our results show both transcriptional and translational effects of Bortezomib in TRAIL-resistant cells. Bortezomib increased Bid levels 2-fold in A172-R cells and 1.3-fold in T98G-R cells compared with untreated cells. Even if Caspase-3/7 activity was not elevated by Bortezomib alone in TRAIL-resistant cells, when we inhibit the caspases with general caspase inhibitor, sensitization reversed and resistant cells continued to survive. Additionally, studies showed that anti-apoptotic proteins decreased with Bortezomib treatment, and suggested that these suppression is realized through NF-kB pathway [149], and/or PI3K/Akt pathway [150] in different cell lines. Specifically, we observed Bortezomib-mediated upregulation of DR4/5, Bid, or Noxa and downregulation of decoy receptor-2 (DcR2), Bcl-2, Bcl-xL, or Survivin in accordance with earlier studies [49,151–154]. In addition to studies showing increased death receptor levels, Bychkov et al showed that apoptotic signaling shifted from DR4 to DR5 with Bortezomib and TRAIL combination in colorectal carcinoma cell lines [155]. These findings were consistent with our results, DR5 expression levels significantly upregulated with Bortezomib in all TRAIL-resistant cell lines. Our results also demonstrated the essentiality of DR5 in Bortezomib mediated TRAIL re-sensitization by CRISPR/Cas9 mediated DR5 silencing in resistant cells. Overall, Bortezomib can be a powerful reagent to revert tumor cell apoptotic resistance that evolve over long time. However, given the reports on possible hepatotoxicity of TRAIL/Bortezomib combination [151], using novel on-site delivery systems or different proteasome inhibitors such as MG132 and PS-341[156] might be alternative approaches to overcome resistance.

Bcl-2 and Bcl-xL expression related with TRAIL-resistance, but cannot override Bortezomib-mediated re-sensitization

An important class of apoptosis regulators, which we reported to be altered in resistance and Bortezomib-mediated re-sensitization is the Bcl-2 family proteins. Bcl-2 family proteins, one of the largest regulators of apoptosis, have Bcl-2 homology (BH) domains and interact with each other. It is well established that the balance in expression and activity of pro- and anti-apoptotic Bcl-2 family members is critical in deciding cells' fate during apoptotic state, and this balance is controlled by several signaling pathways [157–159]. Increasing of anti-apoptotic Bcl-2 family members, such as Bcl-xL, can be seen during TRAIL resistance generation, even during transient resistant conditions [145]. To this end, BH3 mimetics were designed for inhibitor or activator function of specific target proteins with

BH3 domain [160]. Our work specifically on the apoptosis regulators demonstrated that Bcl-2 and Bcl-xL expression played a major role in regulating the TRAIL response. For this purpose, we used sh-RNAs for knockdown of Bcl-2 and Bcl-xL, and ABT-737 [161] and ABT-263 [162] for pharmacologically targeting. Furthermore, functional modulation of Bcl-2 and Bcl-xL, or BH3 mimetic applications, changed the apoptotic outcome of GBM cell lines. Forced overexpression of Bcl-2 or Bcl-xL acquired resistance to TRAIL in sensitive cells, but it was not sufficient to brake Bortezomib-mediated re-sensitization. Knock-down of these proteins did not show functional effect to TRAIL, however, using BH3 mimetics ABT-737 or ABT-263 in combination with TRAIL was effective for both TRAIL-sensitive and TRAIL-resistant cells. Knock-down of Bcl-2 and Bcl-xL proteins could not be enough for overcoming the functional effect, and cells compensated this. However, pharmacological inhibition can target from wide spectrum (Bcl-2, Bcl-xL, and Bcl-w inhibition, and/or accumulation of pro-apoptotics) and achieved overcoming the resistance. These results support earlier findings on the combinatorial efficacy of small molecule Bcl-2 inhibitors and TRAIL [163–167], and are novel to demonstrate this efficacy in acquired TRAIL-resistance models.

Gene expression profiling reveals the alteration of multiple pathways in TRAIL-resistance

Our genome wide transcriptional analysis on the paired TRAIL-sensitive and TRAIL-resistant cell populations revealed high number of differentially expressed genes and pathways in our GBM cell models. Of note, a well-known pro-survival PI3K/Akt pathway was among activated networks in A172-R cells. PI3K/Akt pathway is one of the active pathways, and PTEN, a negative regulator of PI3K signaling, is frequently mutated in GBM. Additionally, several PI3K pathway inhibitors are evaluated in clinical trial studies alone or in combination with TMZ, or other anti-cancer drugs in GBM. [45,46]. Given the reports on the cooperation of PI3K inhibitors and TRAIL in tumor cells [97,150], we tested the ability of the well-known PI3K inhibitor, LY294002, to re-sensitize TRAIL-resistant cells. However, PI3K inhibition was not sufficient to override acquired TRAIL-resistance. We have seen that similar effect with PPARG inhibition and HES1 overexpression **(Appendix A)**. *PPARGC1A* gene was one of the upregulated genes in all TRAIL-resistant cells and expression was decreased Bortezomib treatment. Inhibition of this pathway with PPARG antagonist partially sensitized A172-R cells to TRAIL. Similarly, *HES1* was a downregulated gene in all TRAIL-

resistant cells. Overexpression of HES1 decreased cell viability in A172-S cells, and again partially sensitized A172-R cells to TRAIL. Functional manipulation of either of these molecules were not enough to overcome TRAIL resistance as much as Bortezomib. These findings suggest the role of other existing networks.

On the other hand, insulin like growth factor binding protein-2 (IGFBP-2) was highly elevated in U87MG TRAIL-resistant sub-populations (U87MG-R250) **(Appendix C)**. IGFBP-2 is associated with chemoresistance in different type of cancers including GBM (Hoeflich et al. 2001; Lin et al. 2009). In addition, increased plasma levels of IGFBP-2 in high grade glioma patients (Han et al. 2014) were reported. However, molecular function of IGFBP-2 in GBM has not been known. Studies suggested that IGFBP-2 plays invasion related role in GBM [171], and its inter-cellular regulation is controlled by PTEN [172]. Elevation of IGFBP-2 in TRAIL resistant cells may be controlled by different survival associated pathways including PI3K/Akt signaling because of the PTEN, which is negative regulator of both IGFBP-2 and PI3K. However, manipulation of IGFBP-2 expression did not change the outcome in our U87MG cells against to TRAIL, similar with the inhibition of PI3K pathway in TRAIL-resistant A172 cells. In contrast, exogenous IGFBP-2 treatment partially increased the cell proliferation and TRAIL-resistance in our cells. Additionally, IGFBP-2 as a target of NF-kB network was known for promoting colon cancer cells [173], suggesting inhibition of NF-kB pathway may decrease the expression levels of IGFBP-2 and contribute to overcome of TRAIL resistance in GBM.

NF-kB family is one of the major transcriptional factors to control of cell proliferation, inflammatory response and apoptosis. After receiving the activation signals from DR4 and DR5, via RIP (RPA-interacting protein), sub-units go to nucleus to start transcriptions of its target genes including pro- and anti-apoptotic proteins [66]. NF-kB pathway was a commonly affected pathway in our TRAIL-resistant cells. It was activated in A172-R cells but silenced in the other resistant models. The activation of NF-kB pathway was in accordance with previously published work on the interaction between inflammation and apoptosis, and its activity increased upon TRAIL exposure [124,174,175]. Earlier studies reported that the sensitization of tumor cells to TRAIL-induced apoptosis by inhibition of NF-kB pathway. [176,177] Additionally, enhancing of survival or proliferation by NF-kB has been tried to explain by increasing the anti-apoptotic and inhibiting the pro-apoptotic

proteins. Different role of NF-kB sub-units of RelA and c-Rel has been proposed to regulate TRAIL-induced apoptosis. Overexpression of RelA decreased expression of death receptors and caspase-8, while increasing of apoptosis inhibitory proteins (c-IAP1 and 2) upon TRAIL treatment. In contrast, c-Rel overexpression increased death receptor and Bcl-Xs expressions, and inhibited anti-apoptotic proteins such as surviving and c-IAP1 and 2 [66,178,179]. In our study, we also showed the ability of an NF-kB inhibitor, QNZ, to sensitize all tumor cells to TRAIL. Taken together, our results suggest that inflammatory associated pathways are markedly altered in acquired TRAIL-resistant cell line models and manipulation of this pathway can alter TRAIL response of resistant cells. Our work is the first to show the alteration of the NF-kB network in persistent resistant cells and that its manipulation as a potential future therapy approach to overcome resistance.

One of the reasons for the therapeutic resistance of GBM is intratumoral heterogeneity [11,117,118] which is one of the hallmark of tumor and the biggest challenge of the clinical success. Indeed, the resistant "drug-tolerant" cell populations exhibit large scale genetic and epigenetic variety [119,120]. Therefore, the acquired therapy resistance might be a consequence of both the clonal expansion of already existing resistant tumor cells and the acquisition of resistant state during the treatment period. Clonal growing populations accumulate driver mutations as a result of althered DNA-damage response pathways during the chemotherapy treatment, and members of tumor population exhibit heterogenic response to chemotherapeutic agents [22]. On the other hand, inter-cellular protein dynamics may be enough to contribute the heterogenic phenotype of population. In this context, earlier studies showed that dying cells exhibit duration variety intervals between TRAIL exposure of cells and death from minutes to hours [121]. This "fractional killing" depends on the differences of expression levels of pro- and anti-apoptotic proteins [122,123]. Interestingly, our live cell experiments clearly revealed this time differences, there was at least 6 hours death time differences between sensitive and resistant populations in combination treatment with TRAIL and Bortezomib. In contrast with earlier works, our acquired TRAIL resistant cells never reset the resistant phenotype, suggesting heritable molecular alterations causing the resistance.

Together, our findings, which are summarized as a model in **Figure 4.1**, show that different TRAIL-resistant populations can be generated from GBM cell lines by long term TRAIL exposure and that the resistance is maintained and heritable. Proteasome inhibition, targeting or modulating NF-kB activity can revert the acquired resistant cells back to sensitive state by altering the apoptotic machinery in favor of apoptosis. Therefore, combination of proteasome inhibitors with locally delivered pro-apoptotic ligands can serve as excellent therapeutic approaches in therapy-resistant GBMs.

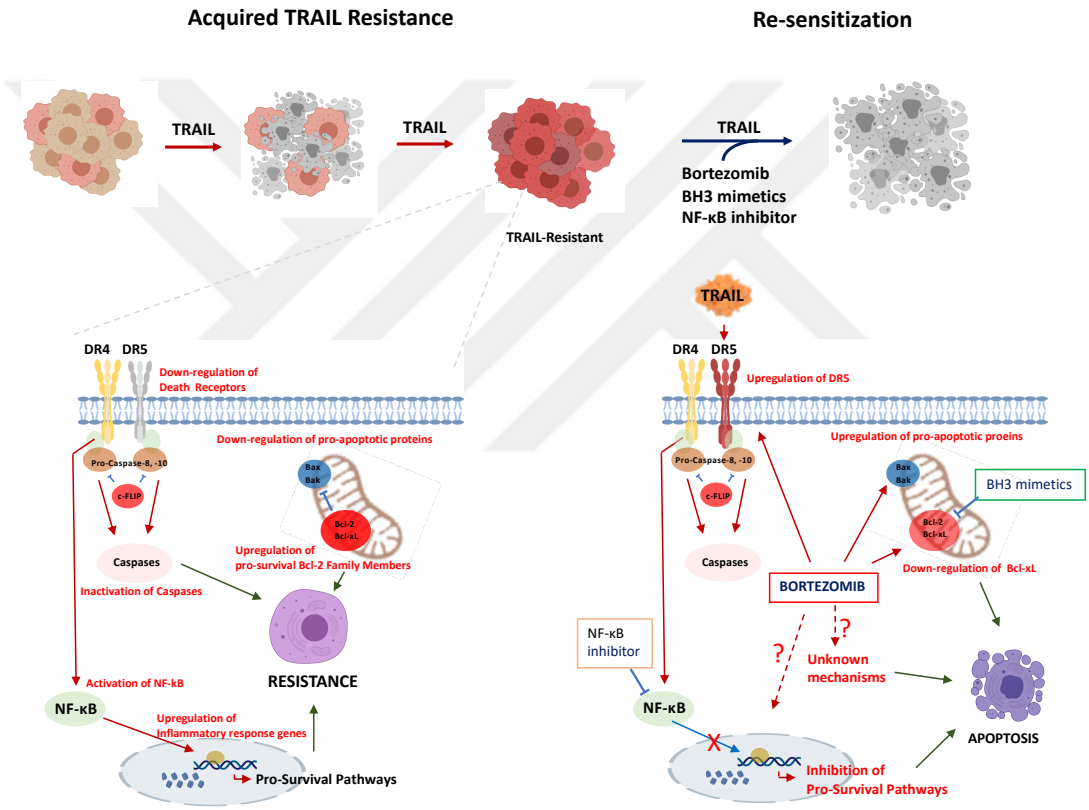


Figure 4.1. Model for generation of TRAIL resistance and re-sensitization of resistant cells with different agents.

5 Appendix I

5.1 Knock-Out of Up-Regulated Genes by CRISPR/Cas9

Up-regulated common genes obtained from RNA-seq data were knocked-out by CRISPR/Cas9 system in A172-S and -R cells. gRNA sequences were picked from GeCKO Library v2 [131], and all gRNAs target the first exon of genes **(Figure 5.1)**.

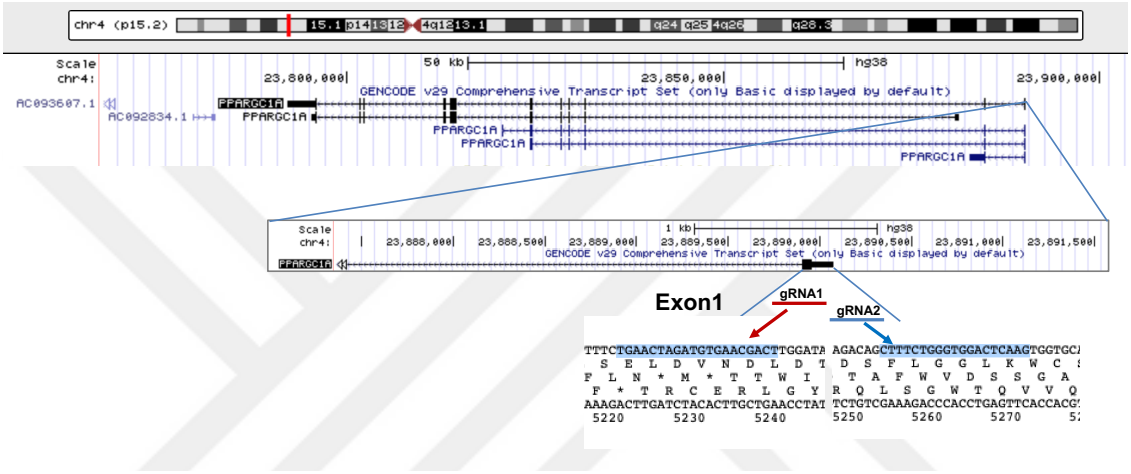


Figure 5.1. Representative showing of genomic map of PPARGC1A gene. gRNAs were designed based on the first exon of gene located on chromosome 4.

Gene		Sequence
gCXCL14-1	F	CACCGGCACCAAGCGCTTCATCAAG
	R	AAACCTTGATGAAGCGCTTGGTGCC
gCXCL14-2	F	CACCGGCCAAAGTACCCGCACTGCG
	R	AAACCGCAGTGCGGGTACTTTGGCC
gDAAM-1	F	CACCGGCACCAAGCGCTTCATCAAG
	R	AAACCTTGATGAAGCGCTTGGTGCC
gDAAM-2	F	CACCGGCCAAAGTACCCGCACTGCG
	R	AAACCGCAGTGCGGGTACTTTGGCC
gMEST-1	F	CACCGCATCGACCGCATCAATTCCA
	R	AAACTGGAATTGATGCGGTCGATGC
gMEST-2	F	CACCGGAGTCTGTACGCGTTTGATG
	R	AAACCATCAAACGCGTACAGACTCC
gPPARGC1A-1	F	CACCGCTTTGGCTTCAGTGACAAAC
	R	AAACGTTTGTCACTGAAGCCAAAGC
gPPARGC1A-1	F	CACCGGAAGTTCAGAAGGCGCTGGG
	R	AAACCCCAGCGCCTTCTGAACTTCC
g-NT1	F	CACCGACGGAGGCTAAGCGTCGCAA
	R	AAACTTGCGACGCTTAGCCTCCGTC

Table 5.1. List of gRNA sequences used in CRISPR/Cas9 experiments.

Knocked-out cells were tested for TRAIL response; however we have not seen any significant sensitization effect to TRAIL in A172-R cells **(Figure 5.2)**.

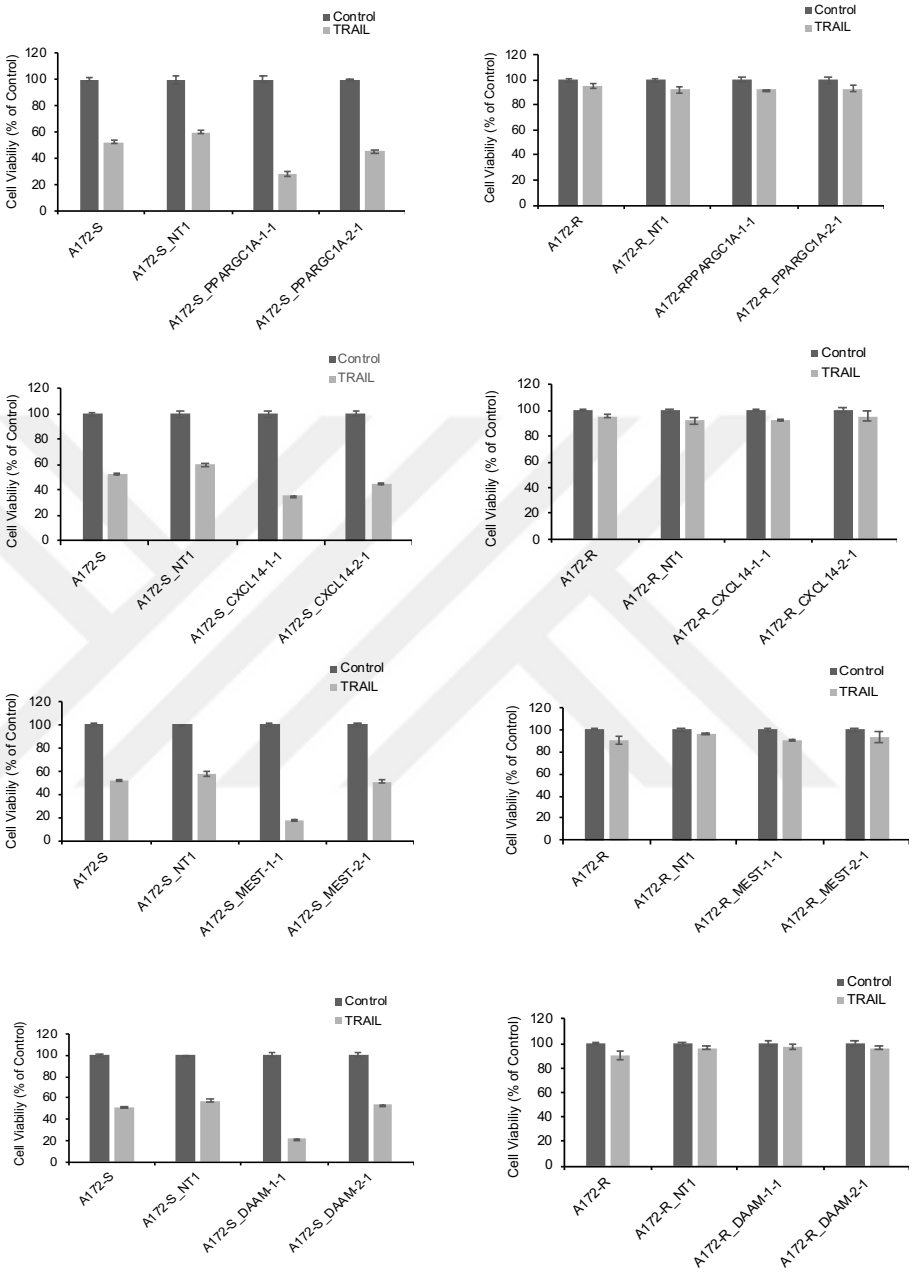


Figure 5.2. Viability of PPARGC1A, CXCL14, MEST, and DAAM genes by CRISPR/Cas9 in A172 cells treated with TRAIL (50 ng/ml) for 24 h.

5.2 Overexpression of HES1 Gene

HES1, a major downregulated gene in all TRAIL-resistant cells, was overexpressed in A172 cells. For overexpression, HES1 vector was purchased from DNASU (#HsCD00043345) and cloned to pLEX307 (Addgene plasmid #41392) vector by Gateway cloning. After the lenti-viral packaging, A172 cells were transduced and antibiotic selection was performed. HES1 overexpression was tested with qRT-PCR **(Figure 5.3)**.

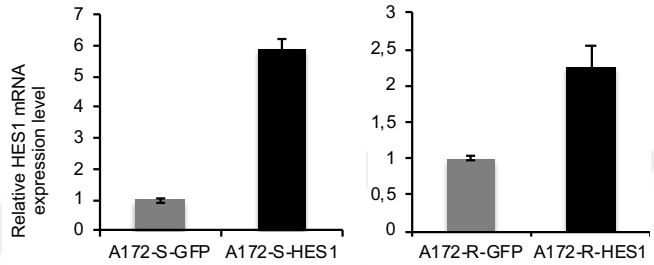


Figure 5.3. qRT-PCR confirmation of HES1 overexpression in A172-S and R cells.

After the confirmation, TRAIL response of HES1 overexpressed A172-S and -R cells were tested, and treated with TRAIL (50 ng/ml) for 24 hours. Viability results showed that HES1 overexpression partly sensitized A172 cells to TRAIL, suggesting its possible role in regulating TRAIL sensitivity **(Figure 5.4)**.

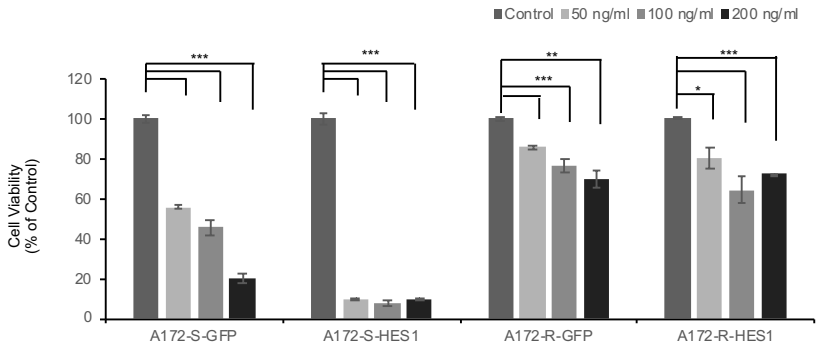


Figure 5.4. Viability of HES1 overexpressed A172-S and -R cells treated with TRAIL (50 ng/ml) for 24 h.

5.3 Inhibition of PPARG Pathway

PPARGC1A gene is one of the upregulated gene in all TRAIL-resistant cells and expression was decreased Bortezomib treatment. For this reason, we inhibited the PPARG by using GW9662, which is a selective PPARγ antagonist. First, drug was applied with different doses for 24, 48, and 72 hours **(Figure 5.5)**.

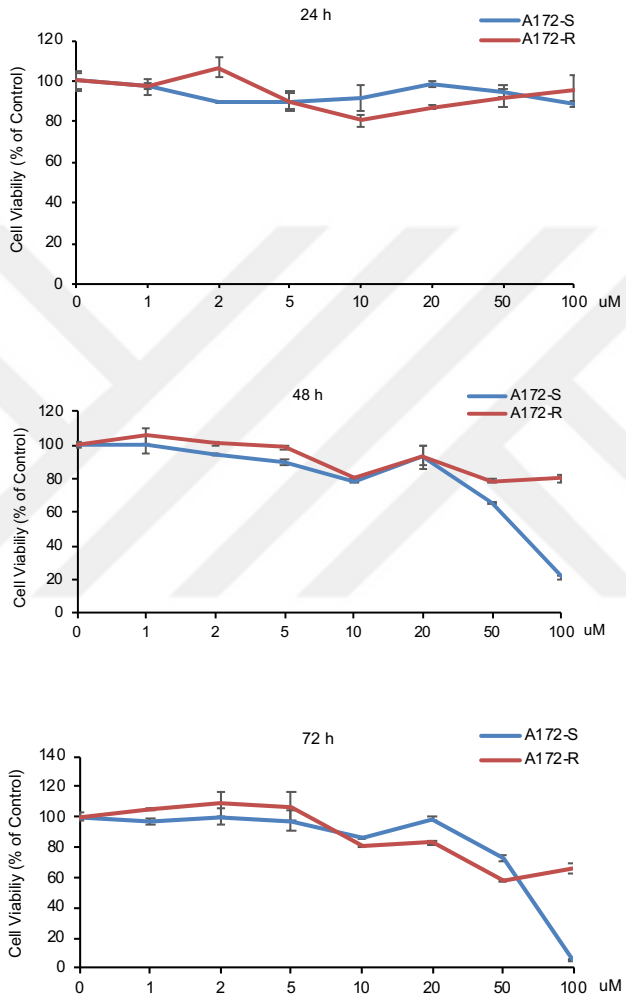
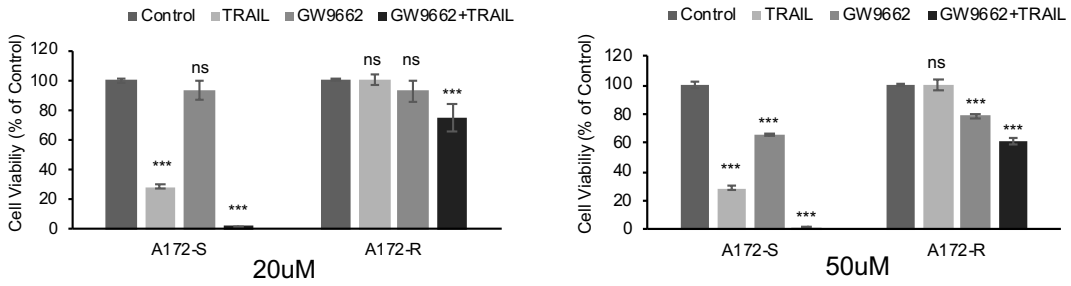


Figure 5.5. Viability of A172-S and -R cells treated with GW9662 for 24, 48, and 72 hours.

Then, GW9662 and TRAIL combination was applied, and viability results showed the PPAR inhibition significantly sensitized A172-S cells and partially sensitized A172-R cells to TRAIL in both 48, and 72 hours **(Figure 5.6)**.

48 hours:



72 hours:

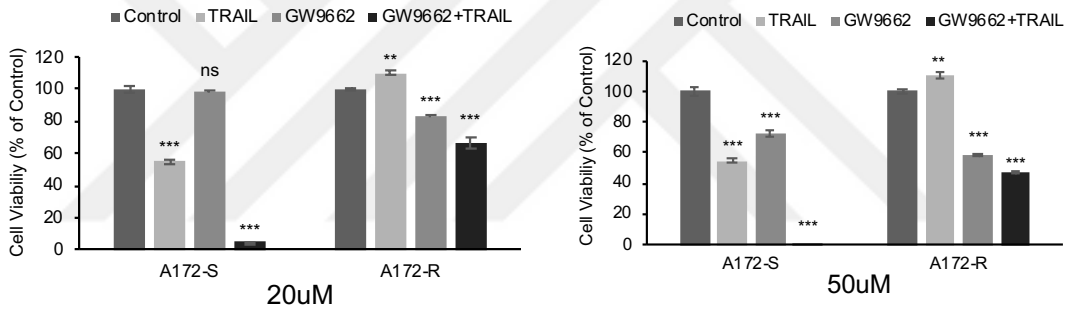


Figure 5.6. Viability of A172-S and -R cells treated with GW9662 and TRAIL combination for 48, and 72 hours.

6 Appendix II

6.1 RNA sequencing of U87MG TRAIL-resistant Sub-Populations

In addition to 4 different GBM TRAIL-resistant cell lines, to focus on specifically TRAIL resistant R50 and R250 cells derived from U87MG, we did RNA-sequencing. Because U87MG cells are mid-sensitive to TRAIL and sub-populations were selected with fixed TRAIL doses (50 ng/ml and 250 ng/ml) in less-time compared with other three cell lines (A172, LN18, and T98G).

For RNA sequencing, three biological replicates of R0 (control), R50 and R250 cells were seeded on 10 cm plates and after 24 hours, cells were collected by trypsinization. Total RNA of all samples was isolated using RNeasy RNA Isolation Kit (QIAgen). High quality RNA samples (A260/280 > 2) were sent for RNA-sequencing, and it was performed at Weill Cornell Medical College (WCMC) epigenomics core. Statistical and functional analysis of the RNA-seq data was carried out by Dr. Zeynep Hülya Gümüş. Differentially expressed genes (DEGs) of R50 and R250 against to R0, control, were detected.

6.2 Functional Analysis of RNA-Seq Data of R50 and 250 Cells

To correlate between the functional groups and gene alterations in R50 and R250 cells, Ingenuity Pathways Analysis (IPA) analysis were performed. Accordingly, cancer and cell death and survival related “disease and functions” groups were activated in U87MG-TRAIL resistant cells **(Figure 6.1)**.

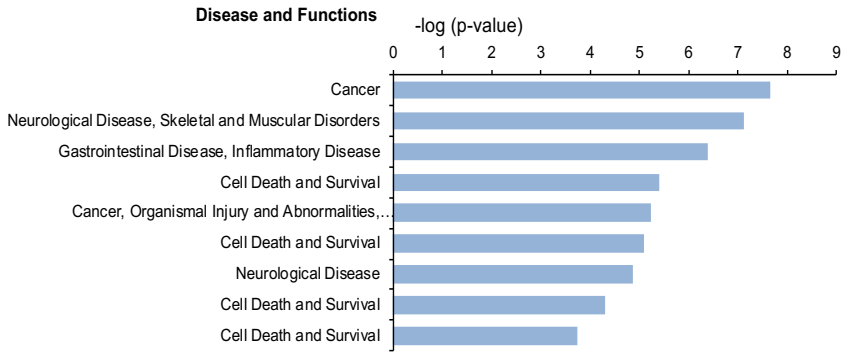


Figure 6.1. Disease and Functions of IPA analysis in U87MG TRAIL-R cells.

Additionally, IPA analysis of DEGs revealed major alterations in canonical pathways upon acquired TRAIL resistance. Similar with other 4 cell lines, inflammation and immune activation related pathways were involved in top of the list, such as NF-κB signaling, acute phase response signaling, IL-6 signaling were inhibited in both R50 and R250 U87MG TRAIL-resistant cells (with negative activation z-scores). In contrast, PPAR signaling and LXR/RXR activation were activated. In addition, upstream regulators of transcription factors were analyzed by "upstream regulator analysis" in IPA, and results supported to altered pathways. For example, RelA, JUN, FOS were among inhibited upstream regulators in U87MG-R50 and R250 cells **(Figure 6.2)**.

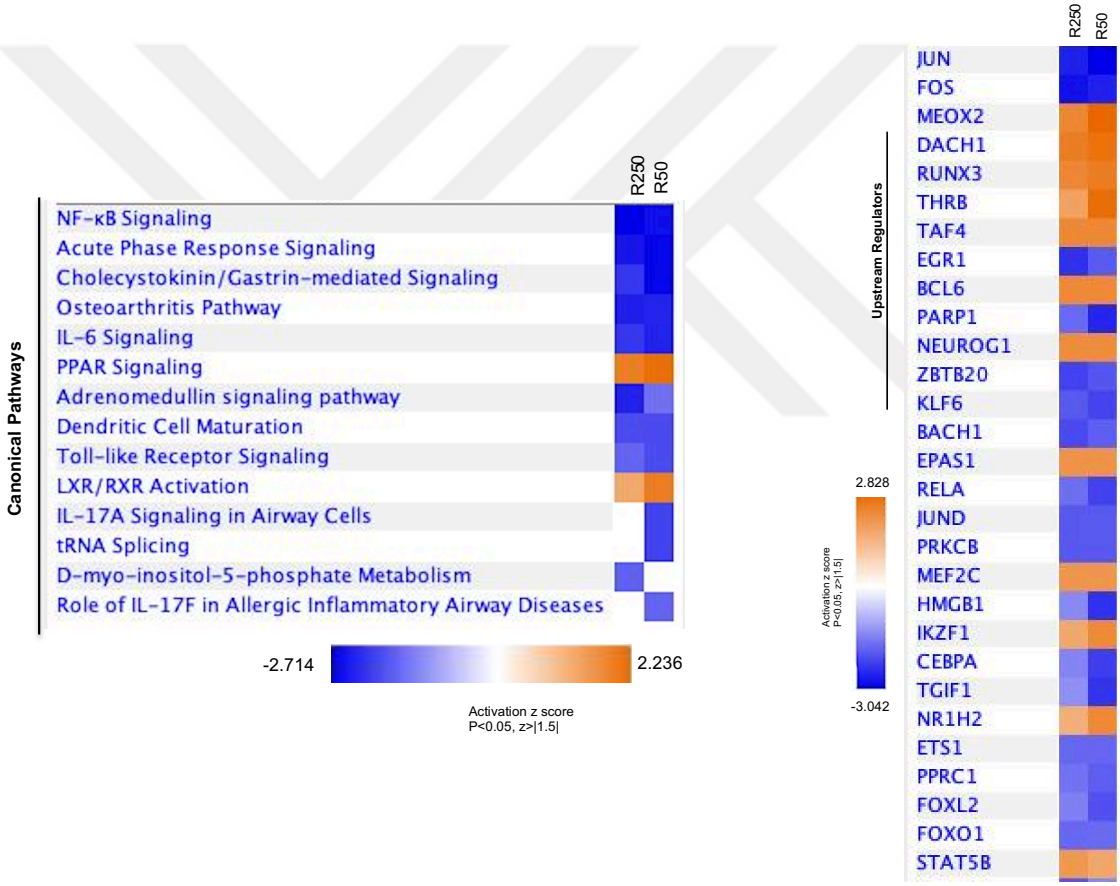


Figure 6.2. Canonical pathways and upstream regulators of R50 and R250 cells.

6.3 Differentially Expressed Gene Alterations

To focus on the transcriptional alterations, DEGs were compared between the R50 and R250 cells and common top 25 up- and down-regulated genes were detected **(Figure 6.3)**.

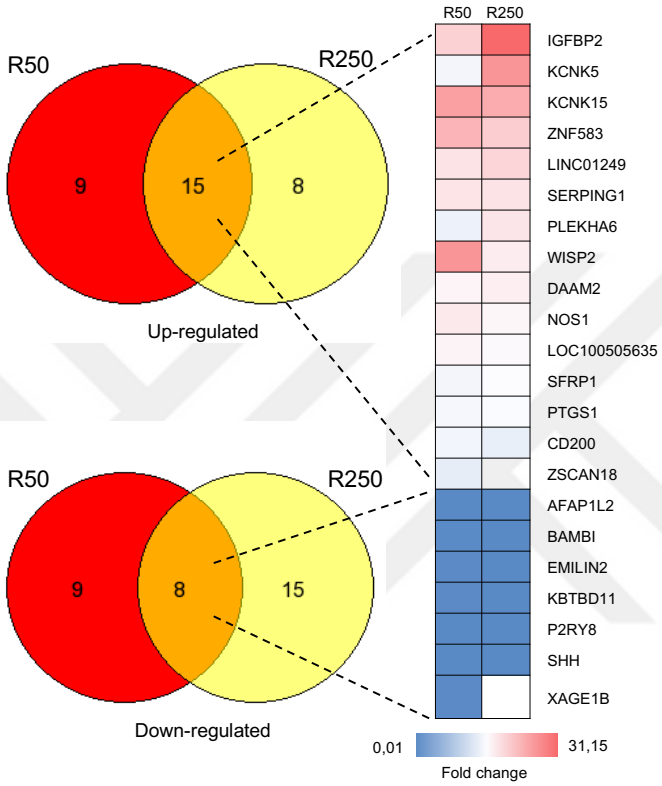


Figure 6.3. Common top 25 up- and down-regulated genes in U87MG-R50 and R250 cells.

These genes were listed in **Table 6.1** (up-regulated) and **Table 6.2** (down-regulated).

R50			Common genes					R250		
Gene names	Fold Change	P Adj	Gene names	Fold Change	P Adj (R50)	Fold Change	P Adj (R250)	Gene names	Fold Change	P Adj
CTAG2	10,46	4,2E-02	CD200	7,78	5,6E-06	7,31	1,6E-05	CXCL14	7,66	9,3E-152
DAPK1	7,73	1,5E-43	DAAM2	9,53	4,4E-33	10,49	3,3E-119	DLX5	8,69	3,5E-33
DOK5	8,26	2,4E-20	IGFBP2	15,02	1,8E-111	31,15	3,2E-270	ICAM2	7,58	9,0E-07
ERMN	11,31	3,3E-02	KCNK15	22,79	2,6E-11	20,84	1,1E-09	SERINC2	8,59	0,0E+00
MIR519A2	32,61	5,4E-04	KCNK5	7,79	4,1E-02	24,42	1,9E-09	SPANXD	7,98	9,6E-05
RIMS4	24,42	3,7E-03	LINC01249	12,14	2,2E-32	14,38	4,4E-41	VCX3A	14,23	1,6E-02
RORC	7,64	4,1E-03	LOC100505635	9,67	5,6E-12	8,79	3,3E-07	ZFP28	16,64	4,0E-02
THY1	9,71	2,5E-27	NOS1	11,23	3,5E-22	9,30	1,4E-103	ZNF808	7,18	1,9E-07
TRABD2B	8,38	2,2E-36	PLEKHA6	7,50	1,1E-34	11,83	4,2E-68			
			PTGS1	7,91	4,4E-08	8,18	1,2E-08			
			SERPING1	12,07	7,0E-10	12,29	3,2E-10			
			SFRP1	7,79	8,8E-03	8,31	4,0E-03			
			WISP2	24,38	2,3E-24	10,84	8,9E-14			
			ZNF583	19,35	8,9E-11	15,65	3,0E-10			
			ZSCAN18	7,17	3,3E-08		2,9E-29			

Table 6.1. Table showing of common top 25 up-regulated genes in U87MG-R50 and R250 cell lines.

R50			Common genes					R250		
Gene names	Fold Change	P Adj	Gene names	Fold Change	P Adj (R50)	Fold Change	P Adj (R250)	Gene names	Fold Change	P Adj
C10orf47	0,11	1,5E-03	AFAP1L2	0,06	8,7E-06	0,01	1,5E-07	BCL11B	0,04	2,7E-25
CCND2	0,10	5,8E-03	BAMBI	0,09	1,3E-04	0,01	1,0E-06	EIF1AY	0,05	1,6E-08
FLJ25801	0,07	5,3E-10	EMILIN2	0,07	1,1E-30	0,06	3,1E-31	FLJ26245	0,05	2,1E-02
HES1	0,11	5,1E-04	KBTBD11	0,08	2,4E-15	0,01	8,9E-22	GPR158-AS1	0,06	5,8E-03
HOXC10	0,11	1,1E-03	P2RY8	0,04	2,5E-50	0,04	5,4E-51	HOTAIR	0,04	1,6E-02
IL1F8	0,08	1,6E-222	SHH	0,05	1,4E-06	0,03	4,3E-07	KDM5D	0,04	5,5E-09
MAGEE1	0,11	1,1E-04	XAGE1B	0,08	3,4E-04		1,2E-06	LHB	0,05	1,9E-05
TFCP2L1	0,07	8,9E-03						LOC100505501	0,04	1,6E-02
ZNF569	0,01	1,7E-07						PAK3	0,04	4,3E-89
								PLEKHG3	0,04	7,2E-06
								SAGE1	0,06	6,9E-11
								TEAD2	0,04	1,9E-19
								TXLNGY	0,02	3,2E-06
								XAGE1E		1,2E-06
								ZNF613	0,05	2,9E-02

Table 6.2. Table showing of common top 25 down-regulated genes in U87MG-R50 and R250 cell lines.

7 Appendix III

7.1 Insulin-like Growth Factor Binding Proteins (IGFBPs)

Insulin-like growth factors are members of growth-stimulating peptides in insulin superfamily, and the most abundant polypeptides overall [180]. There are two types of insulin-like growth factor ligands (IGF-1 and IGF-II) that interact with specific IGF receptors (IGF1R and IGF2R) in IGF system [181], and they share hetero-tetrameric receptors. IGFs are separated from insulin by interaction with six high affinity binding proteins (IGFBPs).

Secreted IGFBPs can interact with IGFs without IGF-IGF1R pathway and this is called IGF1R-independent IGFBP function. The biological role of IGFBPs is to increase half-life of IGFs and bioactivity in circulation, or transportation of IGFs to target tissue. They release IGFs in a controlled manner and rapidly under specific conditions. Released IGFs quickly interact with IGF receptors and promote cell growth, differentiation and display anti-apoptotic functions [180,181].

7.1.1 IGF-Binding Protein-2 (IGFBP-2)

IGFBP-2 mRNA is expressed in both embryonic and fatal development. In addition, expression of IGFBP-2 is started in preimplantation of embryos. In the postnatal period, IGFBP-2 is the second high IGFBP in tissues, circulation and biological fluids. Serum level of IGFBP-2 depends on many physiological or non-physiological situations, and increases in shock, fasting, hypoxia and traumata conditions [168].

On the other hand, IGFBP-2 is significantly expressed in different tumor types and interestingly, it is correlated with the grade levels of tumors. Effects of IGFBP-2 on tumor growth are shown in many types of cancer. IGFBP-2 and activated KRAS were shown to promote astrocytoma in mice [182]. Additionally, IGFBP-2 overexpression or exogenous protein increased cell growth and metastasis in different cancer models including ovarian (Chakrabarty 2006), prostate [183], and glioblastoma [171]. Interestingly, downregulation of this gene inhibited cell growth [180].

Also, IGFBP-2 levels in serum increased in some cancer types, including lung , colon, prostate, and CNS [168]. Serum IGFBP-2 concentrations were positively correlated with specific tumor antigens. IGFBP-2 combination with carcinoembryonic antigen were determined in highly metastatic and recurrent colon cancer patients' serum [184,185]. It is positively correlated with CA 125, ovarian tumor marker, in ovarian cancer patients; and with PSA (prostate specific antigen) in prostate cancer patients [168]. In CNS tumors, IGFBP-2 level was elevated in cerebrospinal fluid (Muller 1994). Moreover, circulating IGFBP-2 increased in glioma patients [186]. These findings suggest that IGFBP-2 might use as specific tumor marker in both serum and other biological fluids.

7.1.2 IGFBP-2 in Glioblastoma

As another tumor types, recent studies showed that IGFBP-2 overexpressed in glioblastoma multiforme (GBM). Fullet et al. [187] showed that IGFBP-2 overexpression in GBM as a first time. After this discovery, many studies confirmed that IGFBP-2 level and glioma tumor grade progression [168,188–192]. However, molecular function of IGFBP-2 in GBM has not been known well. When binding of IGFs by IGFBP-2, growth and migration are inhibited, other mechanisms are correlated with IGFBP-2 expression and tumor grade levels. There are some proposed mechanisms IGFBP-2-mediated tumor progression, (i) including RGD-dependent or independent cell surface interactions of IGFBP-2, (ii) as behavior IGF reservoir, and resulting in effected IGF concentration in the microenvironment of pericellular area, (iii) stimulation of cancer cell proliferation in IGF-independent function [171].

Most studies of IGFBP-2 in GBM suggest that played potential important role in invasion. Engineered overexpression of IGFBP-2 increased cellular invasive capacity, therefore invasion-related proteins, such as MMP-2 was upregulated [193,194]. Moreover, knock-down of IGFBP-2 significantly reduced invasion capacity of GBMs [171]. Furthermore, there may possible link between IGFBP-2 and angiogenesis, because IGFBP-2 and VEGF (vascular endothelial growth factor) are synchronically upregulated in pseudopalisading area of GBM [191].

IGFBP-2 expression is controlled by different hormones or transcription factors. The IGFBP-2 expression level is negatively correlated with PTEN expression in glioma. Also,

serum IGFBP-2 level may be used as a biomarker of PTEN and PI3K-Akt pathway activation [172,195]. IGFBP-2 downstream targets are little known but identified IGFBP-2-induced signaling are correlated with invasive growth-related genes in GBM, such as MMP-2, integrin α5/6, thrombospondin, fibronectin and VEGF [187,191,192,194]. Additionally, the relation of IGFBP-2 expression with ERK1/2, SAPK/JNK, WNT-β-catenin signals, NF-kB, and N-myc were shown in different type of cancer [173,196,197]

7.1.3 IGFBP-2 was Common Upregulated Top Gene

According to the RNA-sequencing results, "Insulin-like growth factor binding protein-2" (IGFBP-2) gene was top upregulated gene in U87MG TRAIL-resistant (R250) cells with 31,15 fold increase. Endogenous IGFBP2 expression levels were tested by qRT-PCR in all TRAIL resistant cells (R10, R50 and R250) derived from U87MG. R0 was control (TRAIL-sensitive U87MG cells) **(Figure 7.1)**. qRT-PCR results confirmed the RNA sequencing.

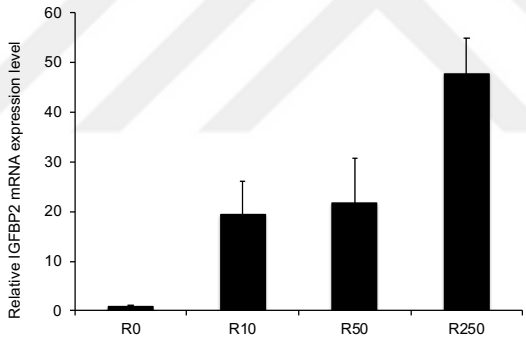


Figure 7.1. qRT-PCR confirmation of IGFBP2 gene levels in U87MG-TRAIL-R cells.

7.1.4 Correlation of IGFBP-2 Expression with Patient Survival

According to the survival analysis on TCGA data, IGFBP-2 expression levels significantly correlated with patient survival in both low grade glioma (LGG) and LGG&GBM patients. IGFBP-2 low patients had longer survival rate than high patients. **(Figure 7.2)**. Survival analysis was performed by Dr. Mehmet Gönen.

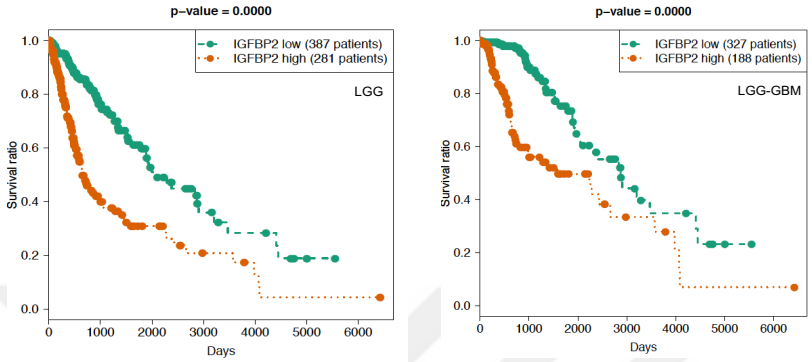


Figure 7.2. Survival analysis of IGFBP-2 expression in both LGG and LGG&GBM patients.

7.2 Knock-down of IGFBP-2 in U87MG-R250 cells

Since IGFBP-2 levels were highly upregulated in TRAIL resistant sub-populations, first, we knocked-down the IGFBP-2 expression. For this purpose, shRNA vectors were designed using RNAiCodex program and cloned to MSCV-PM vector. Cloned vectors were sequenced for confirmation.

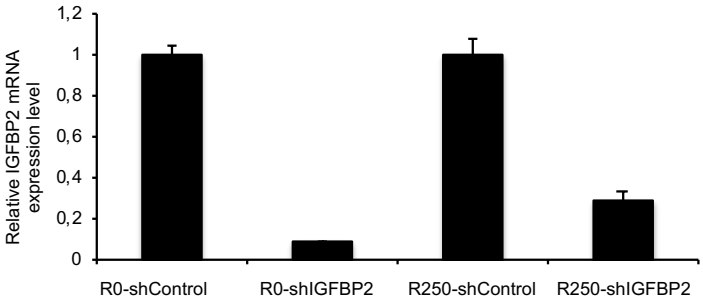


Figure 7.3. qRT-PCR analysis showing shRNA mediated knockdown of IGFBP2 in U87MG-S (R0) and -R (R250) cells.

U87MG-R250 cells were transduced with shIGFBP-2 vector, and after the puromycin selection knock-down efficiency was detected by qRT-PCR **(Figure 7.3)**.

7.3 The Effects of Down-regulation of IGFBP-2 on TRAIL-resistance

To determine the role of IGFBP-2 on TRAIL resistance, TRAIL response of IGFBP-2 knocked-down cells was tested. Viability results showed that silencing of IGFBP-2 did not affect the cell viability upon TRAIL treatment **(Figure 7.4)**.

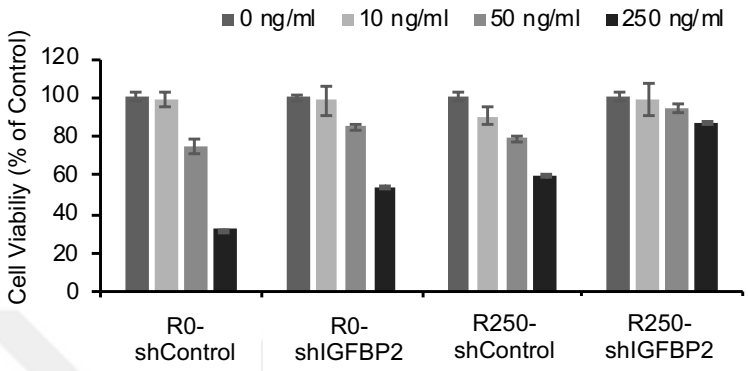


Figure 7.4. Viability of IGFBP2 knocked-down U87MG-S and R cells treated with TRAIL for 24 hours.

7.4 Overexpression of IGFBP2

In order the test the role of IGFBP-2 on TRAIL resistant IGFBP-2 was overexpressed in U87MG cells. First, overexpression vector was cloned to pBabe-puro (Addgene #1764) retroviral backbone, and cloned vector was sequenced for confirmation. Then, U87MG cells were infected with pBabe-IGFBP2 vector. pBabe-GFP vector was used as control. Overexpression of IGFBP-2 was confirmed by qRT-PCR and western blot **(Figure 7.5)**.

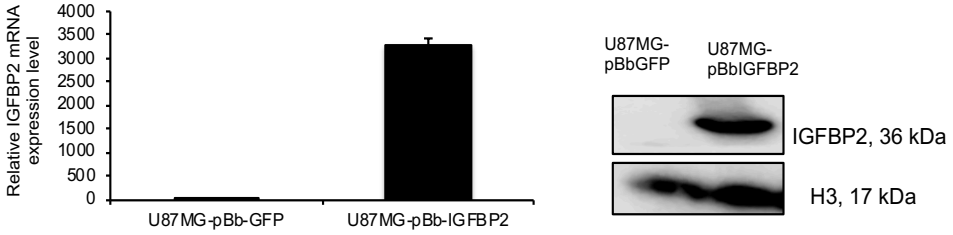


Figure 7.5. qRT-PCR and western blot confirmation of IGFBP-2 overexpression in U87MG cells.

7.5 The Effects of Up-regulation of IGFBP-2 on TRAIL-resistance

In order to test the functional role of IGFBP-2 overexpression against to TRAIL, IGFBP-2 overexpressed-U87MG cells were treated with TRAIL. However, overexpression of IGFBP-2 did not acquire resistance to TRAIL in U87MG cells **(Figure 7.6)**.

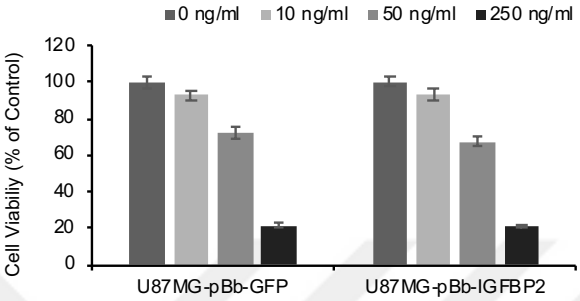


Figure 7.6. Viability of IGFBP-2 overexpressed U87MG cells treated with TRAIL for 24 h.

7.6 The Effects of Secreted IGFBP-2 on TRAIL-resistance

IGFBP-2 is a secreted protein and it has paracrine role. To examine the effects of secreted IGFBP-2 on TRAIL resistance, we treated cells with both recombinant IGFBP-2 protein (500 ng/ml) and condition medium of IGFBP-2 overexpressed-cells following serum starvation for 48 hours. After the IGFBP-2 treatment TRAIL was added in medium for 24 hours **(Figure 7.7)**.

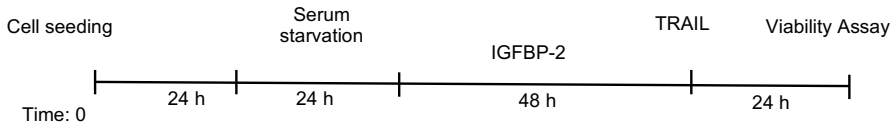


Figure 7.7. Schematic view of IGFBP-2 recombinant protein or conditioned medium experiment timeline.

Cell viability results showed that applying of the recombinant IGFBP-2 increased the cell growth, and partially acquired resistance to TRAIL in serum free conditions **(Figure 7.8, 7.9)**.

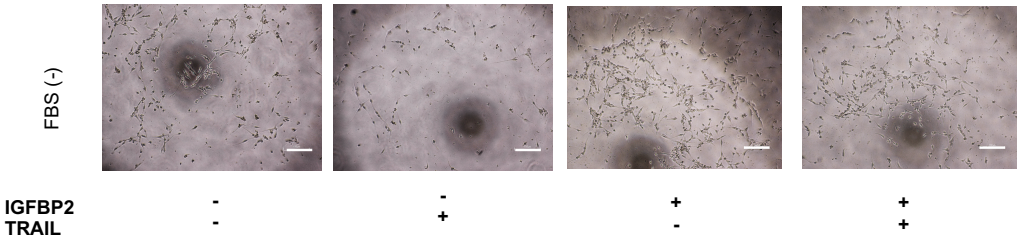


Figure 7.8. Representative snapshots of U87MG cells treated with TRAIL and IGFBP-2.

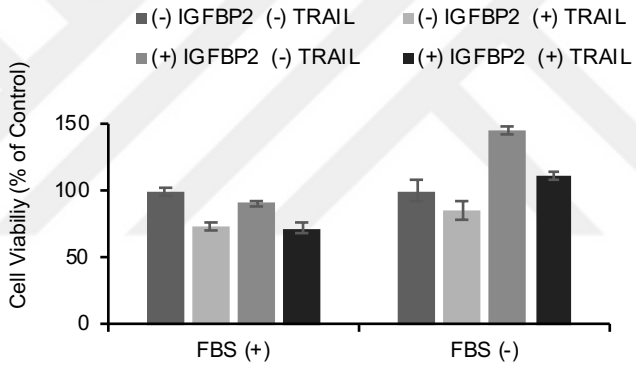


Figure 7.9. Viability of U87MG cells treated with TRAIL for 24 hours following IGFBP-2 treatment for 48 hours.

Additionally, we observed the similar results with conditional medium. In this experiment cell culture medium of IGFBP-2 overexpressed U87MG cells was collected in serum free conditions. Then, conditioned medium was applied on U87MG cells upon 24 hours serum starvation. Similarly, viability results showed that cells acquired partially resistance to TRAIL in IGFBP-2 medium conditions compared with GFP medium **(Figure 7.10)**.

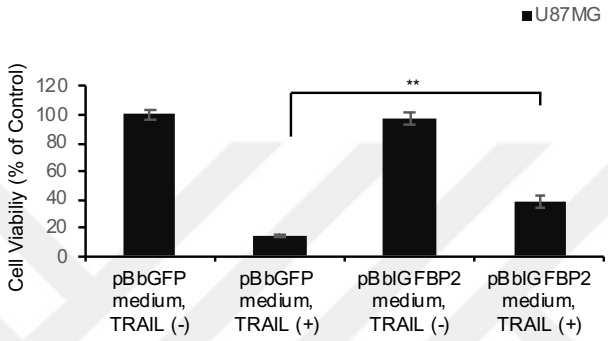


Figure 7.10. Viability of U87MG cells treated with TRAIL for 24 hours upon IGFBP-2 conditioned medium applying.

BIBLIOGRAPHY

1. Drevelegas, A. Extra-axial brain tumors. *Eur Radiol* **15**, 453–467 (2005).
2. Schwartzbaum, J. A., Fisher, J. L., Aldape, K. D. & Wrensch, M. Epidemiology and molecular pathology of glioma. **2**, 494–503 (2006).
3. Jones, C., Perryman, L. & Hargrave, D. Paediatric and adult malignant glioma: close relatives or distant cousins? *Nat. Rev. Clin. Oncol.* **9**, 400–413 (2012).
4. Louis, D. N. *et al.* The 2007 WHO classification of tumours of the central nervous system. *Acta Neuropathol.* **114**, 97–109 (2007).
5. Rich, J. N. & Bigner, D. D. DEVELOPMENT OF NOVEL TARGETED THERAPIES IN THE TREATMENT OF MALIGNANT GLIOMA. **3**, 430–446 (2004).
6. Furnari, F. B. *et al.* Malignant astrocytic glioma: Genetics, biology, and paths to treatment. *Genes Dev.* **21**, 2683–2710 (2007).
7. Jovčevska, I., Kočevar, N. & Komel, R. Glioma and glioblastoma - how much do we (not) know? (Review). *Mol. Clin. Oncol.* **1**, 935–941 (2013).
8. Davis, F. G., Freels, S., Grutsch, J., Barlas, S. & Brem, S. Survival rates in patients with primary malignant brain tumors stratified by patient age and tumor histological type: an analysis based on Surveillance, Epidemiology, and End Results (SEER) data, 1973–1991. *J Neurosurg* **88**, 1–10 (1998).
9. Louis, D. N. *et al.* The 2016 World Health Organization Classification of Tumors of the Central Nervous System: a summary. *Acta Neuropathol.* 1–18 (2016). doi:10.1007/s00401-016-1545-1
10. Li, J., Di, C., Mattox, A. K., Wu, L. & Adamson, D. C. The future role of personalized medicine in the treatment of glioblastoma multiforme. *Pharmgenomics. Pers. Med.* **3**, 111–127 (2010).
11. Huse, J. T. & Holland, E. C. Targeting brain cancer: advances in the molecular pathology of malignant glioma and medulloblastoma. *Nat. Rev. Cancer* **10**, 319–331 (2010).
12. Ostrom, Q. T. *et al.* The epidemiology of glioma in adults: a “state of the science” review. *Neuro. Oncol.* **16**, 896–913 (2014).
13. Rong, Y., Durden, D. L., Meir, E. G. Van & Brat, D. J. Pseudopalisading ` Necrosis in Glioblastoma : A Familiar Morphologic Feature That Links Vascular Pathology , Hypoxia , and Angiogenesis. *J Neuropathol Exp Neurol* **65**, 529–539 (2006).
14. Bonavia, R., Inda, M. D. M., Cavenee, W. K. & Furnari, F. B. Heterogeneity

maintenance in glioblastoma: A social network. *Cancer Res.* **71**, 4055–4060 (2011).

15. Nicholas, M. K., Lukas, R. V, Jafri, N. F., Faoro, L. & Salgia, R. Epidermal Growth Factor Receptor ^ Mediated Signal T. **12**, 7261–7271 (2006).

16. Weinberg, R. A. *The Biology of Cancer, Second Edition*. (2014).

17. Sugawa, N., Ekstrand, A. J., Jamest, C. D. & Collins, V. P. Identical splicing of aberrant epidermal growth factor receptor transcripts from amplified rearranged genes in human glioblastomas. **87**, 8602–8606 (1990).

18. Singh, D. K. *et al.* Oncogenes Activate an Autonomous Transcriptional Regulatory Circuit That Drives Glioblastoma. *Cell Rep.* **18**, 961–976 (2017).

19. Rajasekhar, V. K. *et al.* Oncogenic Ras and Akt Signaling Contribute to Glioblastoma Formation by Differential Recruitment of Existing mRNAs to Polysomes. **12**, 889–901 (2003).

20. Oh, T. *et al.* PI3K pathway inhibitors : potential prospects as adjuncts to vaccine immunotherapy for glioblastoma. **6**, 737–753 (2014).

21. Koul, D. & Koul, D. PTEN Signaling pathways in glioblastoma PTEN signaling pathways in glioblastoma. **4047**, (2008).

22. Lu, Q. R. Developmental origins and oncogenic pathways in malignant brain tumors. 1–23 (2019). doi:10.1002/wdev.342

23. Shangary, S. & Wang, S. Small-Molecule Inhibitors of the MDM2-p53 Protein-Protein Interaction to Reactivate p53 Function : A Novel Approach for Cancer Therapy. 223–243 (2009). doi:10.1146/annurev.pharmtox.48.113006.094723

24. Network, T. C. G. A. R. Comprehensive genomic characterization defines human glioblastoma genes and core pathways. *Nature* **455**, (2008).

25. Cohen, A. L., Holmen, S. L. & Colman, H. IDH1 and IDH2 mutations in gliomas. *Curr. Neurol. Neurosci. Rep.* **13**, 1–7 (2013).

26. Songtao, Q. *et al.* IDH mutations predict longer survival and response to temozolomide in secondary glioblastoma. *Cancer Sci.* **103**, 269–273 (2012).

27. Turcan, S. *et al.* IDH1 mutation is sufficient to establish the glioma hypermethylator phenotype. *Nature* **483**, 479–483 (2012).

28. Gilbert, M. R. *et al.* Autophagy and oxidative stress in gliomas with IDH1 mutations. *Acta Neuropathol.* **127**, 221–233 (2014).

29. Ohgaki, H. & Kleihues, P. Genetic alterations and signaling pathways in the evolution of gliomas. *Cancer Sci.* **100**, 2235–2241 (2009).

30. Ohgaki, H. & Kleihues, P. Genetic Pathways to Primary and Secondary Glioblastoma. *Am. J. Pathol.* **170**, 1445–1453 (2019).

31. Iacob, G. & Dinca, E. B. Current data and strategy in glioblastoma multiforme. **2**, 386–393 (2009).

32. Messaoudi, K. & Clavreul, A. Toward an effective strategy in glioblastoma treatment . Part I : resistance mechanisms and strategies to overcome resistance of glioblastoma to temozolomide. **20**, 899–905 (2015).

33. Zhou, J., Atsina, K., Himes, B. T., Strohbehn, G. W. & Saltzman, W. M. Novel Delivery Strategies for Glioblastoma. **18**, 89–99 (2012).

34. Berens, M. E. & Giese, A. `` . . . those left behind .'' Biology and Oncology of Invasive Glioma Cells. *Neoplasia* **1**, 208–219 (1999).

35. Vleeschouwer, S. De. *Glioblastoma*. (2017). doi:http://dx.doi.org/10.15586/codon.glioblastoma.2017

36. Pelloski, C. E. *et al.* Epidermal Growth Factor Receptor Variant III Status Defines Clinically Distinct Subtypes of Glioblastoma. **25**, (2019).

37. Rich, J. N. *et al.* Phase II Trial of Gefitinib in Recurrent Glioblastoma. **22**, 133–142 (2019).

38. Cohen, M. H., Shen, Y. L., Keegan, P. & Pazdur, R. FDA Drug Approval Summary: Bevacizumab (Avastin威)as Treatment of Recurrent Glioblastoma Multiforme MARTIN. *Oncologist* **14**, 1131–1138 (2009).

39. Reardon, D., Egorin, M. J., Desjardins, A., Vredenburg, J. J. & Beumer, J. H. Phase I Pharmacokinetic Study of the VEGFR Tyrosine Kinase Inhibitor Vatalanib (PTK787) plus Imatinib and Hydroxyurea for Malignant Glioma. *Cancer* **115**, 2188–2198 (2009).

40. Sathornsumetee, S., Desjardins, A., Quinn, J. A., Vredenburgh, J. J. & Rich, J. N. Molecularly Targeted Therapy for Malignant Glioma. (2007). doi:10.1002/cncr.22741

41. Gilbert, M. R. *et al.* NRG oncology RTOG 0625 : a randomized phase II trial of bevacizumab with either irinotecan or dose-dense temozolomide in recurrent glioblastoma. *J Neurooncol* **131**, 193–199 (2017).

42. Vredenburgh, J. J. *et al.* Bevacizumab Plus Irinotecan in Recurrent Glioblastoma Multiforme. *J. Clin. Oncol.* **25**, 4722–4729 (2019).

43. Ellis, L. M. & Hicklin, D. J. Pathways Mediating Resistance to Vascular Endothelial Growth Factor ^ T argeted Therapy. **14**, 6371–6376 (2008).

44. Quant, E. C. *et al.* in recurrent malignant glioma patients who progress on bevacizumab. 550–555 (2009). doi:10.1215/15228517-2009-006

45. Pitz, M. W. *et al.* Phase II study of PX-866 in recurrent glioblastoma Marshall. *Neuro. Oncol.* **17**, 1270–1274 (2015).

46. Massacesi, C. *et al.* PI3K inhibitors as new cancer therapeutics : implications for clinical trial design. 203–210 (2016).

47. Costa, B. *et al.* Human Glioblastoma Multiforme : p53 Reactivation by a Novel MDM2 Inhibitor. **8**, (2013).

48. Touat, M., Idbaih, A., Sanson, M. & Ligon, K. L. Glioblastoma targeted therapy: updated approaches from recent biological insights. *Ann. Oncol. Off. J. Eur. Soc. Med. Oncol.* **28**, 1457–1472 (2017).

49. Unterkircher, T. *et al.* Bortezomib primes glioblastoma, including glioblastoma stem cells, for TRAIL by increasing tBid stability and mitochondrial apoptosis. *Clin. Cancer Res.* **17**, 4019–4030 (2011).

50. Jung, T., Catalgol, B. & Grune, T. The proteasomal system. *Mol. Aspects Med.* **30**, 191–296 (2009).

51. Yin, D. *et al.* Proteasome inhibitor PS-341 causes cell growth arrest and apoptosis in human glioblastoma multiforme (GBM). 344–354 (2005). doi:10.1038/sj.onc.1208225

52. Phuphanich, S. *et al.* Phase 1 clinical trial of bortezomib in adults with recurrent malignant glioma. *J. Neurooncol.* **100**, 95–103 (2010).

53. Kardosh, A. *et al.* Aggravated endoplasmic reticulum stress as a basis for enhanced glioblastoma cell killing by bortezomib in combination with celecoxib or its non-coxib analogue, 2,5-dimethyl-celecoxib. *Cancer Res.* **68**, 843–851 (2008).

54. Kerr, J., Wyllie, A. & Currie, A. Apoptosis: A Basic Biological Phenomenon With Wide- Ranging Implications In Tissue Kinetics. *Br. J. Cancer* **26**, 239–57 (1972).

55. Nagata, S. Apoptosis and Clearance of Apoptotic Cells. (2018).

56. Elmore, S. Apoptosis: a review of programmed cell death. *Toxicol. Pathol.* **35**, 495–516 (2007).

57. Falschlehner, C., Emmerich, C. H., Gerlach, B. & Walczak, H. TRAIL signalling: Decisions between life and death. *Int. J. Biochem. Cell Biol.* **39**, 1462–1475 (2007).

58. Mcilwain, D. R., Berger, T. & Mak, T. W. Caspase Functions in Cell Death and Disease. (2013).

59. Li, J. & Yuan, J. Caspases in apoptosis and beyond. 6194–6206 (2008). doi:10.1038/onc.2008.297

60. Pitti, R. M. *et al.* Induction of apoptosis by Apo-2 ligand, a new member of the tumor necrosis factor cytokine family. *J. Biol. Chem.* **271**, 12687–12690 (1996).

61. Wiley, S. R. *et al.* Identification and characterization of a new member of the TNF family that induces apoptosis. *Immunity* **3**, 673–682 (1995).

62. Pan, G. *et al.* The receptor for the cytotoxic ligand TRAIL. *Science* **276**, 111–113 (1997).

63. Pan, G. *et al.* An antagonist decoy receptor and a death domain-containing receptor for TRAIL. *Science* **276**, 111–113 (1997).

64. Marsters, S. a *et al.* A novel receptor for Apo2L/TRAIL contains a truncated death domain. *Curr. Biol.* **7**, 1003–1006 (1997).

65. Emery, J. G. *et al.* Osteoprotegerin is a receptor for the cytotoxic ligand TRAIL. *J. Biol. Chem.* **273**, 14363–14367 (1998).

66. Mellier, G., Huang, S., Shenoy, K. & Pervaiz, S. TRAILing death in cancer. *Mol. Aspects Med.* **31**, 93–112 (2010).

67. von Karstedt, S., Montinaro, A. & Walczak, H. Exploring the TRAILs less travelled: TRAIL in cancer biology and therapy. *Nat. Rev. Cancer* **17**, 352–366 (2017).

68. Horak, P. *et al.* Contribution of epigenetic silencing of tumor necrosis factor-related apoptosis inducing ligand receptor 1 (DR4) to TRAIL resistance and ovarian cancer. *Mol. Cancer Res.* **3**, 335–343 (2005).

69. Mérino, D. *et al.* Differential inhibition of TRAIL-mediated DR5-DISC formation by decoy receptors 1 and 2. *Mol. Cell. Biol.* **26**, 7046–7055 (2006).

70. Wagner, K. W. *et al.* Death-receptor O-glycosylation controls tumor-cell sensitivity to the proapoptotic ligand Apo2L/TRAIL. *Nat. Med.* **13**, 1070–1077 (2007).

71. Rossin, A., Derouet, M., Abdel-Sater, F. & Hueber, A.-O. Palmitoylation of the TRAIL receptor DR4 confers an efficient TRAIL-induced cell death signalling. *Biochem. J.* **419**, 185–192, 2 p following 192 (2009).

72. Burns, T. F. & El-Deiry, W. S. Identification of inhibitors of TRAIL-induced death (ITIDs) in the TRAIL- sensitive colon carcinoma cell line SW480 using a genetic approach. *J Biol Chem* **276**, 37879–86. (2001).

73. Wang, S. The promise of cancer therapeutics targeting the TNF-related apoptosis-inducing ligand and TRAIL receptor pathway. *Oncogene* **27**, 6207–6215 (2008).

74. Ricci, M. S. *et al.* Direct repression of FLIP expression by c-myc is a major determinant of TRAIL sensitivity. *Mol. Cell. Biol.* **24**, 8541–8555 (2004).

75. Özören, N. & El-Deiry, W. S. Defining Characteristics of Types I and II Apoptotic Cells in Response to TRAIL. *Neoplasia* **4**, 551–557 (2002).

76. Krammer, P. H. CD95's deadly mission in the immune system. *Nature* **407**, 789–795 (2000).

77. Song, J. J., Jee, Y. A., Yong, T. K. & Lee, Y. J. Evidence for two modes of

development of acquired tumor necrosis factor-related apoptosis-inducing ligand resistance: Involvement of Bcl-xL. *J. Biol. Chem.* **282**, 319–328 (2007).

78. Baylin, S. B. & Ohm, J. E. Epigenetic gene silencing in cancer - a mechanism for early oncogenic pathway addiction? *Nat. Rev. Cancer* **6**, 107–116 (2006).

79. Dawson, M. a. & Kouzarides, T. Cancer epigenetics: From mechanism to therapy. *Cell* **150**, 12–27 (2012).

80. Martinez, R. *et al.* CpG island promoter hypermethylation of the pro-apoptotic gene caspase-8 is a common hallmark of relapsed glioblastoma multiforme. *Carcinogenesis* **28**, 1264–1268 (2007).

81. Ropero, S. & Esteller, M. The role of histone deacetylases (HDACs) in human cancer. *Mol. Oncol.* **1**, 19–25 (2007).

82. Pingoud-meier, C. *et al.* Loss of Caspase-8 Protein Expression Correlates with Unfavorable Survival Outcome in Childhood Medulloblastoma Loss of Caspase-8 Protein Expression Correlates with Unfavorable Survival Outcome in Childhood Medulloblastoma. **9**, 6401–6409 (2003).

83. Fröhlich, L. F., Mrakovcic, M., Smole, C., Lahiri, P. & Zatloukal, K. Epigenetic silencing of apoptosis-inducing gene expression can be efficiently overcome by combined SAHA and TRAIL treatment in uterine sarcoma cells. *PLoS One* **9**, (2014).

84. Venza, M. *et al.* The overriding of TRAIL resistance by the histone deacetylase inhibitor MS-275 involves c-myc up-regulation in cutaneous, uveal, and mucosal melanoma. *Int. Immunopharmacol.* **28**, 313–321 (2015).

85. Dolly G. Aguilera. Reactivation of death receptor 4 (DR4) expression sensitizes medulloblastoma cell lines to TRAIL. *J Neurooncol.* **93**, (2009).

86. Trivedi, R. & Mishra, D. P. Trailing TRAIL Resistance: Novel Targets for TRAIL Sensitization in Cancer Cells. *Front. Oncol.* **5**, (2015).

87. Bagci-Onder, T. *et al.* Real-time imaging of the dynamics of death receptors and therapeutics that overcome TRAIL resistance in tumors. **32**, 2818–2827 (2013).

88. Kelley, S. K. *et al.* Preclinical Studies to Predict the Disposition of Apo2L / Tumor Necrosis Factor-Related Apoptosis-Inducing Ligand in Humans : Characterization of in Vivo Efficacy , Pharmacokinetics , and Safety. *Pharmacology* **299**, 31–38 (2001).

89. Schneider, P. *Production of recombinant TRAIL and TRAIL receptor: Fc chimeric proteins. Methods in enzymology* **322**, (ACADEMIC PRESS, 2000).

90. Shah, K., Tung, C. H., Yang, K., Weissleder, R. & Breakefield, X. O. Inducible Release of TRAIL Fusion Proteins from a Proapoptotic Form for Tumor Therapy.

Cancer Res. **64**, 3236–3242 (2004).

91. Ganten, T. M. *et al.* Preclinical differentiation between apparently safe and potentially hepatotoxic applications of TRAIL either alone or in combination with chemotherapeutic drugs. *Clin. Cancer Res.* **12**, 2640–2646 (2006).

92. Berg, D. *et al.* Enforced covalent trimerization increases the activity of the TNF ligand family members TRAIL and CD95L. *Cell Death Differ.* **14**, 2021–2034 (2007).

93. Müller, N., Schneider, B., Pfizenmaier, K. & Wajant, H. Superior serum half life of albumin tagged TNF ligands. *Biochem. Biophys. Res. Commun.* **396**, 793–799 (2010).

94. Kim, T. H. *et al.* PEG-transferrin conjugated TRAIL (TNF-related apoptosis-inducing ligand) for therapeutic tumor targeting. *J. Control. Release* **162**, 422–428 (2012).

95. Kim, T. H. *et al.* PEGylated TNF-related apoptosis-inducing ligand (TRAIL) analogues: Pharmacokinetics and antitumor effects. *Bioconjug. Chem.* **22**, 1631–1637 (2011).

96. Erkoc, P., Cingöz, A., Onder, T. B. & Kizilel, S. Quinacrine Mediated Sensitization of Glioblastoma (GBM) Cells to TRAIL through MMP-Sensitive PEG Hydrogel Carriers. *Macromol. Biosci.* **17**, (2017).

97. Bagci-Onder, T., Wakimoto, H., Anderegg, M., Cameron, C. & Shah, K. A Dual PI3K / mTOR Inhibitor , PI-103 , Cooperates with Stem Cell − Delivered TRAIL in Experimental Glioma Models. *Cancer Res.* **71**, 154–163 (2011).

98. Stuckey, D. W. & Shah, K. TRAIL on trial: Preclinical advances in cancer therapy. *Trends Mol. Med.* **19**, 685–694 (2013).

99. Bhere, D. & Shah, K. *Stem Cell-Based Therapies for Cancer*. *Advances in Cancer Research* **127**, (Elsevier Inc., 2015).

100. Hotte, S. J. *et al.* A phase 1 study of mapatumumab (fully human monoclonal antibody to TRAIL-R1) in patients with advanced solid malignancies. *Clin. Cancer Res.* **14**, 3450–3455 (2008).

101. Camidge, D. R. Apomab: An agonist monoclonal antibody directed against Death Receptor 5/TRAIL-Receptor 2 for use in the treatment of solid tumors. *Expert Opin. Biol. Ther.* **8**, 1167–1176 (2008).

102. Wakelee, H. A. *et al.* Phase I and pharmacokinetic study of lexatumumab (HGS-ETR2) given every 2 weeks in patients with advanced solid tumors. *Ann. Oncol.* **21**, 376–381 (2009).

103. Forero-Torres, A., Shah, J., Wood, T., Posey, J. & Saleh, M. Phase I Trial of

Weekly Tigatuzumab, an Agonistic Humanized Monoclonal Antibody Targeting Death Receptor 5 (DR5). *Cancer Biother. Radiopharm.* **25**, 1–8 (2010).

104. Herbst, R. S. *et al.* Phase I dose-escalation study of recombinant human Apo2L/TRAIL, a dual proapoptotic receptor agonist, in patients with advanced cancer. *J. Clin. Oncol.* **28**, 2839–2846 (2010).

105. Younes, A. *et al.* A Phase 1b/2 trial of mapatumumab in patients with relapsed/refractory non-Hodgkin's lymphoma. *Br. J. Cancer* **103**, 1783–1787 (2010).

106. Fuchs, C. S. *et al.* TRAIL receptor agonist conatumumab with modified FOLFOX6 plus bevacizumab for first-line treatment of metastatic colorectal cancer: A randomized phase 1b/2 trial. *Cancer* **119**, 4290–4298 (2013).

107. Inda, M. del M., Bonavia, R. & Seoane, J. Glioblastoma multiforme:A look inside its heterogeneous nature. *Cancers (Basel).* **6**, 226–239 (2014).

108. Lartigue, J. De. Tumor heterogeneity : a central foe in the. **16**, 167–174 (2018).

109. Singh, S. K. *et al.* Identification of human brain tumour initiating cells. *Nature* **432**, (2004).

110. Anido, J. & Seoane, J. TGF-b Receptor Inhibitors Target the CD44high/Id1high Glioma-Initiating Cell Population in Human Glioblastoma. *Cancer Cell* **18**, 655–668 (2010).

111. Verhaak, R. G. W. *et al.* Article Integrated Genomic Analysis Identifies Clinically Relevant Subtypes of Glioblastoma Characterized. *Cancer Cell* **17**, 98–110 (2010).

112. Wang, Q., Hu, B., Hu, X., Kim, H. & Olar, A. Tumor Evolution of Glioma-Intrinsic Gene Expression Subtypes Associates with Immunological Changes in the Microenvironment Article. *Cancer Cell* **32**, 42–56 (2017).

113. Bhat, K. P. L. *et al.* Mesenchymal Differentiation Mediated by NF-κB Promotes Radiation Resistance in Glioblastoma Krishna. *Cancer Cell* **24**, 1–22 (2014).

114. Lan, X. *et al.* Fate mapping of human glioblastoma reveals an invariant stem cell hierarchy. *Nature* **549**, 227–232 (2017).

115. Holohan, C., Schaeybroeck, S. Van, Longley, D. B. & Johnston, P. G. Cancer drug resistance : an evolving paradigm. *Nat. Publ. Gr.* **13**, 714–726 (2013).

116. Housman, G. *et al.* Drug resistance in cancer: An overview. *Cancers (Basel).* **6**, 1769–1792 (2014).

117. Holland, E. C. Glioblastoma multiforme: the terminator. *Proc. Natl. Acad. Sci. U. S. A.* **97**, 6242–6244 (2000).

118. Stavrovskaya, A. A., Shushanov, S. S. & Rybalkina, E. Y. Problems of

Glioblastoma Multiforme Drug Resistance a b c. **81**, (2016).

119. Hoey, T. Drug resistance, epigenetics, and tumor cell heterogeneity. *Sci. Transl. Med.* **2**, 19–22 (2010).

120. Wilting, R. H. & Dannenberg, J. H. Epigenetic mechanisms in tumorigenesis, tumor cell heterogeneity and drug resistance. *Drug Resist. Updat.* **15**, 21–38 (2012).

121. Albeck, J. G. *et al.* Quantitative Analysis of Pathways Controlling Extrinsic Apoptosis in Single Cells. *Mol. Cell* **30**, 11–25 (2008).

122. Spencer, S. L., Gaudet, S., Albeck, J. G., Burke, J. M. & Sorger, P. K. Non-genetic origins of cell-to-cell variability in TRAIL-induced apoptosis. *Nature* **459**, 428–432 (2009).

123. Bhola, P. D. & Simon, S. M. Determinism and divergence of apoptosis susceptibility in mammalian cells. **43**, 4296–4302 (2009).

124. Flusberg, D. a, Roux, J., Spencer, S. L. & Sorger, P. K. Cells surviving fractional killing by TRAIL exhibit transient but sustainable resistance and inflammatory phenotypes. *Mol. Biol. Cell* **24**, 2186–200 (2013).

125. Lane, D., Côté, M., Grondin, R., Couture, M.-C. & Piché, A. Acquired resistance to TRAIL-induced apoptosis in human ovarian cancer cells is conferred by increased turnover of mature caspase-3. *Mol. Cancer Ther.* **5**, 509–521 (2006).

126. Lee, T. J., Lee, J. T., Park, J. W. & Kwon, T. K. Acquired TRAIL resistance in human breast cancer cells are caused by the sustained cFLIPL and XIAP protein levels and ERK activation. *Biochem. Biophys. Res. Commun.* **351**, 1024–1030 (2006).

127. Chen, W. *et al.* Acquired Activation of the Akt/Cyclooxygenase-2/Mcl-1 Pathway Renders Lung Cancer Cells Resistant to Apoptosis. *Mol. Pharmacol.* **77**, 416–423 (2009).

128. Li, Z., Xu, X., Bai, L., Chen, W. & Lin, Y. Epidermal growth factor receptor-mediated tissue transglutaminase overexpression couples acquired tumor necrosis factor-related apoptosis-inducing ligand resistance and migration through c-FLIP and MMP-9 proteins in lung cancer cells. *J. Biol. Chem.* **286**, 21164–21172 (2011).

129. Olson, A. RNAi Codex: a portal/database for short-hairpin RNA (shRNA) gene-silencing constructs. *Nucleic Acids Res.* **34**, D153–D157 (2005).

130. Onder, T. T. *et al.* Chromatin-modifying enzymes as modulators of reprogramming. *Nature* **483**, 598–602 (2012).

131. Sanjana, N. E., Shalem, O. & Zhang, F. Improved vectors and genome-wide libraries for CRISPR screening. *Nat. Methods* **11**, 783–784 (2014).

132. Stemmer, M., Thumberger, T., del Sol Keyer, M., Wittbrodt, J. & Mateo, J. L.

CCTop: An Intuitive, Flexible and Reliable CRISPR/Cas9 Target Prediction Tool. *PLoS One* **10**, e0124633 (2015).

133. Kim, D., Langmead, B. & Salzberg, S. L. HISAT : a fast spliced aligner with low memory requirements. **12**, (2015).

134. Lawrence, M. *et al.* Software for Computing and Annotating Genomic Ranges. *PLoS Comput. Biol.* **9**, 1–10 (2013).

135. Anders Simon & Huber Wolfgang. Differential expression analysis for sequence count data. *Genome Biol.* **11**, (2010).

136. Kaya-Aksoy, E. *et al.* The pro-apoptotic Bcl-2 family member Harakiri (HRK) induces cell death in glioblastoma multiforme. *Cell Death Discov.* **5**, 64 (2019).

137. Sasportas, L. S. *et al.* Assessment of therapeutic efficacy and fate of engineered human mesenchymal stem cells for cancer therapy. *Proc. Natl. Acad. Sci. U. S. A.* **106**, 4822–4827 (2009).

138. Özören, N. & El-Deiry, W. S. Cell surface death receptor signaling in normal and cancer cells. *Semin. Cancer Biol.* **13**, 135–147 (2003).

139. Chen, G. G., Sin, F. L. F., Leung, B. C. S., Ng, H. K. & Poon, W. S. Glioblastoma cells deficient in DNA-dependent protein kinase are resistant to cell death. *J. Cell. Physiol.* **203**, 127–132 (2005).

140. Singh, T. R., Shankar, S. & Srivastava, R. K. HDAC inhibitors enhance the apoptosis-inducing potential of TRAIL in breast carcinoma. 4609–4623 (2005). doi:10.1038/sj.onc.1208585

141. Nakata, S. *et al.* Histone deacetylase inhibitors upregulate death receptor 5 / TRAIL-R2 and sensitize apoptosis induced by TRAIL / APO2-L in human malignant tumor cells. 6261–6271 (2004). doi:10.1038/sj.onc.1207830

142. Wood, T. E. *et al.* Selective Inhibition of Histone Deacetylases Sensitizes Malignant Cells to Death Receptor Ligands. **9**, 246–257 (2010).

143. Ashkenazi, A. Directing cancer cells to self-destruct with pro-apoptotic receptor agonists. *Nat. Rev. Drug Discov.* **7**, 1001–1012 (2008).

144. Flusberg, D. A., Roux, J., Spencer, S. L. & Sorger, P. K. Cells surviving fractional killing by TRAIL exhibit transient but sustainable resistance and inflammatory phenotypes. *Mol. Biol. Cell* **24**, 2186–2200 (2013).

145. Song, J. J., Jee, Y. A., Yong, T. K. & Lee, Y. J. Evidence for two modes of development of acquired tumor necrosis factor-related apoptosis-inducing ligand resistance: Involvement of Bcl-xL. *J. Biol. Chem.* **282**, 319–328 (2007).

146. Breitschopf, K., Zeiher, A. M. & Dimmeler, S. Ubiquitin-mediated Degradation of the Proapoptotic Active Form of Bid. *J. Biol. Chem.* **275**, 21648–21652 (2000).

147. Fulda, S. Novel insights into the synergistic interaction of Bortezomib and TRAIL: tBid provides the link. *Oncotarget* **2**, 418–421 (2011).

148. Nikrad, M. *et al.* The proteasome inhibitor bortezomib sensitizes cells to killing by death receptor ligand TRAIL via BH3-only proteins Bik and Bim. *Mol. Cancer Ther.* **4**, 443–9 (2005).

149. van Dijk, M. *et al.* The proteasome inhibitor bortezomib sensitizes AML with myelomonocytic differentiation to TRAIL mediated apoptosis. *Cancers (Basel).* **3**, 1329–1350 (2011).

150. Chen, K.-F. *et al.* Bortezomib Overcomes Tumor Necrosis Factor-related Apoptosis-inducing Ligand Resistance in Hepatocellular Carcinoma Cells in Part through the Inhibition of the Phosphatidylinositol 3-Kinase/Akt Pathway. *J. Biol. Chem.* **284**, 11121–11133 (2009).

151. Koschny, R. *et al.* TRAIL/bortezomib cotreatment is potentially hepatotoxic but induces cancer-specific apoptosis within a therapeutic window. *Hepatology* **45**, 649–658 (2007).

152. Koschny, R. *et al.* Bortezomib sensitizes primary meningioma cells to TRAIL-induced apoptosis by enhancing formation of the death-inducing signaling complex. *J. Neuropathol. Exp. Neurol.* **73**, 1034–1046 (2014).

153. de Wilt, L. H. A. M. *et al.* Bortezomib and TRAIL: A perfect match for apoptotic elimination of tumour cells? *Crit. Rev. Oncol. Hematol.* **85**, 363–372 (2013).

154. Naumann, I., Kappler, R., Von Schweinitz, D., Debatin, K. M. & Fulda, S. Bortezomib primes neuroblastoma cells for TRAIL-induced apoptosis by linking the death receptor to the mitochondrial pathway. *Clin. Cancer Res.* **17**, 3204–3218 (2011).

155. Bychkov, M. L., Gasparian, M. E., Dolgikh, D. a. & Kirpichnikov, M. P. Combination of TRAIL with Bortezomib Shifted Apoptotic Signaling from DR4 to DR5 Death Receptor by Selective Internalization and Degradation of DR4. *PLoS One* **9**, e109756 (2014).

156. Ganten, T. M. *et al.* Proteasome inhibition sensitizes hepatocellular carcinoma cells, but not human hepatocytes, to TRAIL. *Hepatology* **42**, 588–597 (2005).

157. Yin, X.-M., Oltvai, Z. N. & Korsmeyer, S. J. BH1 andBH2 domainsofBcl-2 are required for inhibition of apoptosis and heterodimerization with Bax. *Nature* **369**, 321–323 (1994).

158. Matayoshi, E. D. *et al.* Solution structure of the antiapoptotic protein bcl-2. *Proc. Natl. Acad. Sci.* **98**, 3012–3017 (2002).

159. Warren, C. F. A., Wong-Brown, M. W. & Bowden, N. A. BCL-2 family isoforms in

apoptosis and cancer. *Cell Death Dis.* **10**, (2019).

160. Khaw, S. L., Huang, D. C. S. & Roberts, A. W. BH3-mimetics - The solution to chemoresistance? *Leuk. Lymphoma* **50**, 1069–1072 (2009).

161. Oltersdorf, T. *et al.* An inhibitor of Bcl-2 family proteins induces regression of solid tumours. *Nature* **435**, 677–681 (2005).

162. Tse, C. *et al.* ABT-263: A Potent and Orally Bioavailable Bcl-2 Family Inhibitor. *Cancer Res.* **68**, 3421–3428 (2008).

163. Cristofanon, S. & Fulda, S. ABT-737 promotes tBid mitochondrial accumulation to enhance TRAIL-induced apoptosis in glioblastoma cells. *Cell Death Dis.* **3**, e432-11 (2012).

164. Hetschko, H. *et al.* Pharmacological inhibition of Bcl-2 family members reactivates TRAIL-induced apoptosis in malignant glioma. *J. Neurooncol.* **86**, 265–272 (2008).

165. Huang, S. & Sinicrope, F. A. BH3 Mimetic ABT-737 Potentiates TRAIL-Mediated Apoptotic Signaling by Unsequestering Bim and Bak in Human Pancreatic Cancer Cells Shengbing. *Cancer Res.* **68**, 2944–2951 (2008).

166. Schmidt, C. W. *et al.* Small-molecule Bcl-2 inhibitors sensitise tumour cells to immune-mediated destruction. *Br. J. Cancer* **96**, 600–608 (2007).

167. Song, J. H., Kandasamy, K. & Kraft, A. S. ABT-737 induces expression of the death receptor 5 and sensitizes human cancer cells to TRAIL-induced apoptosis. *J. Biol. Chem.* **283**, 25003–25013 (2008).

168. Hoeflich, A. *et al.* Insulin-like Growth Factor-binding Protein 2 in Tumorigenesis : Protector or Promoter ? Insulin-like Growth Factor-binding Protein 2 in Tumorigenesis : Protector or Promoter ? 1. 8601–8610 (2001).

169. Lin, Y. *et al.* Plasma IGFBP-2 levels predict clinical outcomes of patients with high-grade gliomas. *Neuro. Oncol.* **11**, 468–476 (2009).

170. Han, S., Li, Z., Master, L. M., Master, Z. W. & Wu, a. Exogenous IGFBP-2 promotes proliferation, invasion, and chemoresistance to temozolomide in glioma cells via the integrin β1-ERK pathway. *Br. J. Cancer* **111**, 1400–1409 (2014).

171. Fukushima, T., Tezuka, T., Shimomura, T., Nakano, S. & Kataoka, H. Silencing of insulin-like growth factor-binding protein-2 in human glioblastoma cells reduces both invasiveness and expression of progression-associated gene CD24. *J. Biol. Chem.* **282**, 18634–18644 (2007).

172. Levitt, R. J., Georgescu, M. M. & Pollak, M. PTEN-induction in U251 glioma cells decreases the expression of insulin-like growth factor binding protein-2. *Biochem. Biophys. Res. Commun.* **336**, 1056–1061 (2005).

173. Ben-Shmuel, a, Shvab, a, Gavert, N., Brabletz, T. & Ben-Ze'ev, a. Global analysis

of L1-transcriptomes identified IGFBP-2 as a target of ezrin and NF-κB signaling that promotes colon cancer progression. *Oncogene* 1–11 (2012). doi:10.1038/onc.2012.340

174. Diessenbacher, P. *et al.* NF-κB inhibition reveals differential mechanisms of TNF versus TRAIL-induced apoptosis upstream or at the level of caspase-8 activation independent of cIAP2. *J. Invest. Dermatol.* **128**, 1134–1147 (2008).

175. Franco, A. V. *et al.* The Role of NF- B in TNF-Related Apoptosis-Inducing Ligand (TRAIL)-Induced Apoptosis of Melanoma Cells. *J. Immunol.* **166**, 5337–5345 (2001).

176. Thayaparasingham, B., Kunz, A. & Kulms, D. Sensitization of melanoma cells to TRAIL by UVB-induced and NF-κB-mediated downregulation of xIAP. *Oncogene* **28**, 345–362 (2009).

177. Lee, K. Y., Park, J. S., Jee, Y. K. & Rosen, G. D. Triptolide sensitizes lung cancer cells to TNF-realted apoptosis-ligand (TRAIL)-induced apoptosis by inhibition of NF-kB activation. *Exp. Mol. Med.* **34**, 462–468 (2002).

178. Ravi, R. & Bedi, A. Sensitization of tumor cells to Apo2 ligand/TRAIL-induced apoptosis by inhibition of casein kinase II. *Cancer Res.* **62**, 4180–4185 (2002).

179. Bernard, D., Quatannens, B., Vandenbunder, B. & Abbadie, C. Rel/NF-κB Transcription Factors Protect against Tumor Necrosis Factor (TNF)-related Apoptosis-inducing Ligand (TRAIL)-induced Apoptosis by Up-regulating the TRAIL Decoy Receptor DcR1. *J. Biol. Chem.* **276**, 27322–27328 (2001).

180. Baxter, R. C. IGF binding proteins in cancer: mechanistic and clinical insights. *Nat. Rev. Cancer* **14**, 329–41 (2014).

181. Carrick, F. E., Wallace, J. C. & Forbes, B. E. The interaction of Insulin-like Growth Factors (IGFs) with Insulin-like Growth Factor Binding Proteins (IGFBPs): a review. 147–153 (2002).

182. Dunlap, S. M. *et al.* Insulin-like growth factor binding protein 2 promotes glioma development and progression. *Proc. Natl. Acad. Sci. U. S. A.* **104**, 11736–11741 (2007).

183. Chatterjee, S., Park, E. S. & Soloff, M. S. Proliferation of DU145 prostate cancer cells is inhibited by suppressing insulin-like growth factor binding protein-2. *Int. J. Urol.* **11**, 876–884 (2004).

184. Renehan, A. G., Jones, J., Potten, C. S., Shalet, S. M. & Dwyer, S. T. O. Elevated serum insulin-like growth factor (IGF) -II and IGF binding protein-2 in patients with colorectal cancer. **83**, 1344–1350 (2000).

185. Renehan, A. G. *et al.* Circulating Insulin-Like Growth Factor II and Colorectal

Adenomas *. **85**, 3402–3408 (2000).

186. Li, Y. *et al.* cancers : evidences from glioma and colorectal carcinoma studies. 1–8 (2012). doi:10.1093/annonc/mds007

187. Fuller, G. N. *et al.* Reactivation of insulin-like growth factor binding protein 2 expression in glioblastoma multiforme: a revelation by parallel gene expression profiling. *Cancer Res* **59**, 4228–4232 (1999).

188. Elmlinger, M. W. *et al.* In vivo expression of insulin-like growth factor-binding protein-2 in human gliomas increases with the tumor grade. *Biochem. Biophys. Res. Commun.* **142**, 1652–1658 (2001).

189. Sallinen, S. L. Identification of differentially expressed genes in human gliomas by DNA microarray and tissue chip techniques. *Cancer Res.* **60**, 6617–6622 (2000).

190. Zhang, W., Wang, H., Song, S. W. & Fuller, G. N. Insulin-like growth factor binding protein 2: gene expression microarrays and the hypothesis-generation paradigm. *Brain Pathol.* **12**, 87–94 (2002).

191. Godard, S. *et al.* Classification of Human Astrocytic Gliomas on the Basis of Gene Expression: A Correlated Group of Genes with Angiogenic Activity Emerges As a Strong Predictor of Subtypes. *Cancer Res.* **63**, 6613–6625 (2003).

192. Zhou, Y.-H., Hess, K. R., Liu, L., Linskey, M. E. & Yung, W. K. A. Modeling prognosis for patients with malignant astrocytic gliomas: quantifying the expression of multiple genetic markers and clinical variables. *Neuro. Oncol.* **7**, 485–94 (2005).

193. Wang, G. K., Hu, L., Fuller, G. N. & Zhang, W. An interaction between insulin-like growth factor-binding protein 2 (IGFBP2) and integrin α5 is essential for IGFBP2-induced cell mobility. *J. Biol. Chem.* **281**, 14085–14091 (2006).

194. Wang, H. *et al.* Insulin-like growth factor binding protein 2 enhances glioblastoma invasion by activating invasion-enhancing genes. *Cancer Res.* **63**, 4315–4321 (2003).

195. Mehrian-Shai, R. *et al.* Insulin growth factor-binding protein 2 is a candidate biomarker for PTEN status and PI3K/Akt pathway activation in glioblastoma and prostate cancer. *Proc. Natl. Acad. Sci. U. S. A.* **104**, 5563–5568 (2007).

196. Chakrabarty, S. & Kondratick, L. Insulin-like growth factor binding protein-2 stimulates proliferation and activates multiple cascades of the mitogen-activated protein kinase pathways in NIH-OVCAR3 human epithelial ovarian cancer cells. *Cancer Biol. Ther.* **5**, 189–197 (2006).

197. Chambéry, D., Mohseni-Zadeh, S., de Gallé, B. & Babajko, S. N-myc regulation of type I insulin-like growth factor receptor in a human neuroblastoma cell line. *Cancer Res.* **59**, 2898–2902 (1999).